Doctoral Thesis

Study on Indoor Environmental Quality for Four-bed Ward with Ceiling Induction Diffusers

(天井吹出し型誘引ユニットを有する

４床病室における室内環境に関する研究)

Ying Li

Department of Architectural Engineering,

Division of Global Architecture,

Graduate School of Engineering,

Osaka University

July, 2018

ABSTRACT

Indoor environmental quality is essential to people who stay in the room. Inappropriate indoor environmental quality would lead to some uncomfortable feelings and make people upset.

Air conditioning system is a kind of multifunctional facilities in medical buildings. In recent years, especially, the ceiling induction air conditioning has attracted widespread attention, because this kind of air conditioning systems presented the excellent properties both on the high quality of indoor environment and energy conservation.

In this study, a full-scaled model room with four beds was assigned to simulate a real hospital ward and verified the characteristics of the air-conditioning system with Ceiling Induction Diffusers (CID). In order to examine the practicability and validity of CID system, several experiments were conducted in a simulation sickroom where the size and appearance were designed by reference to a real sickroom. In order to simulate the real environment of the ward, manikins who can exhale the gas mixture (density is near to the air) composed by carbon dioxide (CO_2) and helium (He) emitted from the chests of manikins. were arranged and black lamps were also set for simulating the heat generated by household appliances such as TV, refrigerator etc. Moreover, the gauge points in the monitoring process were widely arranged, including the horizontal and vertical distributions. The layout of device and decoration in the ward probably has influence on the indoor environment, therefore, these factors were also considered in this study.

We collected measurement data such as temperature distribution, tracer gas concentration, the age of air and air velocity and radiation. Among the measurement data, the age of air requires further calculation from the tracer gas concentration. There are existing methods for the calculation of age of air, e.g., pulse method, step-up method and step-down method, however, these method requires pulse, step-up and step-down injection of tracer gas which is impossible in the case of CID system due to the returning air. Therefore, we adopted a modeling approach, making an assumption of the concentration response function and identifying a few parameters from the measured data in the certain local point, then the local mean age of air can be calculated numerically based on the least square method.

Keywords: Indoor environmental quality; Ceiling Induction Diffusers (CID); Tracer gas method; Temperature distribution; Tracer gas concentration; Air velocity; Radiation; Impulse response function; Local mean age of air

ACKNOWLEDGEMENTS

First and foremost, to my supervisor, Professor Toshio Yamanaka, I want to extend my sincere gratitude for his considerate inspiration and tireless support. I have benefited a lot from his knowledge and high standards in research at Ph.D. course in Osaka University. His research sprite and responsibility behind top researcher will guide me in the future.

I would like to express my deepest gratitude to Professor Kondo who reviewed and commented my doctoral thesis, and gave me the valuable comments.

I am particularly grateful to Professor Kobayashi, who is also one of the reviewers of my doctoral thesis, for his comments and useful suggestions.

I also want to give my heartfelt thanks to the late Professor Hisashi Kotani for his patience, encouragement.

I would like to express my deepest gratitude to Professor Kazunobu Sagara for his encouragement, and of course, valuable suggestions.

I am thankful to Professor Yoshihisa Momoi for his help I have received.

What`s more, I am appreciated the assistant from the laboratory secretary, Mrs. Iida and all the students in laboratory 4. It is my pleasure to study with all of you.

I wish to express my gratitude to all the professors who taught me in my life. Without the knowledge I learned, it is impossible for me to complete this thesis.

The financially support from the Japanese Government (MONBUKAGAKUSHO MEXT) scholarship is gratefully acknowledged.

Last but not the least, I am indebted to my family. They are standing behind me and supporting me silently all the time.

CONTENTS

NOTATIONS

d [m]: Depth of experimental room

w [m]: Width of experimental room

h [m]: height of experimental room

Q_{OA} [m^3/h]: Air flow rate of outdoor air

Q_{SA} [m^3/h]: Air flow rate of supply air

Q_{EA} [m^3/h]: Air flow rate of exhaust air

M [m^3/h]: Emission rate of tracer gas

C_{OA} [ppm]: Concentration of outdoor air

C_{SA} [ppm]: Concentration of supply air

C_{EA} [ppm]: Concentration of exhaust air

C_e [ppm]: Air concentration near the suction inlet in equipment room

C_i [ppm]: Indoor air concentration.

θ_i [℃]: Temperature of indoor air

C_p [ppm]: Steady-state concentration at each measurement point

R_P (t) [ppm]: The concentration of tracer gas at point P caused by injecting a unit amount of tracer gas

V [m^3]: Volume of the room

t_n [s]: Nominal ventilation time

$<\tau>$ [s]: Average age of air

τ_p [s]: Local mean age of air

t : Time [s]

h_r [-]: Ratio of tracer gas distributed in the experimental room.

η_{eff} [-]: Coefficient efficiency

E [W/m^2]: Irradiance,

U [V]: Voltage output

σ [W/(m^{2}K^4)]: Stefan-Boltzmann constant

θ [℃]: Instrument body temperature

S [V/(W/m^2)]: Sensitivity

$_{-EA}$: Exhaust air

$_{-OA}$: Outdoor air

$_{-SA}$: Supply air

$_{-e}$: Equipment room

$_{-i}$: Indoor air

Chapter 1 INTRODUCTION

1.1 History

Indoor environmental quality is a conception that some indicators are comprised, which can influence occupants in buildings. Generally, thermal comfort, humidity, indoor air velocity and the concentration of contaminant are the main indicators to evaluate the indoor environmental quality in public buildings. Natural ventilation is an important and useful approach to make air circulate at dwelling buildings. Especially, cross-ventilation is an effective way that brings flesh wind and benefits the indoor air quality. In summers, keeping the windows and doors that are in opposite positions open is a usual and efficient way to improve indoor thermal comfort and take away much dampness. However, the way that open windows and introduce natural wind dependents on the weather and seasons to much extent. During the monsoon or winters, natural ventilation cannot relieve indisposed feelings caused by unfriendly indoor environment.

In addition, this original way shows its limitations with the development of buildings. In order to meet various needs of human beings, buildings have had others functions except for inhabiting, such as office buildings, commercial buildings, schools, hospitals etc. These types of buildings hardly achieve the designs of natural ventilation, due to spacious rooms and few windows. Actually, in Japan, the Building Standards Law has been enacted in the early 21st century, which enforce mechanical ventilation devices to be installed for residences. As for those public buildings, mechanical ventilation or hybrid ventilation cannot satisfy the service function. Therefore, the advent of air-conditioner expects to solve this dilemma.

Vacuum Reducer Valve (VRV), ie. central air-conditioning system, is usually installed in public building to modify indoor environment. Various working principles for refrigeration system have been researched and developed since this kind of machine was invented. Cooling water system, fresh air system and fan-coil unit system were designed and improved continuously to satisfy comfort of people who are staying in the indoor room. Unlike the old inner circulation principle or unhealthy method of fresh-old wind mixture, developed transformation of new wind is mainly applied the type of displacement that outdoor fresh air can be indrawn into rooms by negative pressure. The process of dedusting and filtrating can be conducted when new wind is below through the fresh air inlet to house. Indoor pipelines linked with exhaust outlets form the circulation system which would exhale the exhaust gas and facilitate good circulation. With technology developing and conception creating, fan coil unit (FCU) was created as an ideal terminal product, which process the indoor air, cooling or heating, and make processed air circle

in the room under the forced triggering by the fan. New wind can be carried into house by make-up air unit, and the fresh air volume can be up to the standard of air conditioning room. There are thin pipes for water and new wind rather than large air duct in this type of equipment, based on the heat convection simply, therefore public place where people have a short stay usually employ it. Undoubtedly, air conditioning system has become the most efficient device to control and modify indoor environment and the scope of application for it has been expanding. However, there is only water pipe and thin fresh air tube instead of air duct in the fan coil cooling unit. Fig. 1.1 illustrates that a water pipe with a small size can transport the same cooling energy as a much bigger air duct. Chilled beams can facilitate to dramatically reduce air handler and ductwork sizes and make both horizontal and vertical interior space more efficient. This kind of air conditioning system is usually installed in those rooms that have small areas and require the lower precision for temperature and humidity.

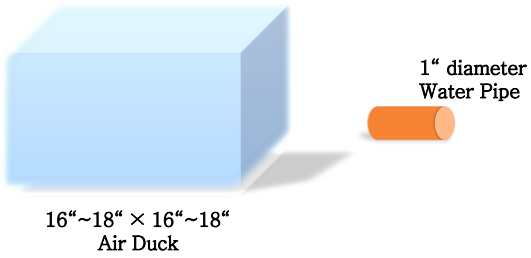

Fig. 1.1 Cooling energy transport economies of air and water

In modern times, air conditioning system is a kind of multifunctional facility in a hospital. In recent years, especially, the chilled beam systems have attracted widespread attention (Kosonen and Tan 2005)1-1), because this kind of air conditioning presented the excellent properties both on the high quality of indoor environment and energy conservation.

1.2 What is the chilled beam system?

Chilled beam systems are an alternate method to traditional air conditioning. It uses chilled water pipes installed to the ceiling to cool air in a space. In the chilled beams, ventilation is the only matter which needs to deliver to the occupied space, and the warmer water which cannot be used in conventional fan-coil units can be used in chilled beams. Moreover, chilled beams improve thermal comfort, air quality, and have lower than conventional installation costs. Two types of chilled beam systems are designed and widely used: passive beams and active beams. The natural buoyancy of air is the impetus for passive chilled beams to circulate through the

heat exchange coils to make the air cool. Hot air rises in a room and is stuck in an overhead space in chilled beams, then the air will naturally fall back into the room when it interacts with the lower temperature beams. Compared with the passive chilled beams, active chilled beams are complex and both interior and outdoor air are involved in heat exchange process. Air is oriented through the nozzles to the cooling/heating coils, and active systems tend to be about double as efficient as passive systems due to the forced convection required. It is worth noting that any other mechanical process would not be used in both passive and active systems in the cooling process. Chilled beams have been used in Europe continent as well as Australia for over decades and before long this kind of systems have been introduced to North America due to the minimal installation space requirements. Fig.1.2 presents the operational principles for passive chilled beams and active chilled beams.

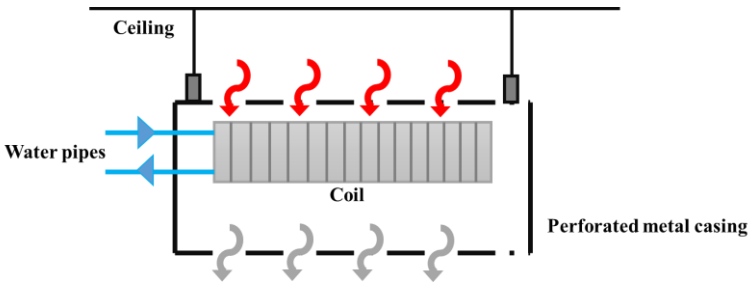

a) Passive chilled beam operation

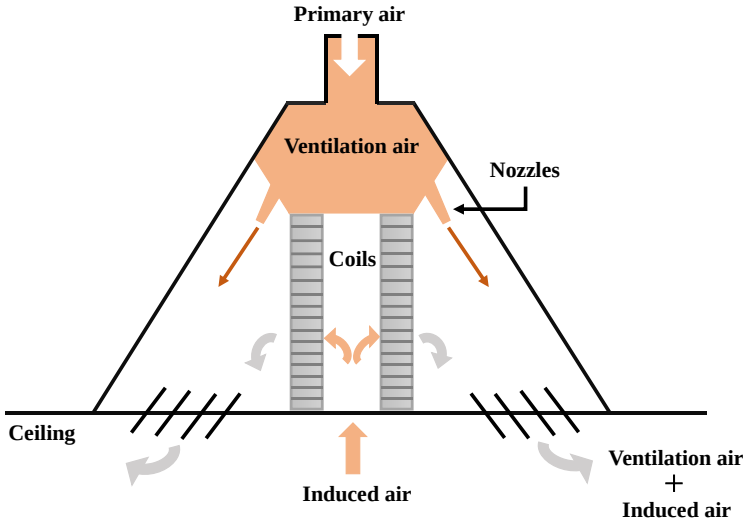

b) Active chilled beam operation

Fig. 1.2 Operational principles for Chilled beam systems

1.3 Chilled beam systems and ceiling induction diffuser units

Installing chilled beam systems to an existing building has many practical benefits on environment and people. Applying water with high specific heat capacity as a transfer medium instead of air enables the system to be far less fan energy than a conventional air-based system, and temperature for water in chilled beams is far less demanding than that for conventional air systems. Hence, chilled water systems are more efficient than a conventional system. Chilled beam systems make cool air be distributed more evenly as well as in higher quantities around a room which results in less energy consumed to supply the room's desired temperature and humidity. Consequently, the costs associated with chilled beams systems are lower than the traditional system, for example, the operating cost and maintenance of some mechanical components. The energy costs for operating chilled beams are remarkably lower than that for all-air systems, and operational efficiencies of pumps are higher than fans, resulting in the lower energy transport costs. As for the maintenance, chilled beams exclude those moving parts (fans, motors, damper actuators, etc.) and most chilled beams can be filters-free. Table 1.1 lists the lifetime maintenance and replacement costs for active chilled beams and FCU, based on an expected lifetime for FUC of 20 years (Virta M. 2004) [1-2)].

Table 1.1 Life cycle maintenance costs Fan coil unit vs. Active chilled beam

	Fan coil unit	Active chilled beam
Filter changes		
Frequency	Twice yearly	NA
Cost per change	$30.0	$0.0
Cost over lifetime (20 years)	$1,200.0	$0.0
Clean coil and condensate system		
Frequency	Twice yearly	Every four years
Cost per event	$30.0	$30.0
Cost over lifetime	$1,200.0	$150.0
Fan motor replacement		
Frequency	Once during lifetime	NA
Cost per event	$400.0	$0.0
Cost over lifetime	$400.0	$0.0
Life cycle (20 years) maintenance cost	$2,800.0	$150.0

It assumes that each beam or FCU serves a perimeter floor area of 150 square feet. And the floor-to-slab height will be shrunk due to the small size of water pipe replaced air trunk. Specifically, chilled beams can be mounted in ceiling spaces as small as 8 to 10 inches vertically while all-air systems typically require to over twice.

In terms of comfort and indoor air quality (IAQ) benefits of chilled beam systems, properly designed chilled beam systems generally lead to enhanced thermal comfort and indoor air quality (Trox USA, Inc.) [1-3]. The constant airflow rate delivery of primary air to the active chilled beam helps assure that the design space ventilation rates and relative humidity levels are closely maintained. However, chilled beams are hardly used in Japan because the high humidity environment makes those systems inefficient. Ceiling induction diffuser (CID) units evolved from chilled beam systems are a good alternative, which remove the heating coils. Now, there are three types of CID units being used in Japan.

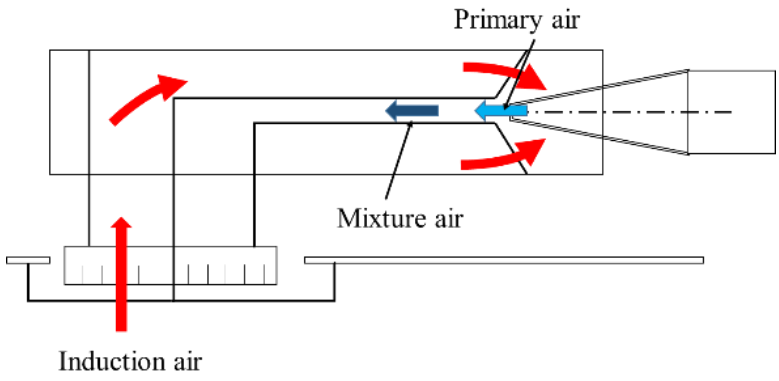

a) The diffuser with large temperature difference

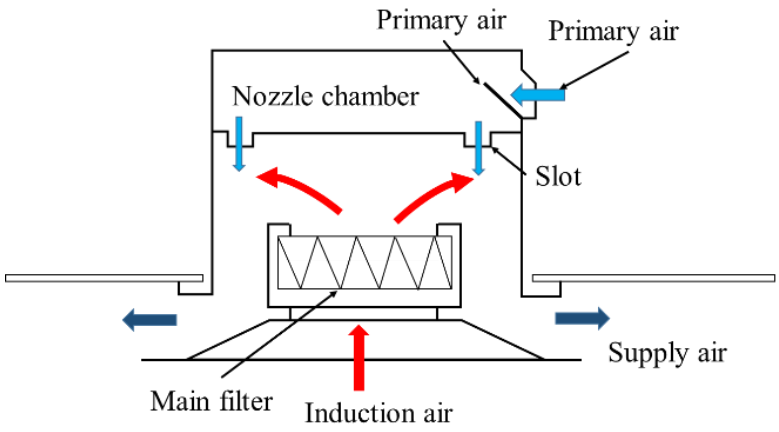

b) The unit with purification device

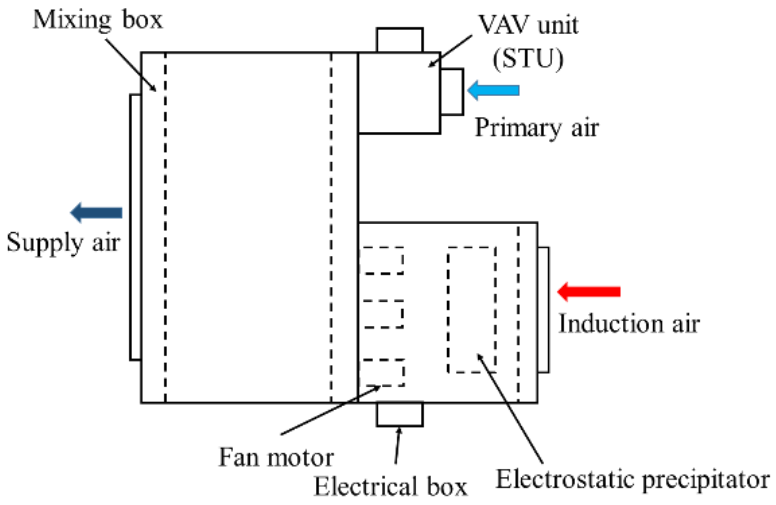

c) Circulation fan VAV units

Fig. 1.3 Induction unit used in Japan

Firstly, the diffuser with large temperature difference (Fig.1.3 a)) can facilitate to provide wind with low temperature at the minimum of 5℃, which can induce the air around the ceil of the room. The induction ratio of this unit is 50 ~ 120%. They are widely installed in shopping malls and department stores. In addition, the unit with purification device (Fig.1.3 b)), whose induction ratio is 50 ~ 100%, is a unit that enables induced air in room to be purified, with a low pressure loss high performance filter built in it. Coupled with the mentioned two types, circulation fan can control the indoor temperature through VAV units (Fig.1.3 c)) and make the recirculating air over 50% to ensure air distribution. There are five features for induction units:

1) The reduced amount of air output for once caused by blowing cool wind can facilitate to a smaller size of air conditioning system, which is conducive to an economy plan for construction and power delivery.

2) The space for devices and equipment is less needed and more building space can be fully used.

3) The thermal comfort can be improved because of the lower indoor humidity (relative humidity 30~40%), but it is disadvantaged to energy conservation.

4) There is no cool water pipe in this system, where the water leakage will be eliminated.

5) The maintenance cost can be reduced because fans are unnecessary for inducing nozzles.

1.4 Introduction of CID System

Fig. 1.4 shows the mechanism of CID system. The outdoor air is sucked into the air conditioner placed in the equipment room, cooled or heated, dehumidified or humidified, and sent to the air beam. Air is supplied from the air beam and exhausted to the outside of the room through the exhaust fan.

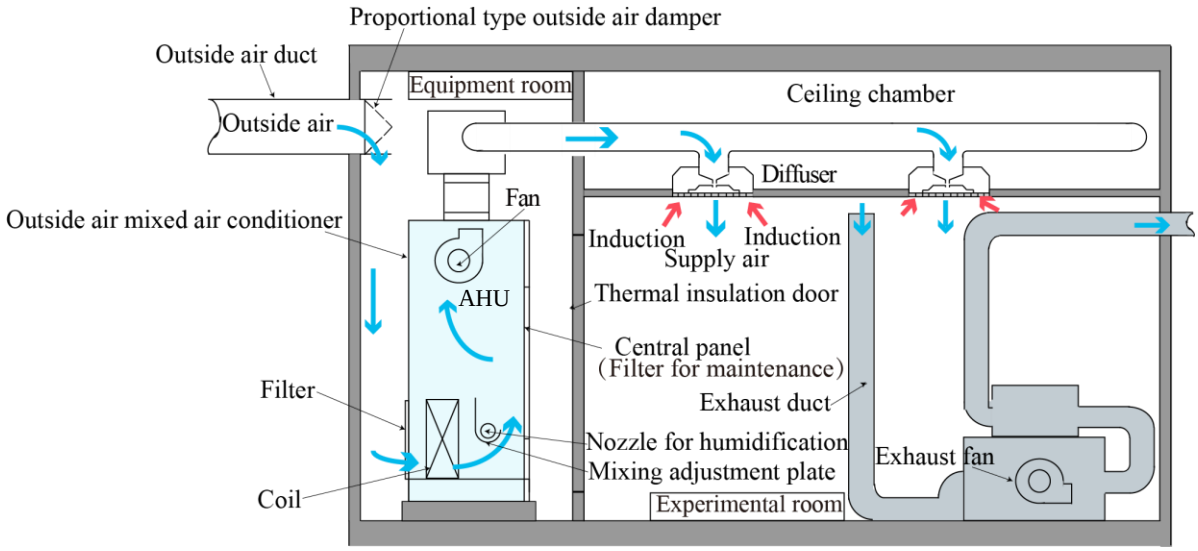

Fig. 1.4 Schematic diagram of CID system

AHU used in CID system, an improved air handling unit, has been being of interests since it was invented because of its effectiveness as well as energy saving. Rolled elliptic cylinder tubes are laid in the unit as heat exchange pipes, where fins are designed for air flowing along the length of pipe. Its significant superiority can be described as follow:

(a) Elliptic cylinder tubes, compared with traditional cylinder tubes blocked more than 40% area of air intake, enables to enlarge the internal flow area of air and improves the effective area of ventilation. This kind of design witnesses its excellent air flowing performance outside the shell of pipe. That air flows against the wall of elliptic-shaped pipes streamlines the airflow, and airstream can flow past smoothly. This situation results in a delayed split-off point between airflow and the shell, which contributes to reduce the eddy flow zone (shown in Fig. 1.5) to form. Therefore, flow loss caused by Karman vortex street declines significantly which means the air side resistance in elliptic-shaped pipe is averagely lower than that in rounded pipe. Feeding power of wind turbine only dependents on the air drag, when the heat exchange capacity and airflow rate have the certain arrangements. It achieves decrease of energy

consuming of the wind turbine. Moreover, the pipe cluster is easy to arrange compactly for shrinking the size of the unit and reducing installing spaces; and the smaller heat exchange surface is needed for elliptic-shaped pipe than that for circular pipe.

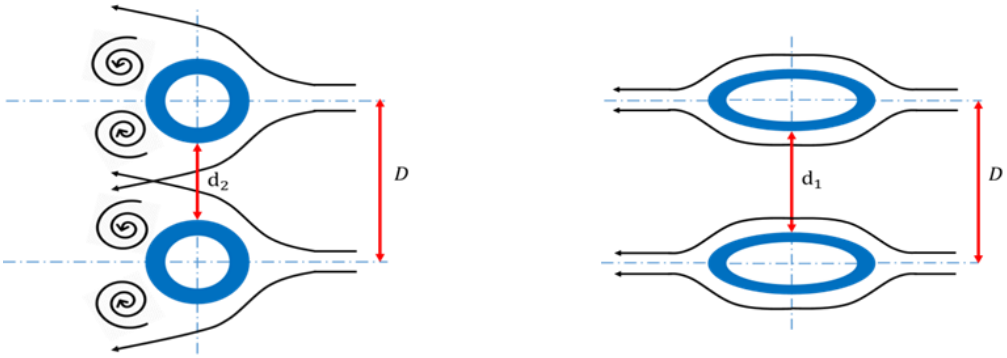

Fig. 1.5 Comparison of air flowing through the elliptic-shaped pipes and rounded pipes

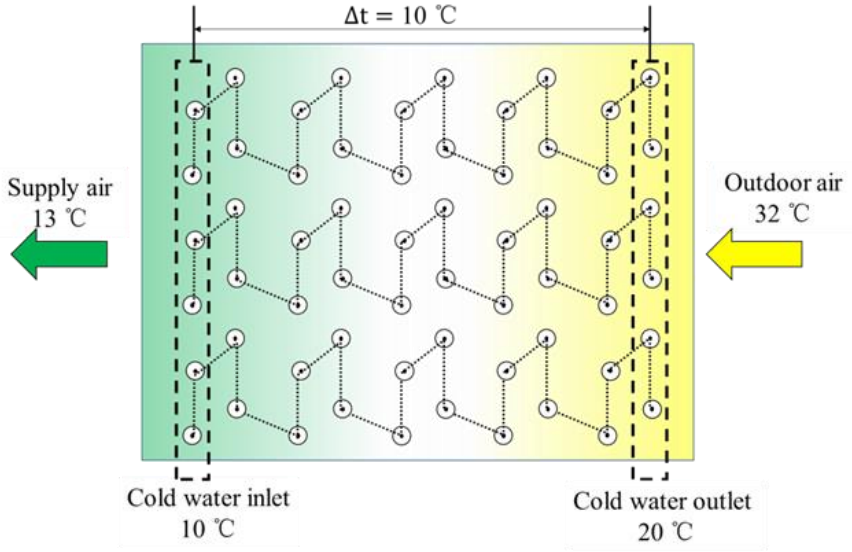

Fig. 1.6 The schematic diagram of elliptic-shaped heat exchanger with fins under the cooling condition

(b) Perimeter of elliptic-shaped pipe is longer than that of rounded pipe, when they have the same cross-sectional area. The bigger contact area between the pipe and airflow is conducive to heat exchange. More heat exchange tubes, enlarged the effective heat transfer area, can be laid in the tank of heat exchanger. Basically, compared with rounded pipes, the coefficient of heat transfer for fins on elliptic-shaped pipes is higher. Take the cooling condition as an example illustrated in Fig. 1.6. In order to achieve the process of cooling dehumidification for the blending wind formed by indoor return air and fresh air converging into the mixing chamber,

the unit takes fully use of the circular chilled water with 10℃/20℃. The blending wind cools down to 13℃ from 16℃ (the conventional temperature) and then goes into the indoor induction unit. When indoor comfort can be satisfied, under the situation of low temperature air supply, the higher temperature difference make 30% air quantity be saved as well as 30% power of air supply. Obviously, the consumption of energy and operating expense decline. The smaller area of air duct occupies the fewer building space due to the same reason.

However, the energy consumption seems to be increased resulting from the supply water with high temperature which aims at achieving the higher temperature difference between supply and return water. This also leads to a deteriorated effect on heat exchanger, therefore several rows of coilers have to be installed to cater for the supplied-air temperature at 13℃. The drawback caused by this practical problem can be solved by the elliptic-shaped design, because the small air resistance but high performance overcomes the increasing wind resistance of more coilers. It can be considered that the advantages of this air-conditioning system to be embodied by its higher temperature difference and lower airflow rate.

Moreover, this kind of air-conditioning system is able to regulate the process of heat and humidity changing in the air, due to the fact that elliptic-shaped fin type heat exchanger is used as an important component of intensive air handling unit improved induced air-conditioning system. The pipe cluster has a compact structure, hence making a small volume of equipment facilitates to save building space. In comparison with those traditional rounded pipes, airflow experiences good flowing performance outside the shell of elliptic-shaped pipes. It can be seen that, in the Fig. 1.6, the streamline flows against the shell of elliptic-shaped pipes and a backward detached position between the air and the pipe is observed. This results in forming smaller vortex regions, and then decreases the air flow resistance. Meanwhile, both of wetted perimeter and heat exchange area extend because of the elliptic cross section, which declines the internal thermal resistance of the pipe. Coupled with the high coefficient of heat transfer for elliptic-shaped pipes, the thermal exchanging performance is improved effectively. Therefore, increasing the number of coiler enables to cool the outside air down to 13℃ by effective utilization of 10℃/20℃ freezing water, and the air resistance is also controlled in a suitable range.

There are three advantages through applying air-conditioning unit with an elliptic-shaped fin type heat exchanger. It utilizes the medium temperature of chilled water, decreases supply air temperature and raises evaporating temperature. The three strengths are listed as follow:

(1) Energy consumption of circulating pump declines markedly, because using chilled water in this system makes a high temperature difference to 10℃. Compared with the traditional temperature difference (about 5℃), the higher one is conducive to low energy consumption.

(2) Small building spaces are needed to install the unit. The lower supply air temperature of 13℃, compared with the conventional supply air temperature of 18℃, reduces air output and achieves a small air duct.

(3) Energy efficiency ratio of the unit (COP) can be improved by decreasing work done during compression and input work of compressor. The temperature of the chilled water has an influence on the evaporating temperature of the unit, the high water temperature meaning the high evaporating temperature. A lower pressure difference experiences between evaporator and condenser, which makes compression ratio decline.

Inlet, the terminal device of air-conditioning system, supplies the treated air in the air-conditioning rooms directly. Diffusion properties at the position of downstream jet-flow are significantly influenced by the geometrical structures of the terminal devices. The way of air supply via induced air outlets is definitely efficient and qualified, though in 1970s induction unit was replaced by fan coil unit (FCU) for a variety of reasons. In recent years, Japan, the U.S. and many countries in the European continent have been tending to reuse this kind of unit because of the extensive attention of the related researchers and manufactures. Particularly, some national manufactures and engineers are of interests on it. As shown in Fig. 1.7, the unit system consists of plenum box, chamber, nozzles and rectification panel etc. Primary air treated by the intensive air conditioning unit is ejected by the nozzles through passing the plenum box. According to the venturi effect, a negative pressure zone is formed around the nozzles after ejecting and the differential pressure enables to induct the indoor return air to mix with the air in the negative pressure zone. Then the mixed air with moderate temperature is rectified through the rectification panel and blown in the indoor space at the speed of 0.2~0.8m/s from the strip typed opening. A high induction ratio designed in this system, the ratio of primary airflow rate to inducted airflow rate of 6:4, can decrease the speed of ejecting air out to achieve the mute

environment. Thereinto, the indoor air makes up 40% and the primary air accounts for 60% of the total mixed air.

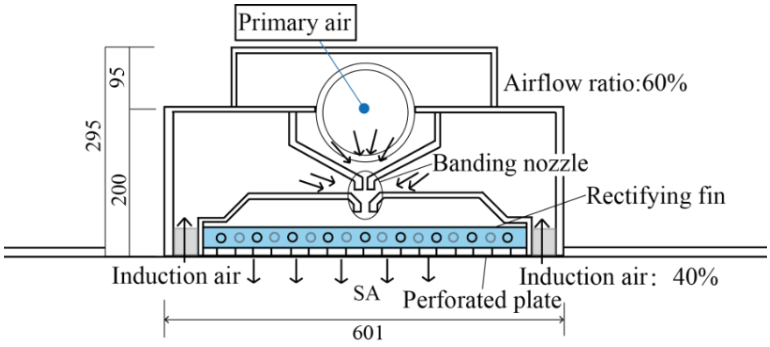

Fig. 1.7 CID system

In order to avoid the occurrence of dewing, much lower temperature is unreasonable for setting the air supply temperature of the air conditioning under cooling condition. The air supply temperature of traditional air conditioning, for example, is generally 16℃. In terms of CID system, the supplied air can be blown from the air-conditioning system with ceiling induction diffusers at 13℃. As the indoor air makes up 40% of the total mixed air, the primary air accounting for 60%, the temperature of the mixed air is determined by the temperature-weighted for the air proportions. For instance, the mixed air temperature of 18℃contains indoor air at 26℃and primary air at 13℃.

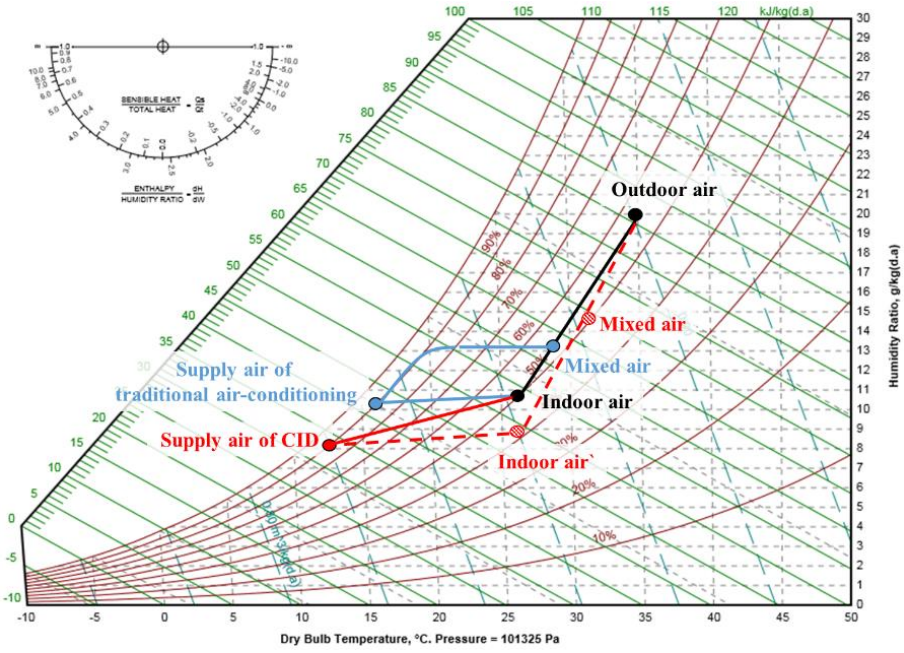

Fig. 1.8 Psychrometric chart

In order to avoid the occurrence of dewing, much lower temperature is unreasonable for setting the air supply temperature of the air conditioning under cooling condition. The air supply temperature of traditional air conditioning, for example, is generally 16℃. In terms of CID system, the supplied air can be blown from the air-conditioning system with ceiling induction diffusers at 13℃. As the indoor air makes up 40% of the total mixed air, the primary air accounting for 60%, the temperature of the mixed air is determined by the temperature-weighted for the air proportions. For instance, the mixed air temperature of 18℃ contains indoor air at 26℃ and primary air at 13℃. According to the Fig.1.8， it's obvious that the enthalpy difference between the supply air and the indoor air of CID system is larger than that of traditional air conditioning. In the figure, the red ones represent the CID system and the blue ones represent the traditional air-conditioning system. When the two systems show the same total heat capacity, the airflow rate of CID system is reduced and fan power is reduced accordingly. Therefore, condensation-free energy saving is facilitated in the CID system.

There are four main advantages as follows:

Convection is the useful way that achieves to induce indoor air having a good effect. All air induction unit enables to mix partial return air before fresh air is supplied, which increases the volume of air supply and multiplies indoor air changes. Air supply temperature difference shrinks due to the way of induced draught, hence the uncomfortable shock caused by large temperature difference is eliminated. Indoor environmental comfort of non-blowing feeling can be created through induce indoor air and rectify air supply which dispel individual feeling of air flowing. This comfortable indoor environment attributes to the improved inducted unit with big area of air duct, reasonable ratio of primary airflow rate to inducted airflow rate and low speed air supply through the trepanning on the rectification panel.

Small size blast pipe saves much more raw material and space than traditional all-air system. It benefits from the end device of ceiling inducer improved efficiently, the compact structure of equipment as well as the flexible layout that only fresh air ducts and a few air exhaust pipes needs to be arranged for air supply system in ceiling. Some buildings with strict restrictions to the space of air supply unit can take into account this kind of system, when they rebuild or renovate. And this improved system is also appropriate for some silence demanding places, because the design that remove draught fans and supply air at a low speed is conducive to indoor noise controlling. Integration of installing the air-conditioning equipment and illuminators in

ceiling can save installation cost, and the heat quantity released by fluorescent lamps would have a utilization of winter heating and reheat in summer.

The steadiness of system is able to put the technology of low temperature air supply with large temperature difference into practical service, and the problem of condensation of moisture is solved. Through inducing hybrid cool air is supplied at 19℃ as rectifier air, the temperature of supplying air is far higher than the indoor dew-point temperature. Therefore, the phenomena of condensation and dewfall, leaking water and breeding bacterium etc. hardly happen.

This improved induced system makes energy saving come true. Induction chamber takes effectively use of the indoor afterheat carried by induced air to reheat the primary air that is about 13℃. The energy consumption of reheater declines effectively, and mixing part of indoor return air during air supplying achieves the energy saving because of small airflow rate of air to be treated.

1.5 The current study of the hospital

Known and recognized concept of hospitals as places of treatment and recuperation can date back to the past two centuries. Hospitals are primarily a place for people to recover from illness, disease and injury, where patients as well as medical staff require improved environmental quality that facilitates to enhance the efficient of recovery and increase productivity. Hygiene and indoor air quality are the main indicators to assess the environmental level for hospitals currently, because patients probably suffer new infections during the healing process and bad smell would have influence on medical staff. The existing references show that previous studies focused on the indoor environment of hospital to obtain or seek the suitable and reasonable indexes for indoor environment.

1.5.1 The meaning of indoor environmental quality in hospitals

Compared with others public buildings, there is a relative higher rate of human occupancy in an average ward, where 2~4 patients live in one room with 20~30m^2. Regarding to the patients, it is very important to control respiratory disease transmission (Tang et al. 2006)[1-4)], which has been proved to be one of main reasons for the outbreak of the Severe Acute Respiratory Syndrome (SARS) in 2003 (Li et al. 2004)[1-5)]. Poor environmental conditions of wards would delay recovery times of patients or even cause deterioration. The latent crises include cross-

infection, viruses breeding, insanitary environment and so on. The undesired consequences result in the waste of medical resource and severe psychological stress for patients. The existing research results have found that a suitable indoor air climate can shorten the patients' length of stay at hospital (Azizpour et al. 2011)[1-6].

Medical staff are also influenced by the indoor environment of sick-rooms. Inferior quality of indoor environment would lead to some uncomfortable feelings and make people upset. Inappropriate temperature, bad smells, lack of fresh air probably distract them, as they take care of patients at wards. Therefore, working in comfortable conditions benefits both productivity and performance of medical staff (Parsons K.C. 2003)[1-7].

1.5.2 The current study on indoor environmental quality in hospitals

In order to learn about and improve the conditions of wards and office rooms in hospitals, many researchers have studied the indoor environment of hospitals. Several corresponding standards and codes have been established to ensure the beneficial indoor environment for patients.

ASHRAE Applications Handbook (ASHRAE 2003)[1-8] recommended several factors that can estimate the indoor environment of healthcare buildings. Temperature, relative humidity, minimum air changes per hour and some others were taken into consideration in this criterion. The indoor environment is considered comfortable for inpatients as well as can minimize the spread of contamination, as these factors show appropriate values. Kameel and Khalil (2006)[1-9] stated that air temperature and relative humidity can influence the breeding and transmission of germs, and infection control as well as comfort can be achieved by adjusting these two factors. In the light of hospital indoor environment, Sutida S. et al. (2017)[1-10] concluded that healthcare occupants in Thai hospitals (tropical region) prefer slightly colder temperature than neutral. Specifically, the acceptable temperature ranges for patients, visitors, and caregivers are at 21.8–27.9℃, 22.0–27.1℃, and 24.1–25.6 ℃ respectively. A questionnaire about the subjective responses on thermal environment given by patients and medical staff has been finished in a hospital in winter (Hashiguchi et al., 2008)[1-11]. The survey indicated that introducing humidifiers in hospitals during winters can alleviate the discomfort for staff. (Balaras et al., 2007)[1-12] focused on the indoor thermal conditions in hospital operating rooms, which require efficient HVAC installations to achieve the demanding indoor environmental conditions. However, referring to the various international standards, regulations and guidelines, the

majority of the audited subjects in this study did not conform to the strict optimum indoor thermal conditions.

And the existing study also gives attention to the contaminants in hospitals. (Wang et al., 2006)[1-13] collected the indoor air PM2.5 and PM10 samples from the different types of indoor environment in the four hospitals and their adjacent outdoor environments in Guangzhou, China, during the summertime. Indoor organic carbon concentrations were much higher than outdoors, which might be due to volatile organic matters emissions from indoor sources such as the extensive use of detergent, disinfectant and preservative inside the hospitals. (Mendes et al. 2015) [1-14] monitored the PM10, PM2.5 as well as some others harmful substance in 22 elderly care centers (ECCs) of Portugal. The overall PM2.5 mean concentration of the 22 ECC was above international reference levels, and maintaining natural and passive ventilation could provide health benefits to ECC inhabitants and medical staff.

An efficient air conditioning system for sickrooms in hospitals is essential. It not only can provide the high comfortable environment to recover, also can reduce the concentration of bacteria and contaminants. Making suitable air conditioning systems serve in hospitals has aroused extensive interests and concerns of public.

1.6 Purpose and scope of this study

In this study, the practicability and validity for using CID in hospitals will be examined through several series of experiments. Energy saving, eliminating smell of body odor and reasonable air flow from air conditioning are the main factors when make the experimental designs and plans. The experiments will be conducted in a simulation sickroom where the size and the display accord with the real one. Some indicators related to the indoor environment quality of ward will be collected and analyzed, such as indoor temperature, the concentration of contaminants and local mean age of air etc., under different conditions. The gauge points in the monitoring process will be widely arranged, including the horizontal and vertical distributions. The layout of device and decoration in the ward probably has influence on the indoor environment, therefore, these factors will also be considered in this study. In order to cater to the real environment of the ward, manikins who can exhale the gas with contaminants will be arranged in the simulation sickroom. Therefore, the concept of the gas mixture composed by carbon dioxide (CO_2) and helium (He) used as tracer gas, whose density is near to the air was proposed.

Moreover, as the existing methods for the calculation of age of air is inapplicable to the air conditioning system due to the returning air, the improved calculation method of local mean age of air based on tracer gas step-up method was proposed. Therefore, we adopted a modeling approach, making an assumption of the concentration response function and identifying a few parameters from the measured data in the certain local point, then the local mean age of air can be calculated numerically based on the least square method.

1.7 Composition of Dissertation

This thesis is composed of eight chapters in total. Fig. 1.9 illustrates the layout of the whole dissertation. The detailed composition of this thesis is shown as follow:

Chapter 1. Introduction

In this chapter, the background of chilled beam systems was presented, and the overview about indoor environment in hospitals was provided. The CID systems derived from chilled beams was introduced. Meanwhile, some existing studies and frontier research related to indoor air quality in hospitals were summarized. At last, the mechanism and principles of this type of system are elaborated and the main features of the induction units are introduced in this chapter.

Chapter 2. Measurements for Cooling Condition

With the purpose of studying CID Systems served in sickrooms, several series of experiments are conducted. In order to examine the practicability of CID system in the ward under the cooling condition, the corresponding experiments are conducted after the specific arrangement of the simulation sickroom. The exact design and layout of the simulation sickroom as well as the positions of gauging points are described and illustrated in this section. The experimental results on the indoor environment such as the temperature distribution, concentration distribution of contaminants and local mean age of air are analyzed. Air velocity and radiation are also the research targets of this chapter, and the corresponding discussion and conclusions are presented through analyzing the collected data during the experiments.

Chapter 3. Related Experiments under Heating Condition

Following the last chapter, the application of CID system in the ward under heating condition is also investigated. The experiments are conducted after modifying some parameters of device.

The collected data of the temperature distribution, concentration distribution of contaminants and local mean age of air under this condition are analyzed and discussed.

Chapter 4. Conclusion

Some conclusions based on experiments are drawn. This chapter summarizes the findings under both cooling condition and heating condition.

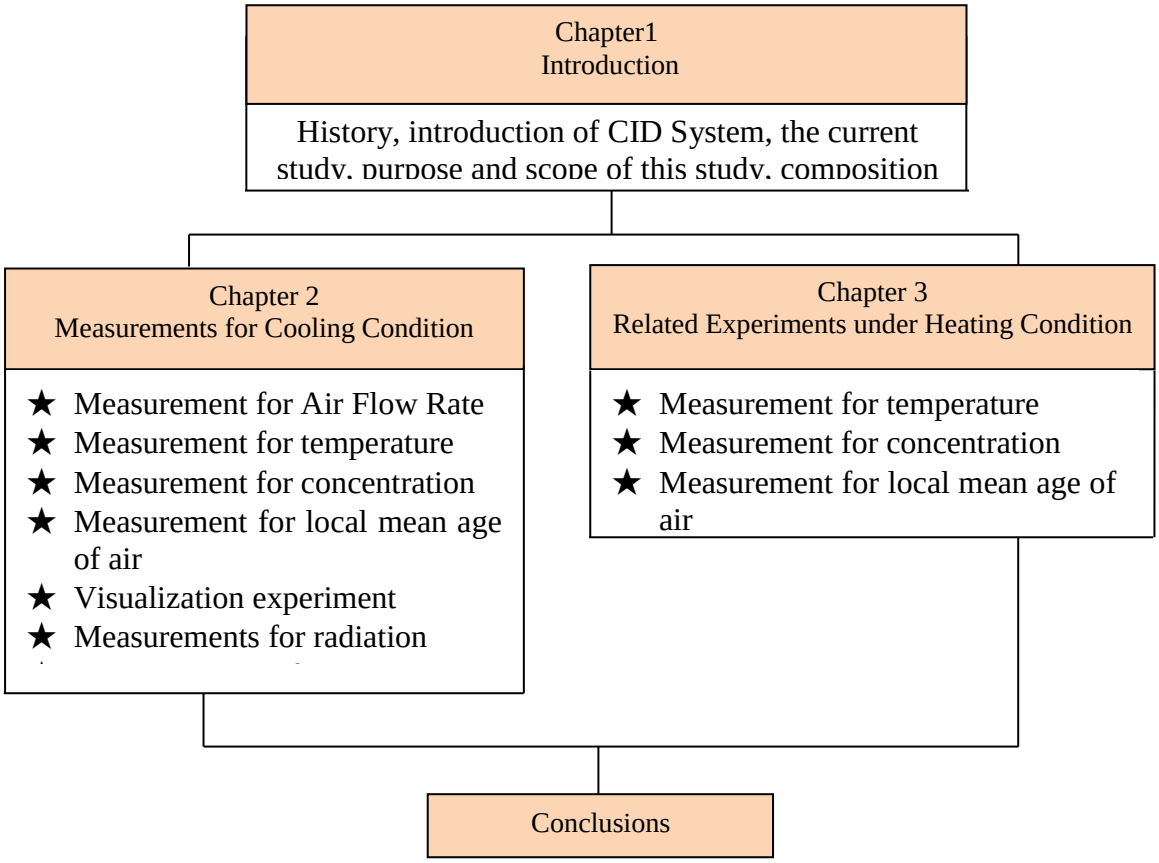

Fig. 1.9 Layout of dissertation

Chapter 2 MEASUREMENTS FOR COOLING CONDITION

2.1 Purpose of the experiments

In order to verify the characteristics of the air-conditioning system with ceiling induction diffusers, a series of experiments were carried out in a full scaled model room. It aimed at examining the relevant parameters which have effect on the following factors, including the distributions of indoor temperature, local mean age of air, contaminant concentration, air velocity and radiation. Meanwhile, the way that these parameters influenced the indoor environmental quality in a sickroom would be discussed.

2.2 Experimental set-ups

All of the experiments were conducted in a showroom of KIMURA KOHKI Corporation in Osaka Japan, which is a full scaled model room with four beds. It is divided into three parts, experimental room, corridor and control room. The operation of air conditioning can be controlled and air flow rate can be adjusted in the control room and equipment room in the northwest part of experimental room. The full view of experimental room is shown in Fig. 2.1.

Fig. 2.1 Full view of experimental room

The dimensions of the experimental room are 7.35m(d)×5.35m(w)×2.42m(h), as shown in Fig. 2.2 and Fig. 2.3. Polystyrene foam with the thickness of 15mm, which was used as insulation material, was pasted on the both north wall and east wall. Four beds were set in the experimental

room. Above each bed, a rectangular supply diffuser (1200mm×500mm) which contains a built-in induction panel was set on the ceiling.

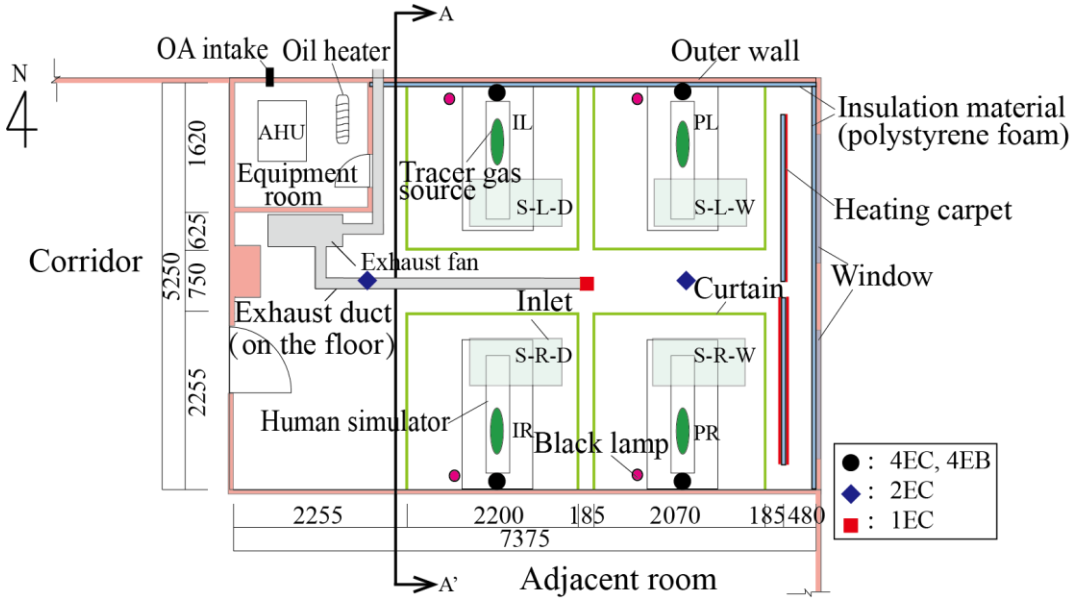

Fig. 2.2 Plan of experimental room [mm]

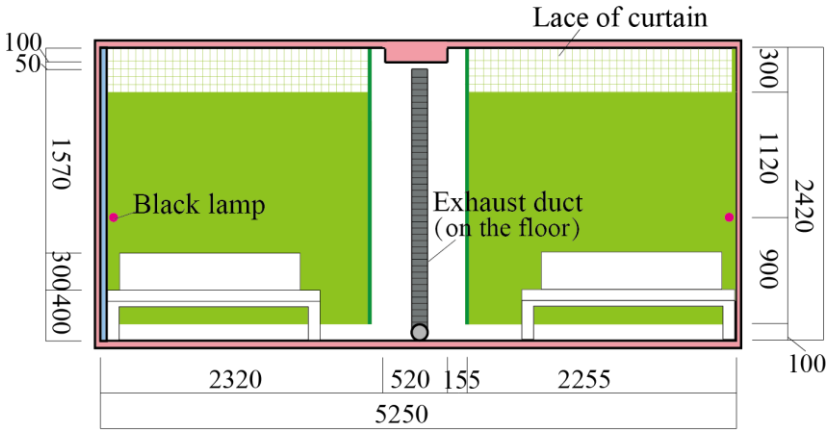

Fig. 2.3 A-A' Section of experimental room [mm]

Fig. 2.4 Exhaust fan

As shown in Fig. 2.4, the exhaust fan (BFS-80SC) produced by Mitsubishi Electric is set in the experimental room, and spiral ducts (φ150mm) are used as the exhaust ducts set in the experimental room. The plane positions of the exhaust ducts are displayed in Fig. 2.2, and the according heights are shown in Table 2.1. The whole test lasted for 19 days, ranging from November 7th, 2016 to November 25th, 2016.

Table 2.1 Positions of exhaust ports

No.	Item	Number of exhaust ports	Position of exhaust ports
A	4EC	4	50mm below the ceiling
B	4EB	4	1200mm above the floor on the wall
C	1EC	1	50mm below the ceiling in the middle of four beds
D	2EC	2	50mm below the ceiling at perimeter and interior side

As we assume that the air conditioning system is running during summer, the outdoor unit is covered with styrofoam in order to reduce the external air load. And the outdoor air temperature could reach to 32℃, due to the fact that the outdoor air was heated by three oil heaters in the equipment room, whose the total heat generation rate is 3300W. The oil heater is shown in Fig. 2.5. And Fig. 2.6 shows the simulated human used in the experiment.

Fig. 2.5 Oil heater in equipment room

Fig. 2.6 Simulated human

On each bed, we set a spiral duct (φ150mm, H1500mm) as a simulated human. We paste 10 meter long winding heating cable on the inner surface of each spiral duct, and cover them with polyester cloth. See Fig. 2.7 for inner surface of spiral duct details. Heat generation rate of each simulator was 40W, which meant one real patient provided the corresponding sensible heat load. Therefore, the total power was set as 160W by the slidac. Moreover, to simulate the breath of human, a PET bottle (φ＝50mm, h=300mm) was set on the center of upper half of each spiral duct. On each bottle, we punch 150 small holes (φ＝4mm) as the tracer gas generation source

and cover the bottle with 10 millimeter thick sponge to restrict the speed of the emitted tracer gas, as shown in Fig. 2.8.

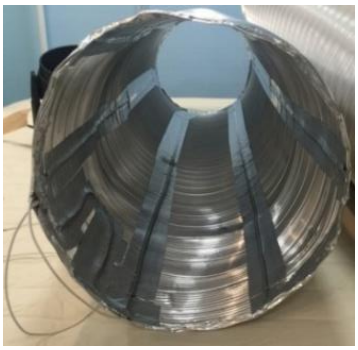

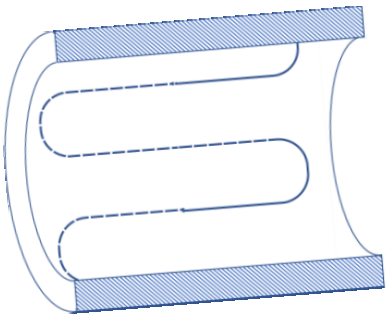

a) Inner surface of spiral duct b) Sectional view of spiral duct

Fig. 2.7 Details for spiral duct

Fig. 2.8 PET bottle

Fig. 2.9 Black lamp

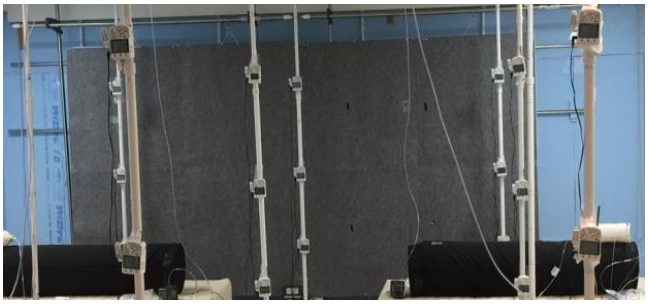

Fig. 2.10 Heating carpets (NU-204)

As shown in Fig. 2.9, black lamps were placed aside of each bed at the height of 1000mm, for imitating the heat generated by household appliances such as TV, refrigerator etc. The power of each lamp was 55W, and 220W-power was supplied by four lamps in total. There were four pieces of heating carpets (NU-204) produced by YAMAZEN Corporation to be pasted on the both sides of polyethylene foam, which function was to simulate the heat gain from windows, as shown in Fig. 2.10. The heat flux of them is controlled by Slidac (V-130-3). However, only three heating carpets (the heat generation rate of every heating carpet was 333.3W) worked normally during the experiment and the total heat flux was 1000W. One heating carpet placed in the inner of a wall was out of order during the experiment. Fig. 2.2 showed the three heating carpets which kept working during the experiment period.

2.3 Measurement for Air Flow Rate

Supply air flow and exhaust air flow were measured by tracer gas method. Carbon dioxide is used as tracer gas to measure air flow rate. In this measurement, CO_2 GAS ANALYZER (MI70, VAISALA), is used to measure and monitor CO_2 concentration. The picture of VAISALA is also shown in Fig. 2.11. Initially, step A, CO_2 is released in equipment room at the position of suction inlet of AHU (Air Handing Unit), marked as ★ in Fig. 2.12 (a). The concentration of supply air and air near the suction inlet, named as C_{SA} and C_e, respectively. Subsequently, step B, CO_2 is emitted in the exhaust duct, marked as ▲ in Fig. 2.12 (b). The concentration of exhaust duct and indoor air were measured and monitored by the same method, named as C_{EA} and C_i, respectively. Specifically, it takes three minutes to collect data at each measurement point.

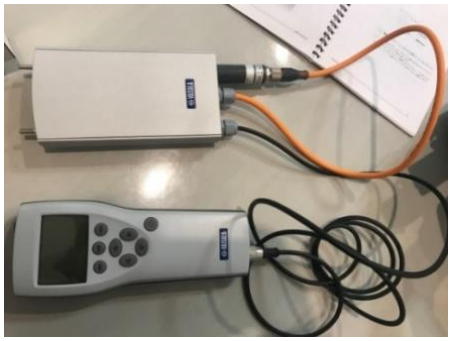

Fig. 2.12 Picture of VAISALA

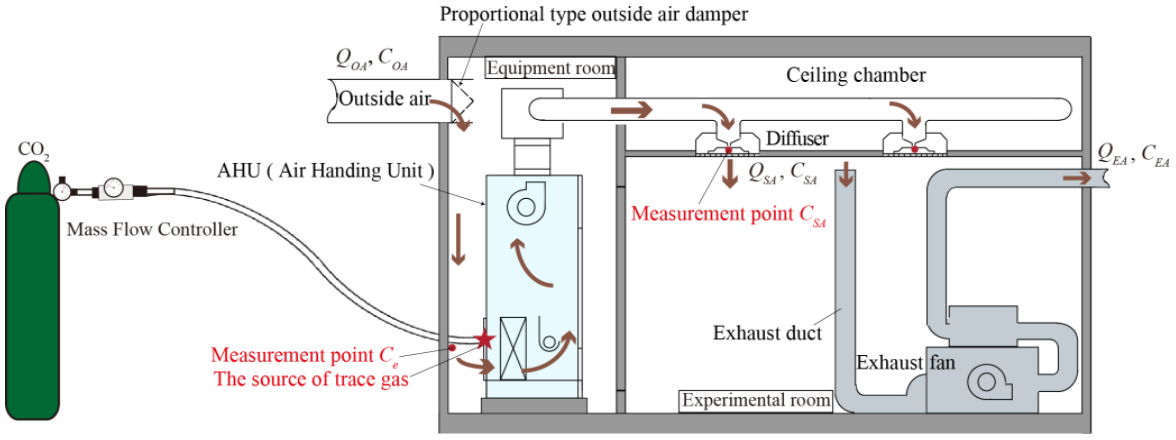

(a) Step A

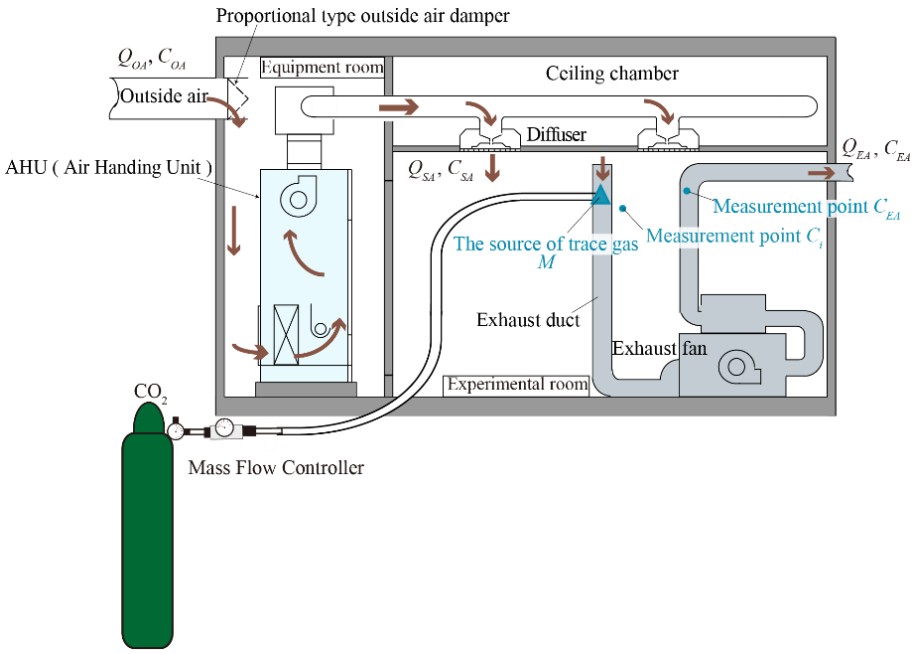

(b) Step B

Fig. 2.11 Measurement diagram for air flow rate

Since a part of tracer gas flowed into the equipment room through a gap between the door of the equipment room and the floor, the airflow rate of supply air can be calculated as equation (2.1):

$$Q_{SA}=\frac{M}{(C_{SA}-C_e)}\times\frac{(273+\theta_i)}{273} \tag{2.1}$$

The airflow rate of exhaust air can be calculated as equation (2.2):

$$Q_{EA}=\frac{M}{(C_{EA}-C_i)}\times\frac{(273+\theta_i)}{273} \tag{2.2}$$

Where, C_{OA}, C_{SA}, C_{EA} [ppm] is the concentration of outdoor air, supply air and exhaust air, respectively. C_e, C_i [ppm] is the air concentration near the suction inlet and indoor air concentration. Q_{OA}, Q_{SA}, Q_{EA} [m^3/h] is the air flow rate of outdoor air, supply air and exhaust air, respectively. M [m^3/h] stands for emission rate of tracer gas and θ_i [℃] is the temperature of indoor air.

As a result, supply air flow rate and exhaust air flow rate have constant rate at 450m^3/h and 380m^3/h, respectively. This discrepancy of supply and exhaust flow rate might be caused by the

returning air to the equipment room through the crack and the exfiltration flow through the other gaps.

2.4 Measurement for temperature, concentration and local mean age of air

2.4.1 Experimental set-up and measurement methods

The method of step-up tracer gas was applied, and the gas mixture (density is near to the air) composed by carbon dioxide (CO_2) and helium (He) was used as tracer gas. The flow rate of CO_2 and He was restricted at 1.5L·min^{-1} and 0.9L·min^{-1} by mass flow controller, respectively. See Fig. 2.13 for the gas mixture generator details.

Fig. 2.13 Picture of gas mixture generator

Table 2.2 Experimental conditions

Condition	Exhaust position	Positions of tracer gas generation	Curtains around bed
4EC-C-4B	4EC	4B	Closed
4EB-C-4B	4EB	4B	Closed
2EC-C-4B	2EC	4B	Closed
1EC-C-4B	1EC	4B	Closed
1EC-NC-4B	1EC	4B	Open
4EC-C-4D	4EC	4D	Closed
4EB-C-4D	4EB	4D	Closed
2EC-C-4D	4EC	4D	Closed
1EC-C-4D	1EC	4D	Closed
1EC-NC-4D	1EC	4D	Open

The main conditions under cooling are listed in Table 2.2. Moreover, the different positions of tracer gas source of 4B and 4D are shown in Fig. 2.14. 4B simulates the contaminant from four patients and 4D means that four diffusers are applied to release the testing gas for analyzing the distribution of local mean age of air. In addition, as shown in Fig. 2.15, around of each bed was outfit with a curtain and those beds were surrounded under the condition with curtain closed (marked with C). From Fig. 2.3, we can see that there are gaps because of the part of lace curtain, which is beneath the ceiling with the distance of 300mm. However, the gaps between the walls and curtains are blocked by adhesive tapes, in order to eliminate the influence on ventilation efficiency. In addition, the same experiments were conducted as curtains were removed, where the condition is named NC.

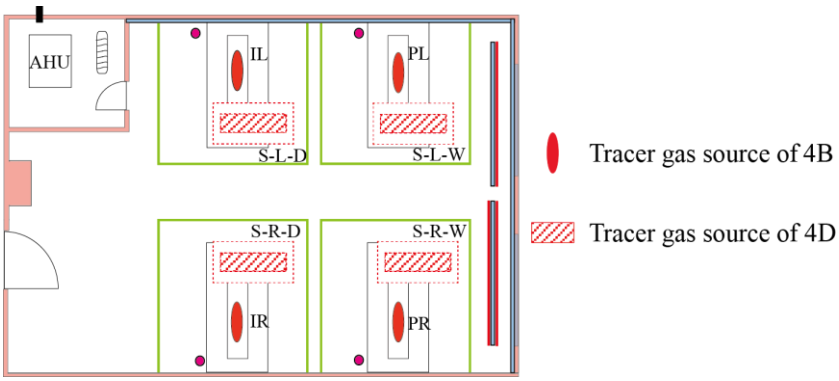

Fig. 2.14 Tracer gas source positions of 4B and 4D

Fig. 2.15 Condition with curtain closed

2.4.2 Measurement points

Wall surface temperature, indoor air temperature and CO_2 concentration were measured, when the indoor environment kept steady state. The measurement points of temperature and CO_2 concentration were given in Fig. 2.16~ Fig. 2.19. The values of wall surface temperature,

captured by T-thermocouple (φ=0.32mm, Data logger Cadac 3, Etodenki Corporation), were collected from 3 heights in a vertical line in the measurement positions W1-W9. It meant that 27 points were involved in testing wall surface temperature in total. In terms of indoor air temperature, the values of indoor air temperature were gotten from measurement positions P1-P12 and there were 11 points along each measurement position vertically, i.e. 128 points in total. It was worth mentioning that there were 10 measurement points at positions P1~P4 (there was no measurement point at the height of 2420mm) because of the existing of a beam. Measurement positions of CO_2 concentration were assigned at P1-P10 and it was measured at 4 points in every position vertically (40 measurement points in total) by CO_2 recorder (RTR-576, TR-76Ui, T&D Corporation). During the testing period, the instantaneous values were recorded per 30 seconds.

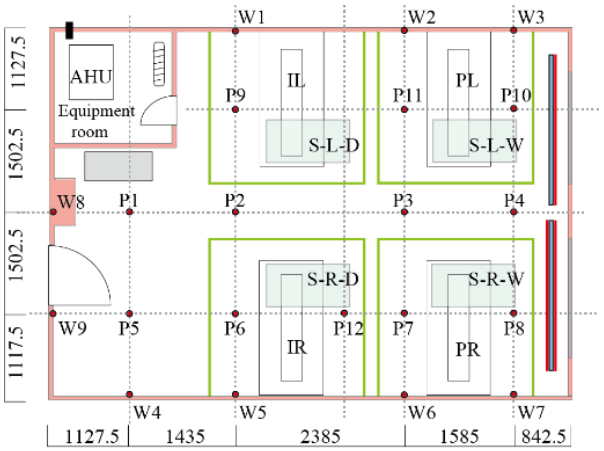

Fig. 2.16 Plane positions of measurement points [mm]

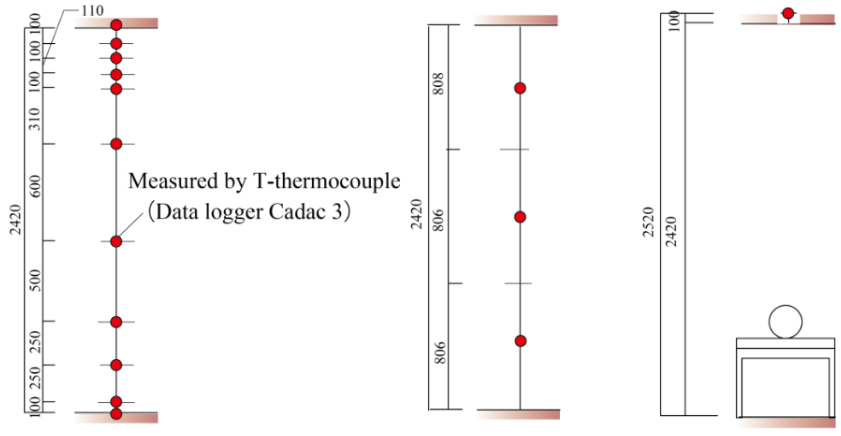

a) Air temperature b) Wall surface temperature c) Supply air temperature (SLW, SLD, SRW, SRD)

Fig. 2.17 Measurement points for temperature

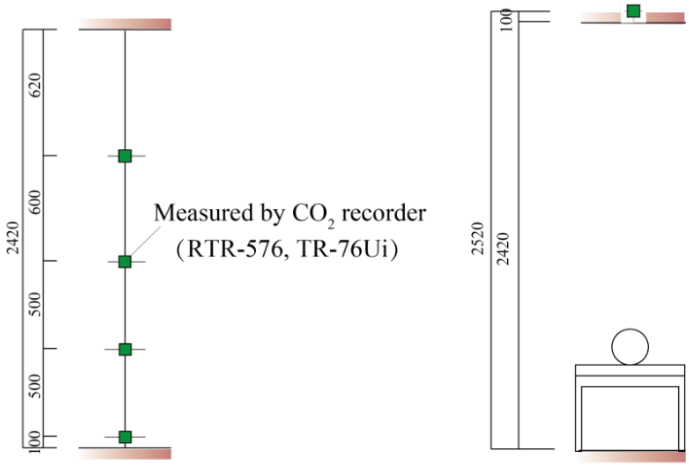

a) Air concentration b) Supply air concentration (SLW, SLD, SRW, SRD)

Fig. 2.18 Measurement points for concentration

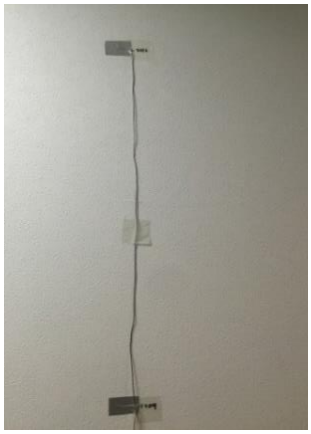

a) Measurement for indoor air temperature

b) Measurement for wall surface temperature

c) Measurement for supply air temperature

d) Measurement for indoor air concentration

e) Measurement for supply air concentration f) Measurement for outdoor air concentration

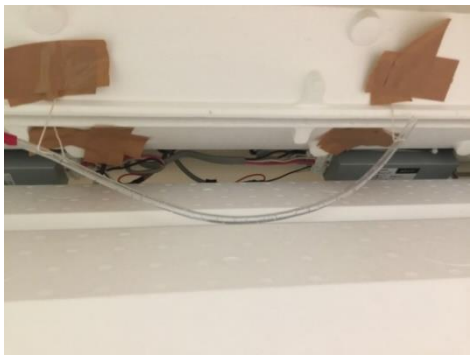

g) Measurement for exhaust air concentration h) Measurement for age of air

Fig. 2.19 Schematic diagram of each measurement point

2.4.3 Measurement instrument

The details information of measurement instruments are shown in Table 2.3.

Table 2.3 List of experiment instrument

Instrument	Manufacuturer	Amount
T-thermocouple		
Data logger (CADAC 3)	Etodenki Corporation	10
CO_2 recorder (RTR-576, TR-76Ui)	T&D Corporation	49
Mass flow controller (FCS-T1000L)	Fujikin	2
Read out model	Fujikin	2
Watt monitor (TAP-TST8N)	Sanwa supply	4
Slidac (V-130-3)	YAMABISHI Corporation	2
Mini pump (MP-Σ500N2)	SIBATA	6

Moreover, we can see the picture of experiment instruments in Fig. 2.20.

a) CO_2 recorder

b) Data logger (Cadac 3)

c) Mass flow controller

d) Read out model

e) Mini pump

f) Watt monitor

g) Slidac

Fig. 2.20 Experiment instruments

It takes about 3 hours from the start to the end of each measurement.

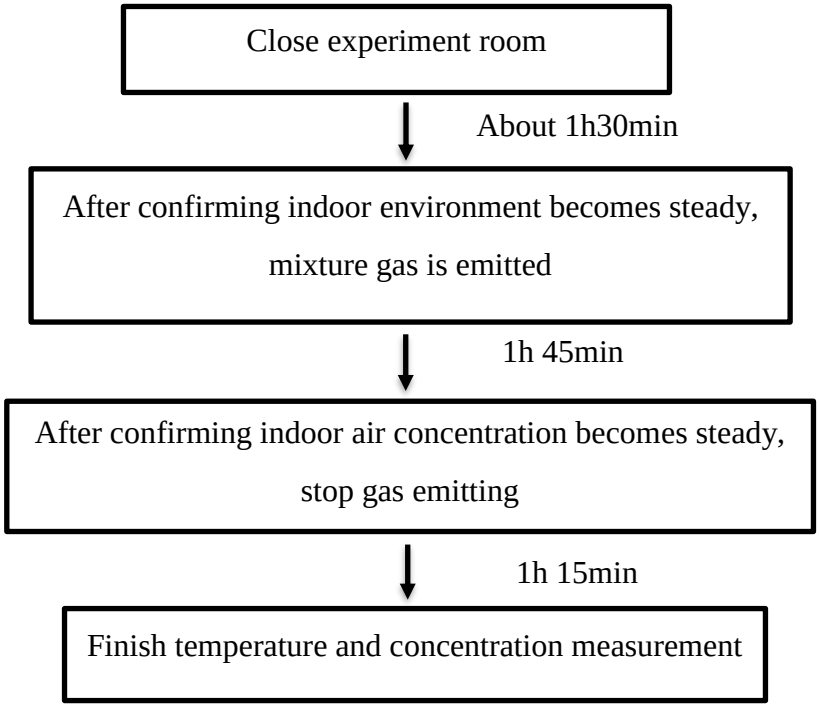

Fig. 2.21 Experiment flowchart

2.4.4 Result and analysis

2.4.4.1 *Temperature distribution*

In order to research how the parameters influence the vertical temperature distributions, we compare the temperature of experiments simulated the contaminants from patients. The vertical temperature distributions show the average temperature at each measurement point during measurement. The vertical axis of the graph is the height [mm], and the horizontal axis is the average temperature at each measurement temperature [°C].

2.4.4.1.1 Influence on vertical temperature distribution caused by the positions of exhaust ducts

Some experiments were carried out under the condition that the curtains were wrapping around the beds and the tracer gas is breathed out from four manikins. By changing the positions of the exhaust ports, these cases were studied. The differences between the two conditions are demonstrated in Table 2.4 and Fig. 2.22~ Fig. 2.25.

Table 2.4 Conditions for three cases

Condition	Exhaust position	Positions of tracer gas generation	Curtains around bed
4EC-C-4B	4EC	4B	Closed
1EC-C-4B	1EC	4B	Closed
2EC-C-4B	2EC	4B	Closed

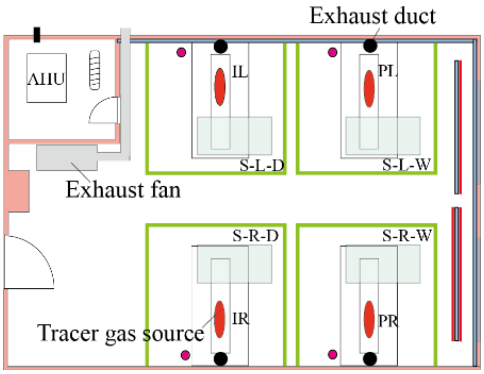

Fig. 2.22 Plan of experimental room
(Exhaust duct of 4EC)

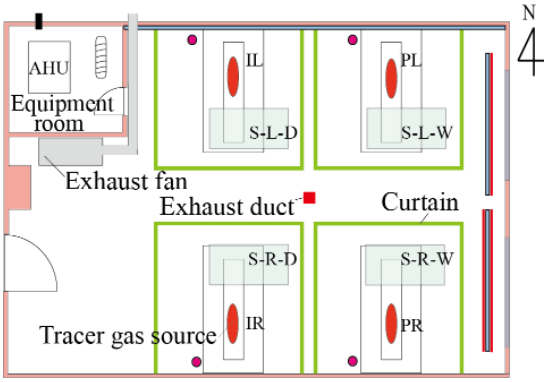

Fig. 2.23 Plan of experimental room
(Exhaust duct of 1EC)

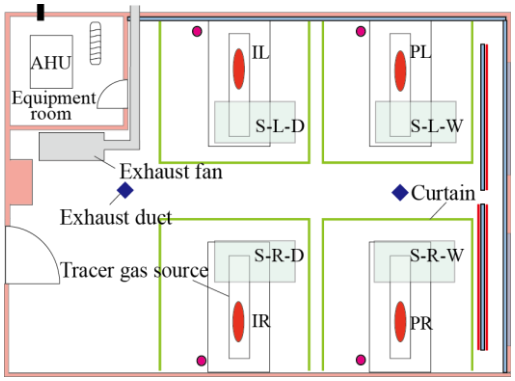

Fig. 2.24 Plan of experimental room
(Exhaust duct of 2EC)

The vertical temperature distribution was shown in Fig. 2.25. In detail, similar vertical temperature distributions were achieved in all cases. In the each of cases, the temperature gaps at the same position were no more than 3℃, which means that comfortable thermal environment was formed. The temperature gaps among the cases were caused by the different outdoor air temperatures probably, where the outdoor air temperature of condition 4EC-C-4B conducted on 11th, Nov., 2016 is 16.0℃ and condition 2EC-C-4B on November 21st and condition 1EC-C-4B on November 24th is 17.2℃and 12.5℃, respectively.

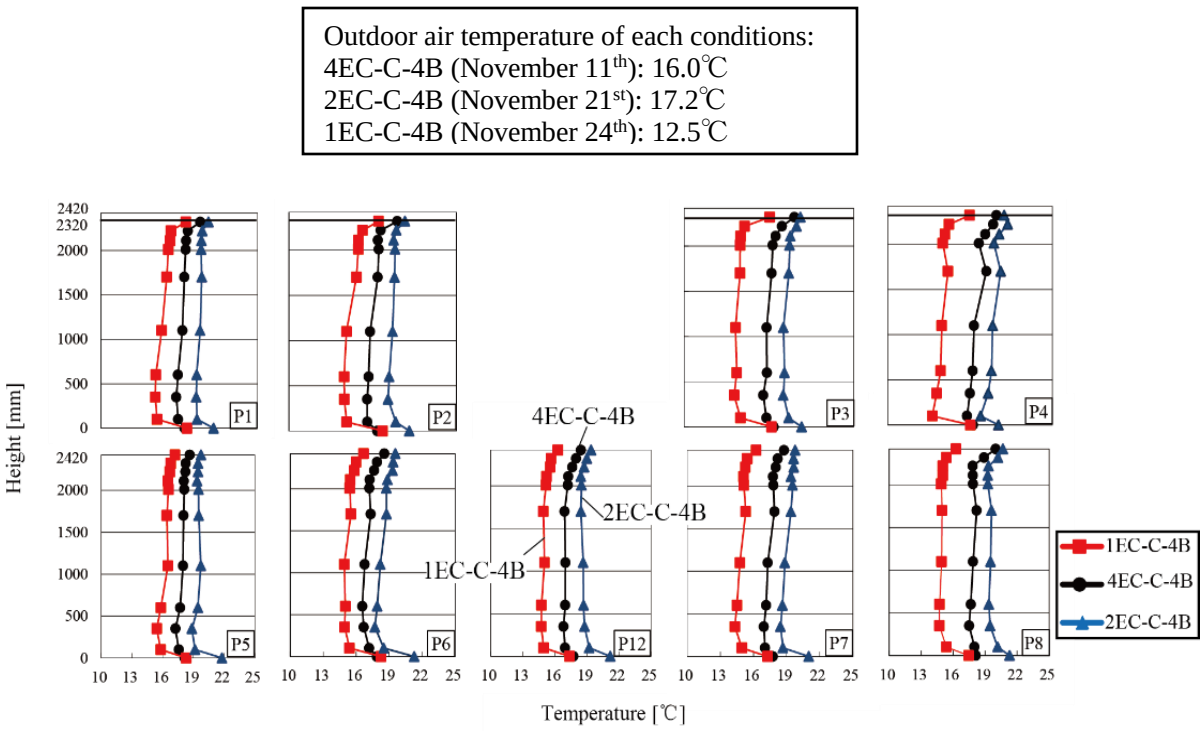

Fig. 2.25 Vertical temperature distributions
(Contaminant source position: 4B, with curtain, position of the exhaust ports: 4EC, 2EC and 1EC)

2.4.4.1.2 Influence on vertical temperature distribution caused by the height of the exhaust ports

In order to research how the height of the exhaust ports had an effect on the vertical temperature distributions and normalised concentration distributions, the other two factors kept fixed (curtains wrapped the beds and tracer gas breathed out of the manikins). Meanwhile, the height of the exhaust ports were designed at two different positions: underneath the ceiling 50 and 1200 mm above the floor, as shown in Table 2.5 and Fig. 2.26~ Fig. 2.27.

Table 2.5 Condition for mentioned cases

Condition	Exhaust position	Positions of tracer gas generation	Curtains around bed
4EB-C-4B	4EB	4B	Closed
4EC-C-4B	4EC	4B	Closed

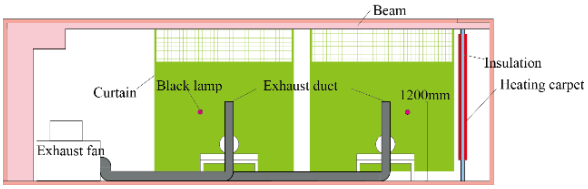

Fig. 2.26 Section of experimental room (Exhaust duct of 4EB)

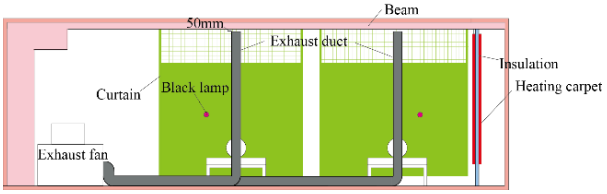

Fig. 2.27 Section of experimental room (Exhaust duct of 4EC)

Vertical profiles of temperature were shown in Fig.2.28. The outdoor air temperature of the two conditions is almost the same, with 16.0℃ (condition of 4EC-C-4B conducted on November 11th) and 15.6℃ (condition of 4EB-C-4B on November 27th), respectively. The similar vertical temperature distribution was collected both in the two cases. There was hardly temperature difference between the two cases except for the positions P3, P4, P7, and P8, which were located near to window.

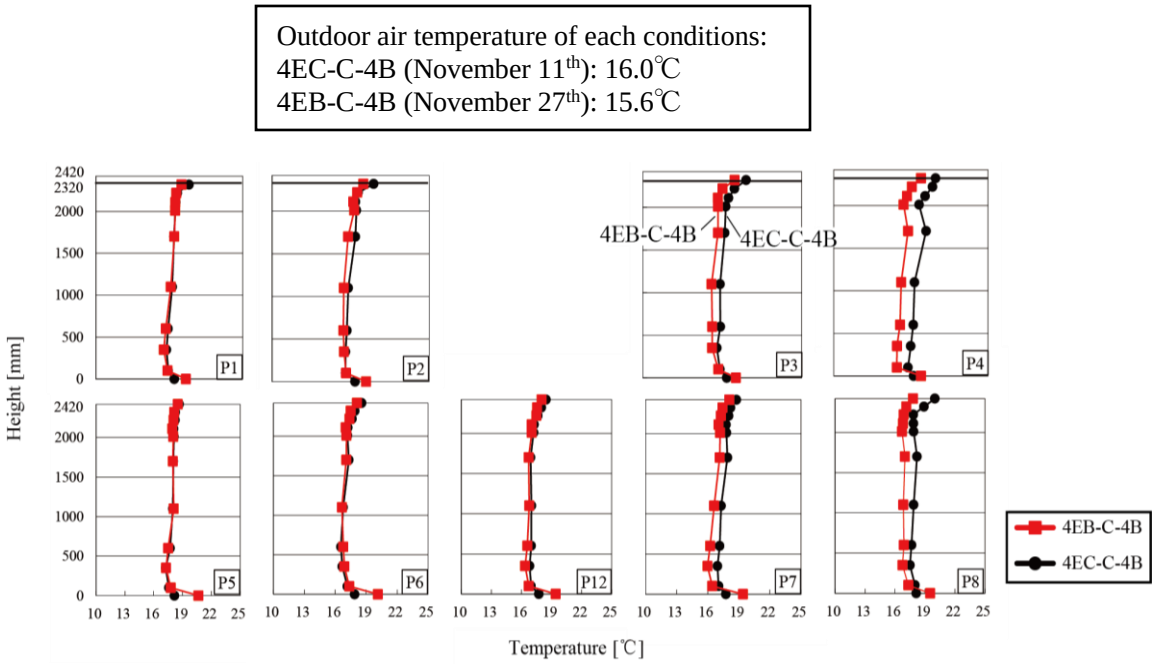

Fig. 2.28 Vertical temperature distributions
(Contaminant source position: 4B, with curtain, position of the exhaust ports: 4EC and 4EB)

2.4.4.1.3 Influence on vertical temperature distribution caused by curtain

Compared with case 4 and case 5, the only difference between them is the situation of curtain, which was demonstrated in Table 2.6 and Fig. 2.29~ Fig. 2.30.

Table 2.6 Condition for mentioned cases

Condition	Exhaust position	Positions of tracer gas generation	Curtains around bed
1EC-C-4B	1EC	4B	Closed
1EC-NC-4B	1EC	4B	Open

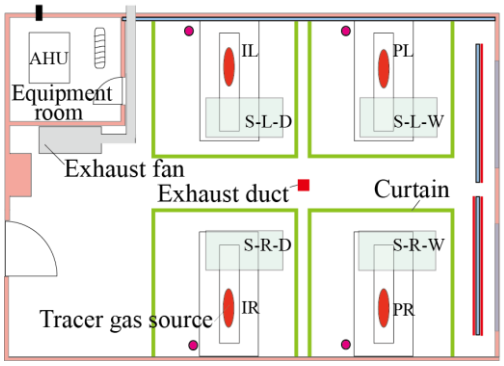

Fig. 2.29 Plan of experimental room (Exhaust duct of 1EC, with curtain)

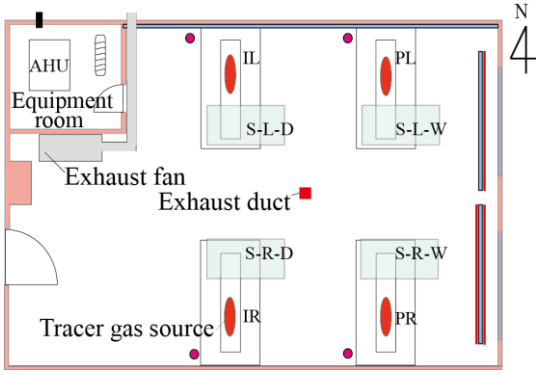

Fig. 2.30 Plan of experimental room (Exhaust duct of 1EC, without curtain)

Outdoor air temperature of each conditions:
1EC-C-4B (November 24th): 12.5℃
1EC-NC-4B (November 25th): 13.3℃

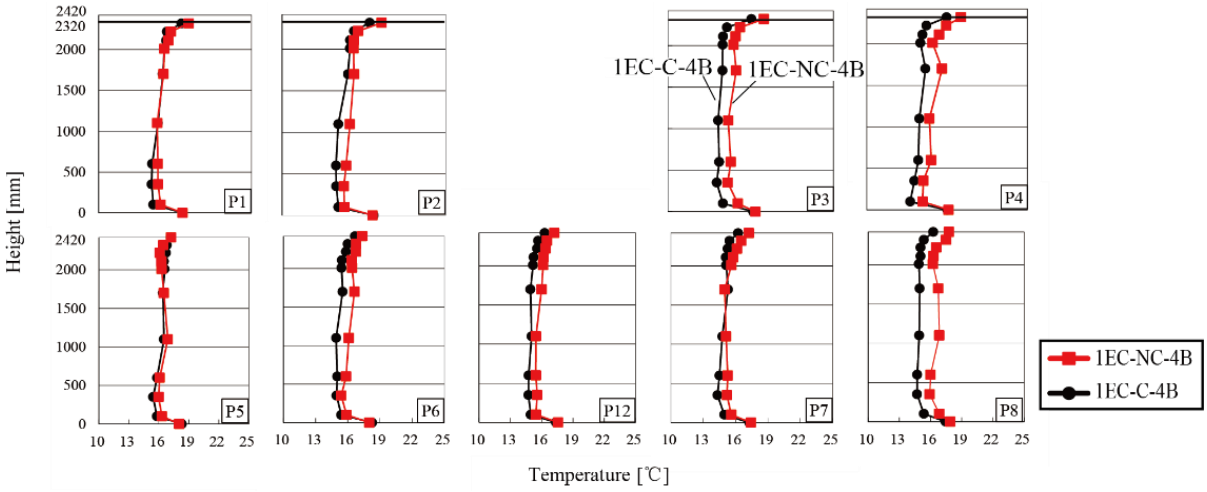

Fig. 2.31 Vertical temperature distributions (Contaminant source position: 4B, position of the exhaust ports: 1EC, with and without curtain)

2.4.4.2 *Concentration distribution*

It can be seen, from Fig. 2.32, a part of tracer gas breathed out of the manikins and then flowed into the equipment room through the crack between the door of the equipment room and the floor. Meanwhile, the ratio of tracer gas remaining in the experimental room was defined as η_r.

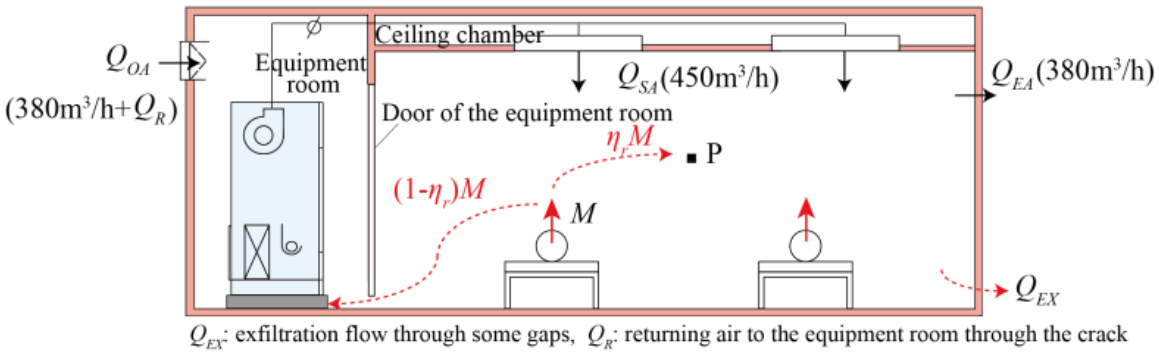

Fig. 2.32 Flow path of tracer gas (tracer gas breathed out of the manikins)

As the result, the concentration of supply air increased. Since the concentration of CO_2 was collected by CO_2 recorder in the experiment, in order to eliminate errors during the process of measurement, CO_2 recorders were calibrated after finishing data collecting, where the data obtained would be used to process experimental data. Seal CO_2 recorders in a polyethelene bag followed by injecting calibration gas into the bag. Three groups of experiments were conducted with different concentration of span gas, 500ppm, 1000ppm and 1500ppm respectively. Values of CO_2 concentration were recorded, when there was no obvious fluctuation during the experiment. Created calibration lines for CO_2 recorders based on the correct gas concentration. These calibration lines are important data to revise the measured concentration. It is an effective way to ensure measurement accuracy.

According to the Equation (2.3), the standardised concentration could be calculated. It is worthy to mention that the equipment room and the ceiling chamber were excluded from the experimental system.

$$C_{OA}Q_{OA} + (1-\eta_r)M = C_{SA}Q_{SA} \tag{2.3}$$

$$Q = Q_{SA} \tag{2.4}$$

Based on the formula (2.3), (2.4), the value of h_r can be calculated as formula (2.5) and shown in Table 3.4.

$$\eta_r = 1 - \frac{(C_{SA} - C_{OA})\ Q}{M} \tag{2.5}$$

Where, C_{OA}[ppm] is the concentration of outdoor air and C_{SA}[ppm] is the concentration of supply air, Q_{OA}, Q_{SA}[m^3/h] is the airflow rate of outdoor air and supply air, respectively, M [m^3/ h] stands for emission rate of tracer gas and h_r was the ratio of tracer gas distributed in the experimental room.

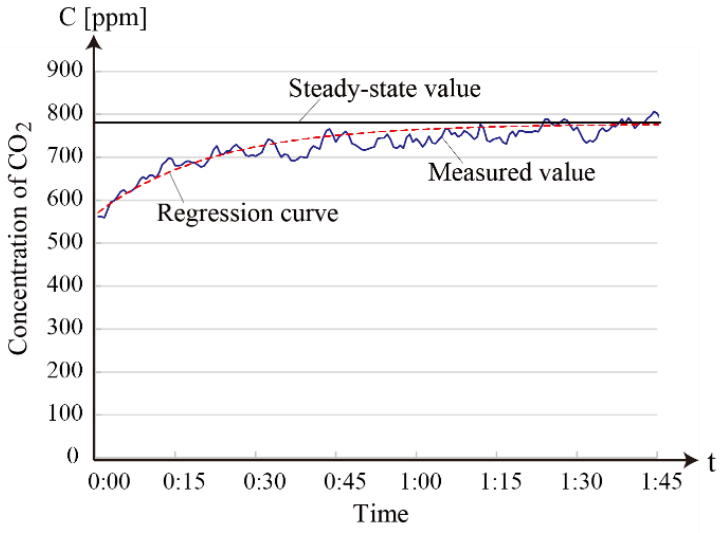

Fig. 2.33 Steady-state concentration

Fig.2.33 illustrated how the steady-state concentration (*Cp*) was calculated by an exponential function, which was a needed parameter in Equation 2.6. And according to the Equation 2.6, the standardised concentration could be calculated. It is worthy to mention that the equipment room and the ceiling chamber were excluded from the experimental system.

$$C_n = \frac{C_p\text{-}C_{SA}}{\frac{\eta M}{Q}} = \frac{C_p\text{-}C_{SA}}{\frac{M}{Q} + C_{OA}\text{-}C_{SA}} \tag{2.6}$$

Meanwhile, the ratio of tracer gas remaining in the experimental room was defined as η_r, which value can be worked out from the Equation 2.6. The values of η_r were shown in Table 2.7.

Normalised concentration distributions in vertical profiles were shown in Fig. 2.34~ Fig. 2.43. Due to the symmetry, the normalised concentration distributions at P1–P8 were shown in this part.

Table 2.7 The values of η_r

Item	Condition	η
Case 1	4EC-C-4B	0.48
Case 2	4EB-C-4B	0.53
Case 3	2EC-C-4B	0.38
Case 4	1EC-C-4B	0.36
Case 5	1EC-NC-4B	0.32
Case 6	4EC-C-4D	0.49
Case 7	4EB-C-4D	0.49
Case 8	2EC-C-4D	0.42
Case 9	1EC-C-4D	0.42
Case 10	1EC-NC-4D	0.33

2.4.4.2.1 Influence on normalized concentration distribution caused by the positions of exhaust ducts

Some experiments were carried out under the condition that the curtains were wrapping around the beds and the tracer gas is breathed out from four manikins. By changing the positions of the exhaust ports, these cases were studied. The differences between the two conditions are demonstrated in Table 2.8 and Fig. 2.34~ Fig. 2.36.

Table 2.8 Conditions for three cases

Condition	Exhaust position	Positions of tracer gas generation	Curtains around bed
4EC-C-4B	4EC	4B	Closed
1EC-C-4B	1EC	4B	Closed
2EC-C-4B	2EC	4B	Closed

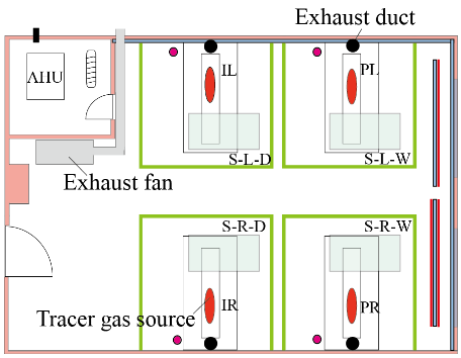

Fig. 2.34 Plan of experimental room
(Exhaust duct of 4EC)

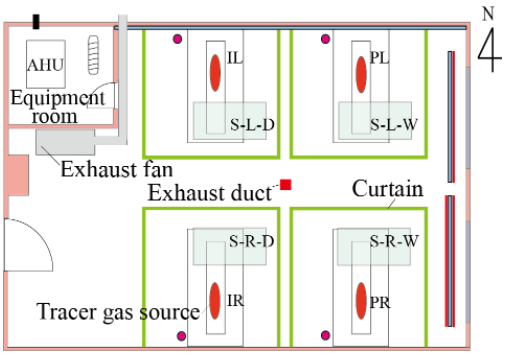

Fig. 2.35 Plan of experimental room
(Exhaust duct of 1EC)

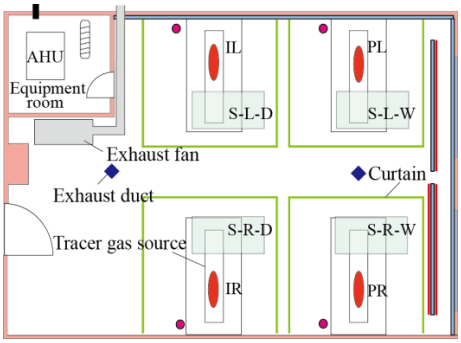

Fig. 2.36 Plan of experimental room
(Exhaust duct of 2EC)

The normalized concentration distribution was shown in Fig. 2.37.

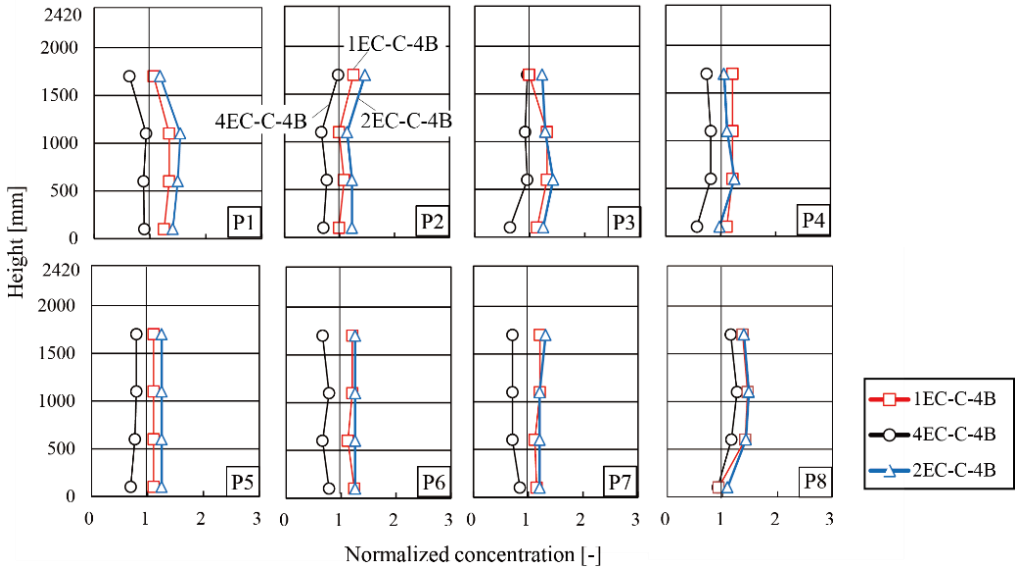

Fig.2.37 Normalized concentration distributions
(Contaminant source position: 4B, with curtain, position of the exhaust ports: 4EC, 2EC and 1EC)

Fig. 2.37 provided some noteworthy data with respect to the vertical concentration distributions. At the beginning of the testing, respectively, outdoor air concentration and the exhaust concentration were defined as 0 and 1. It was clear from the subgraphs that CO_2 spread to the entire room uniformly. It can be seen that the value of normalized concentration in the case 1 was smaller than that of in the other two cases. This showed that contaminants can escape out of the room adequately, as long as the exhaust ports were designed appropriately. For example, the position near the bed was the optimum choice which was the sources of the odor gas.

2.4.4.2.2 Influence on normalized concentration distribution caused by the height of the exhaust ports.

In order to research how the height of the exhaust ports had an effect on the normalized concentration distributions, the other two factors kept fixed (curtains wrapped the beds and tracer gas breathed out of the manikins). Meanwhile, the height of the exhaust ports were designed at two different positions: underneath the ceiling 50 and 1200 mm above the floor, as shown in Table 2.9 and Fig. 2.38~ Fig. 2.39.

Table 2.9 Condition for mentioned cases

Condition	Exhaust position	Positions of tracer gas generation	Curtains around bed
4EB-C-4B	4EB	4B	Closed
4EC-C-4B	4EC	4B	Closed

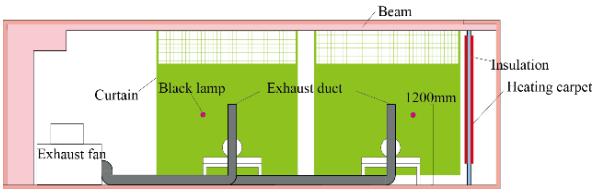

Fig. 2.38 Section of experimental room (Exhaust duct of 4EB)

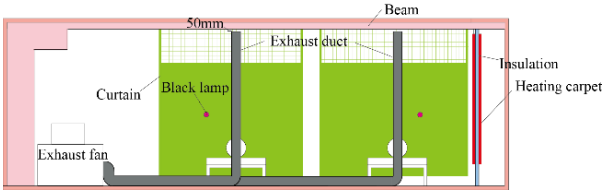

Fig. 2.39 Section of experimental room (Exhaust duct of 4EC)

Furthermore, according to the charts in Fig.2.40, there was no large difference for normalized concentration among all of the measurement points except for P2, P3, and P8. In general, the normalized concentration of exhaust port labelled 4EB was smallest. According to the relevant statistics, it can be concluded that the contaminant will be emitted out of the room more efficiently if the exhaust port is closer to the source of gas generation.

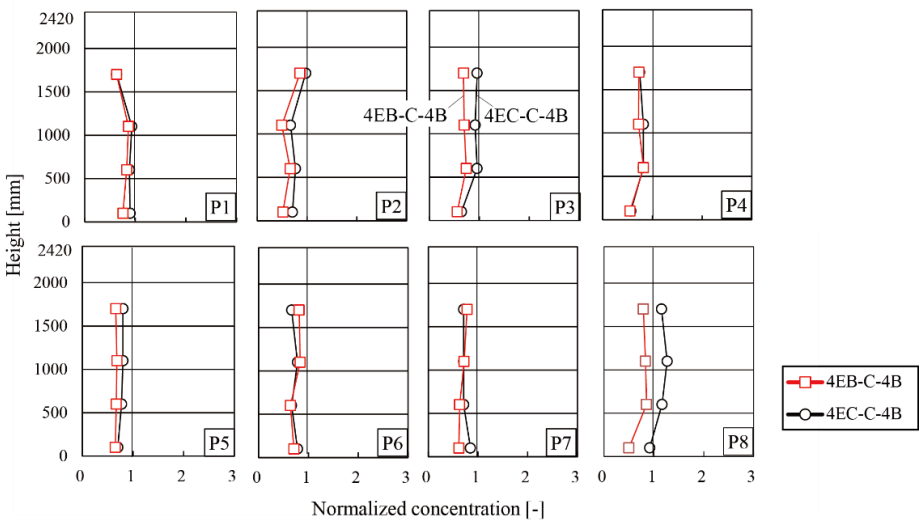

Fig. 2.40 Normalized concentration distributions
(Contaminant source position: 4B, with curtain, position of the exhaust ports: 4EC and 4EB)

2.4.4.2.3 Influence on normalized concentration distribution caused by curtain

Compared with case 4 and case 5, the only difference between them is the situation of curtain, which was demonstrated in Table 2.10 and Fig. 2.41~ Fig. 2.42.

Table 2.10 Condition for mentioned cases

Condition	Exhaust position	Positions of tracer gas generation	Curtains around bed
1EC-C-4B	1EC	4B	Closed
1EC-NC-4B	1EC	4B	Open

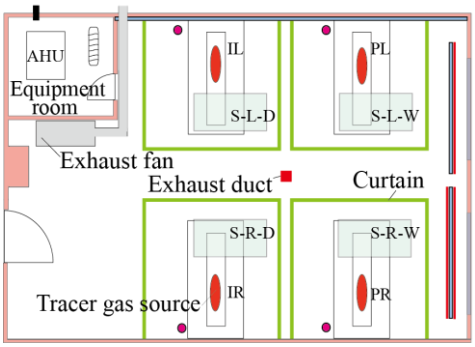

Fig. 2.41 Plan of experimental room
(Exhaust duct of 1EC, with curtain)

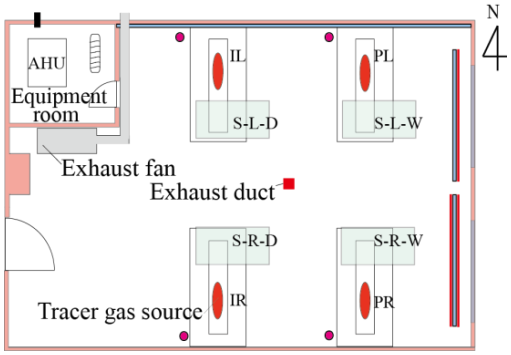

Fig. 2.42 Plan of experimental room
(Exhaust duct of 1EC, without curtain)

In addition, Fig. 2.43 illustrated the normalized concentration distributions in cases 4 and 5. The values of normalized concentration were close to 1 in both cases, but an obvious rising

appeared at P7 and P8 caused by the nearby contaminant source. It can be known that there was a slight difference in the aspect of normalized concentration when the measuring points were placed nearby the contaminant source and inside of the curtains. It meant when in patients panted, the curtains around the bed would prevent the contaminant escaping out.

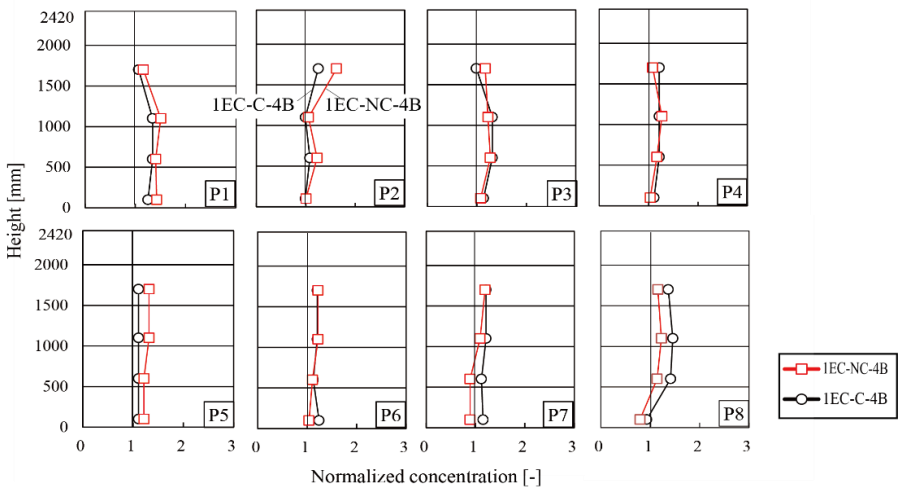

Fig. 2.43 Normalized concentration distributions
(Contaminant source position: 4B, position of the exhaust ports: 1EC, with and without curtain)

2.4.4.3 *Local mean age of air*

2.4.4.3.1 Measurement method

Injecting some tracer gas to experimental room and measuring the consequent concentration change is an effective way to estimate local mean age of air. Typically, three injection methods are widely used: pulse method, tracer gas step-up method and step-down method.

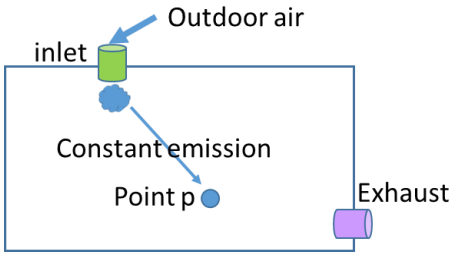

Fig. 2.44 Traditional air conditioning system without returning air

Tracer gas step-up method makes a certain amount of tracer gas be injected from the inlet duct and reaches a steady state. The concentration response at a monitoring point is observed

continuously. The concentration is maintained at the steady state value, when steady state is reached. Tracer gas step-up method is one of the effective ways to estimate local mean age of air with HVAC system without returning air, as shown in Fig. 2.44.

However, it is not applicable in some air-conditioning system with returning air. Therefore, we proposed the improved calculation method of local mean age of air based on tracer gas step-up method.

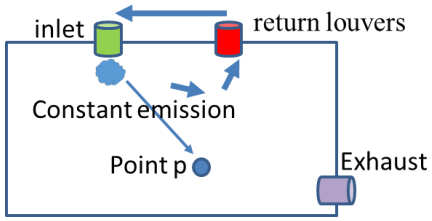

Fig. 2.45 Air conditioning system with returning air

In some air-conditioning system with returning air, the tracer gas injected from the inlet will return back to the air supply inlet via the return louvers and then be injected again, therefore, the tracer gas concentration in the experiment room varied with time, schematic diagram of air flow direction is shown in Fig.2.45. As a result, even though we inject constant flow of tracer gas into experimental room, final gas concentration from inlet is neither pulse nor constant flow due to the returning air.

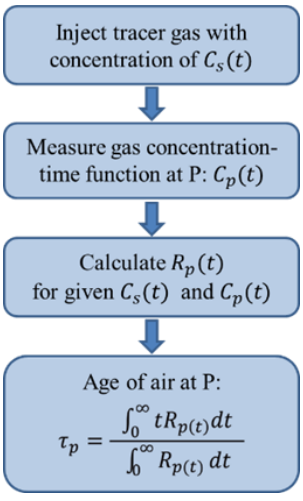

Fig. 2.46 Calculating flow chart of local mean age of air

To solve this problem, we inject tracer gas with concentration of *Cs*(*t*) from diffusers and measure gas concentration *Cp*(*t*) of monitoring P. And then, estimate pulse response *Rp*(*t*) at a

monitoring point based on tracer gas concentration from inlet *Cs*(*t*) [ppm] and the measured concentration in the point *Cpm*(*t*)[ppm]. Finally, local mean age of air at monitoring point P can be calculated by the least square method. The calculating flow chart of local mean age of air is shown in Fig.2.46. R_P (*t*) represents the concentration of tracer gas at point P caused by injecting a unit amount of tracer gas. R_P (*t*) means the function for unit impulse.

If a small amount of injection *M* [m^3] is emitted as shown in Fig. 2.47 a), Eq. (2.7) is for the calculated concentration C_P (*t*):

$$C_p(t) = \int_0^\infty M(t-\tau)R_p(\tau)\mathrm{d}\tau = \int_0^\infty Q \cdot C_s(t-\tau)R_p(\tau)\mathrm{d}\tau \tag{2.7}$$

If no constraint was given, however, in some cases the issue above would be an ill-posed problem. What's more, sometimes, R_p (*t*) result was unreasonable. R_p (t_i) < 0 for some *i* is never acceptable, e.g., because there is no minus concentration in the real world.

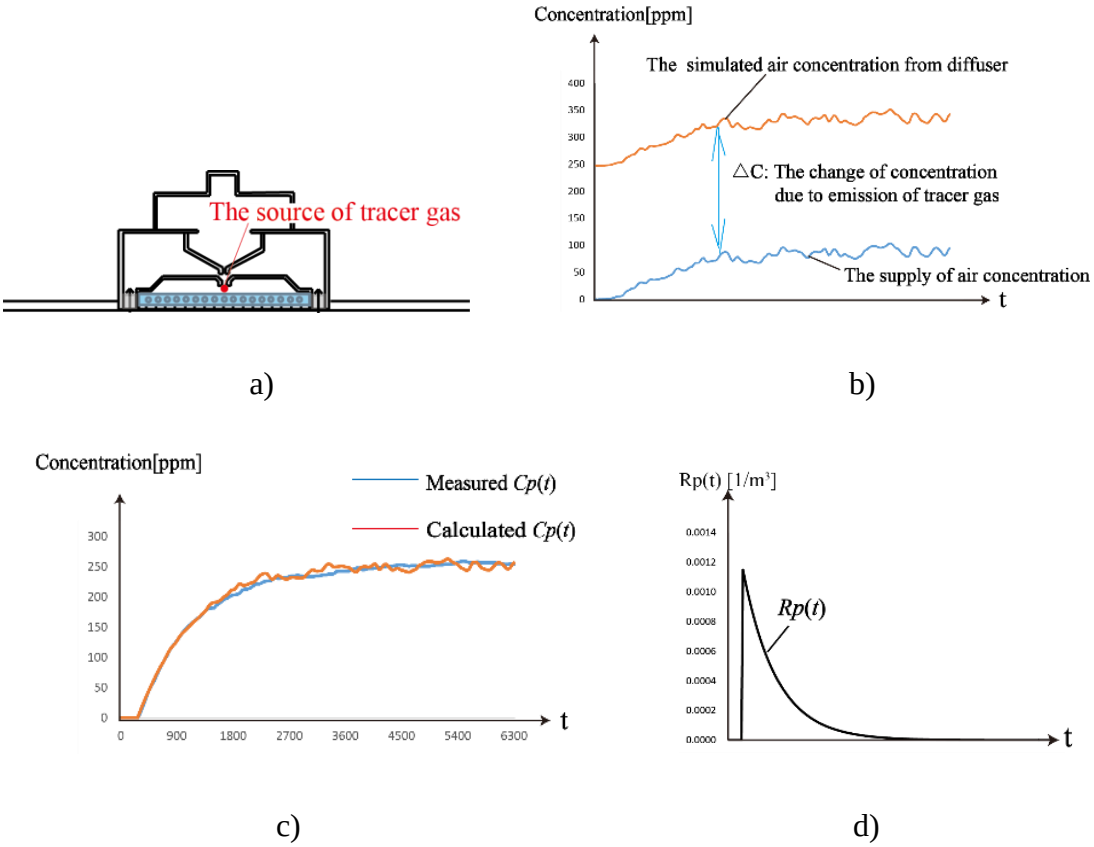

Fig. 2.47 Changes of concentration and response function

a) The position for tracer gas position emitting b) Injected tracer gas from inlet, b) An example for the concentration curve, c) An example for the pulse response *R*p (*t*)

In order to solve this problem, a reasonable model of R_p (t) was assumed as Eq. 2.8

$$R_{\mathrm{p}}(t)=\begin{cases} b\cdot e^{-c(t-a)} & t \succ a \\ 0 & t \le a \end{cases} \tag{2.8}$$

In this way, the optimum R_p (t) was provided. Moreover, it is essential to minimize the following error function by adding constraints. A result for a minimization of sample error was shown in Fig. 2.47 c) and the corresponding result of R_p (t) was shown in Fig. 2.47 d). Based on the calculation of R_p (t), according to the Eq. 2.9, the best response factor a was manually selected and then factor b and c were determined by the modules solver in EXCEL. The local mean age of air τ_p at an arbitrary point P can be easily obtained.

$$\tau_p=\frac{\int_0^\infty tRp(t)\mathrm{d}t}{\int_0^\infty Rp(t)\mathrm{d}t} \tag{2.9}$$

When the local average air age was uniform over the entire room, the room average age of air $<\tau>$ would be available. In addition, the average air distribution performance of the room in the space was characterized by the average air exchange efficiency η_{eff}, and the calculating formula was presented as the Eq. 2.10.

$$\eta_{eff}=\frac{\tau_n}{\langle\tau\rangle} \tag{2.10}$$

The nominal ventilation time τ_n can be gotten by the Eq.2.11, where V [m^3] stood for the volume of the room, and Q [m^3/h] was the supply air flow rate.

$$\tau_n=\frac{V}{Q} \tag{2.11}$$

2.4.4.3.2 Result and analysis

Calculation results for both the average age of air and air exchange efficiency were shown in Table 2.11. Here three sets of results for analysis were listed. Meanwhile, the corresponding analyses and comparison were illustrated in Fig. 2.48 ~ Fig. 2.58.

Table 2.11 Room average age of air and the average air exchange efficiency

τ_n=11.16

Condition	Room average age of air < τ > [min]	Mean air exchange rate η_{eff} [-]
4EC-C-4D	12.26	0.90
4EB-C-4D	11.85	0.93
2EC-C-4D	11.75	0.94
1EC-C-4D	9.55	1.15
1EC-NC-4D	10.41	1.06

Firstly, the influence caused by the positions of exhaust ports on the local mean age of air was analyzed. The conditions of each case are shown in Table 2.12 and Fig. 2.48~ Fig. 2.50. Coupled with the conditions of curtains wrapping around the beds, the positions of the exhaust ports were changed.

Table 2.12 Conditions for three cases

Condition	Exhaust position	Positions of tracer gas generation	Curtains around bed
4EC-C-4B	4EC	4D	Closed
1EC-C-4B	1EC	4D	Closed
2EC-C-4B	2EC	4D	Closed

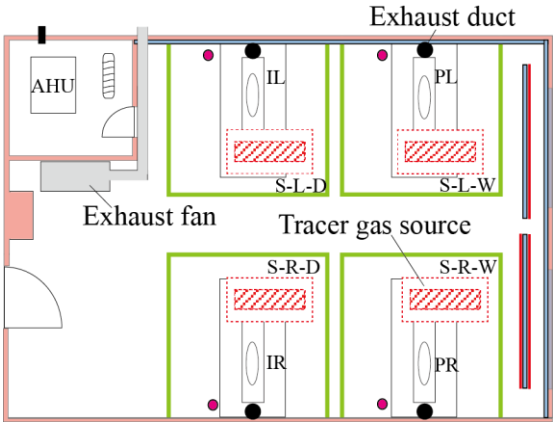

Fig. 2.48 Plan of experimental room
(Exhaust duct of 4EC)

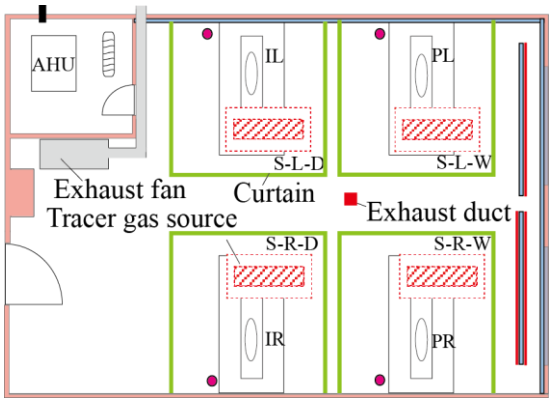

Fig. 2.49 Plan of experimental room (Exhaust duct of 1EC)

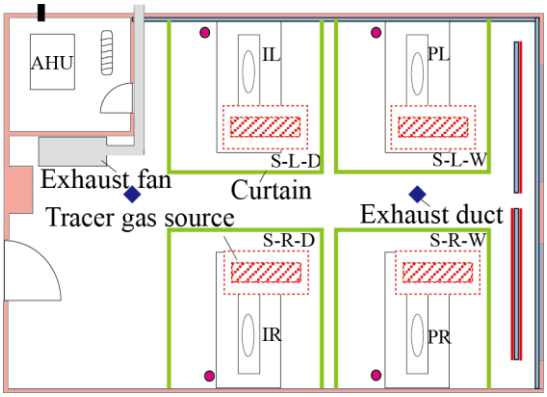

Fig. 2.50 Plan of experimental room (Exhaust duct of 2EC)

The results of the vertical distributions were illustrated in the Fig. 2.51. Moreover, in Table 2.11, the local mean age of air under the condition 1EC is smallest and the rate of the mean air exchange under the condition 1EC showed the maximum value. It can be considered that the ventilation efficiency was excellent with this kind of the exhaust port condition. In terms of the horizontal distributions (Fig. 2.59 a) , c) and d)), the values of local mean age of air showed the maximums under all three conditions when the measuring points were far away from the inlet. It meant that the distance from the inlet to the measuring points had an effect on the air age significantly.

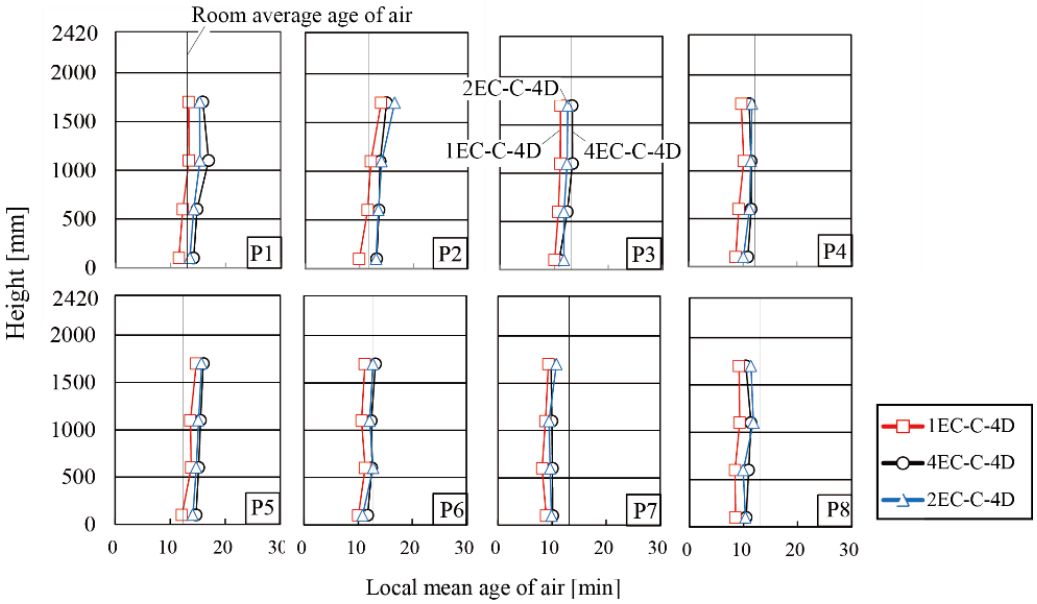

Fig. 2.51 Vertical distributions of local mean age of air (Contaminant source position: 4B, with curtain, position of the exhaust ports: 4EC, 2EC and 1EC)

Then, the influence caused by the height of exhaust ports on the local mean age of air was analyzed. The heights of the exhaust ports were designed at two different positions: underneath the ceiling 50 mm and 1200 mm above the floor. Both the cases were that the curtains were wrapping around the beds.

Table 2.13 Condition for mentioned cases

Condition	Exhaust position	Positions of tracer gas generation	Curtains around bed
4EB-C-4B	4EB	4D	Closed
4EC-C-4B	4EC	4D	Closed

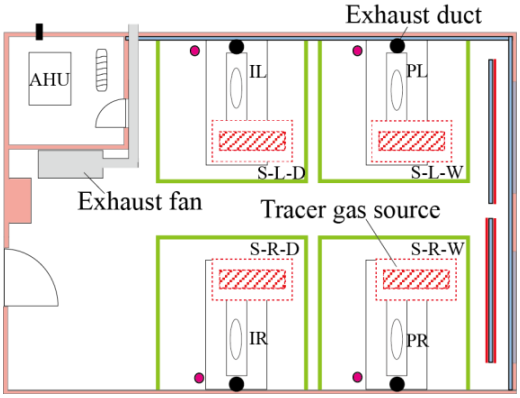

Fig. 2.52 Plan of experimental room
(Exhaust duct of 4EC/4EB)

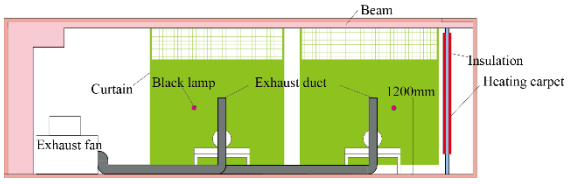

Fig. 2.53 Section of experimental room
(Exhaust duct of 4EB)

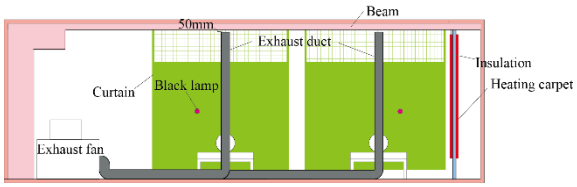

Fig. 2.54 Section of experimental room
(Exhaust duct of 4EC)

From the Fig.2.55, it can be observed that the results of the vertical distributions were close considerably between the both conditions. In addition, the horizontal distributions of the local mean age of air (Fig. 2.59 a) and 2.59 b)) showed the larger values in both conditions when the measuring points were outlying from the inlets. Moreover, the similar values of mean air exchange rate were shown in Table 2.11. It can be considered that there was minor influence on the air age caused by the height of the exhaust port.

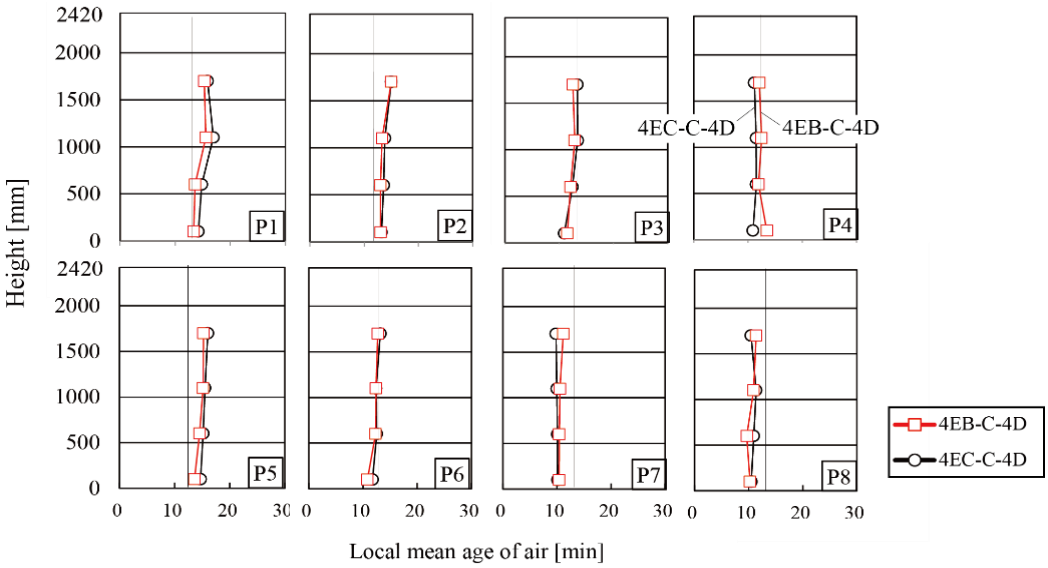

Fig.2.55 Vertical distributions of local mean age of air
(Contaminant source position: 4B, with curtain, height of exhaust port: 50 mm from the ceiling and 1200 mm from the floor)

Eventually, the influence caused by curtains was analyzed. Fig. 2.58 demonstrated the vertical distributions of local mean age of air.

Table 2.14 Condition for mentioned cases

Condition	Exhaust position	Positions of tracer gas generation	Curtains around bed
1EC-C-4B	1EC	4D	Closed
1EC-NC-4B	1EC	4D	Open

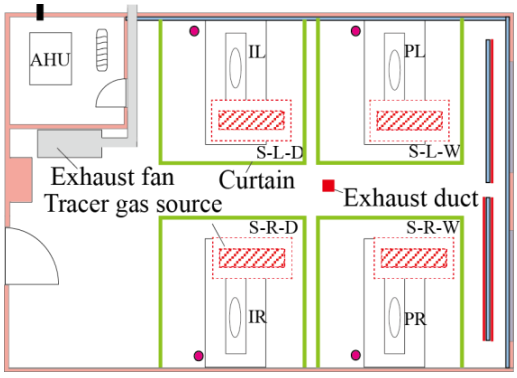

Fig. 2.56 Plan of experimental room
(Exhaust duct of 1EC, with curtain)

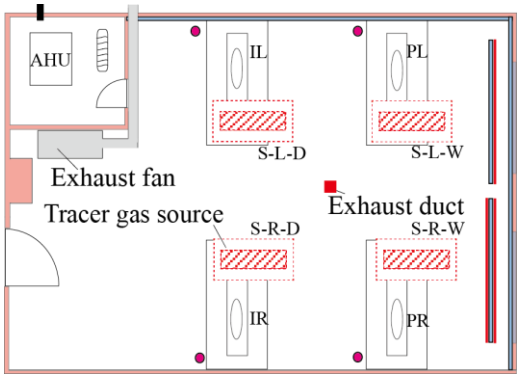

Fig. 2.57 Plan of experimental room
(Exhaust duct of 1EC, without curtain)

The difference was whether the curtains wrapped around the bed or not when the exhaust port condition was 1EC. When the curtains wrapped around the bed, the local mean age of air at

P6~P8 within the space of curtains became small. The air movement was obstructed due to the four inlets were placed inside the curtains. Regarding to the horizontal distributions, the contaminant spread out in the room efficiently when there was no curtain. Moreover, it was apparent that almost the same rates of the mean air exchange were shown in Table 2.11 under the two conditions (Fig. 2.59 d) and e)). This result expressed that the ventilation performance of the whole room presented the same level roughly, although the air flow was affected by the curtains to some extent.

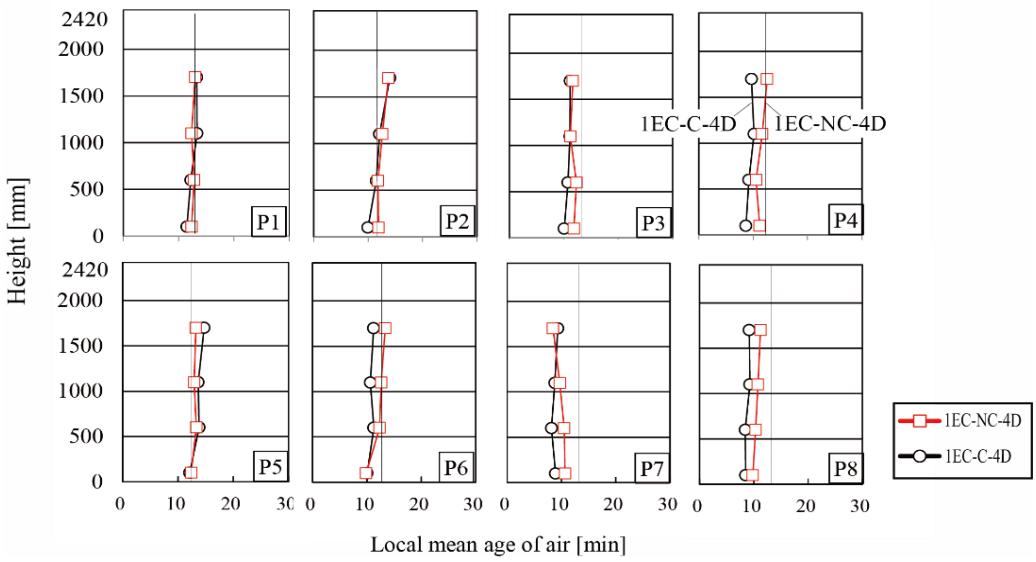

Fig. 2.58 Vertical distributions of local mean age of air
(Contaminant source position: 4B, with curtain, height of exhaust port: 50 mm from the ceiling and 1200 mm from the floor)

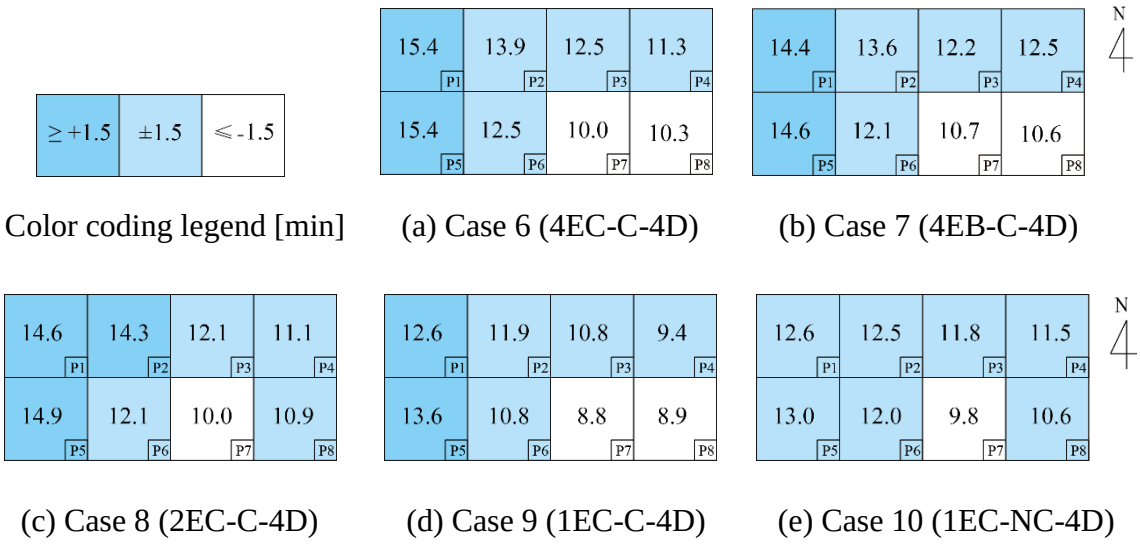

Color coding legend [min] (a) Case 6 (4EC-C-4D) (b) Case 7 (4EB-C-4D)

(c) Case 8 (2EC-C-4D) (d) Case 9 (1EC-C-4D) (e) Case 10 (1EC-NC-4D)

Fig. 2.59 Horizontal distributions of local mean age of air for each case

2.5Visualization experiment

2.5.1 Experimental set-up and measurement methods

To verify the air flow properties, visualization experiment was conducted from 13th to 14th, Dec. 2016. The instruments used are listed in Table 2.15.

Table 2.15 Visualization instrument

Instrument	Manufacturer	Amount
PORTA SMOKE	DAINICHI	1
PIV Laser	Katou co.	1

The instruments are listed in Table 2.15 and the picture of instruments is shown in Fig. 2.60.

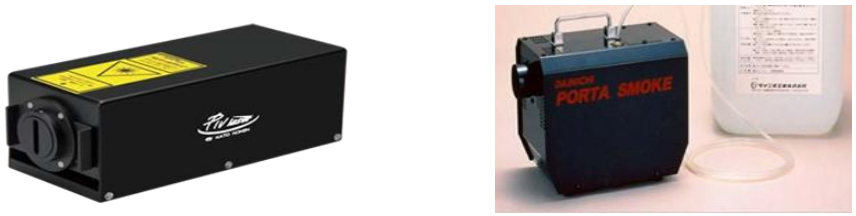

a) PORTA SMOKE b) PIV Laser

Fig. 2.60 Instruments for visualization experiment

Smoke is generated by PORTA SMOKE for about 2 minutes, and the whole process is recorded by video camera. The set-up diagram is illustrated in Fig. 2.61.

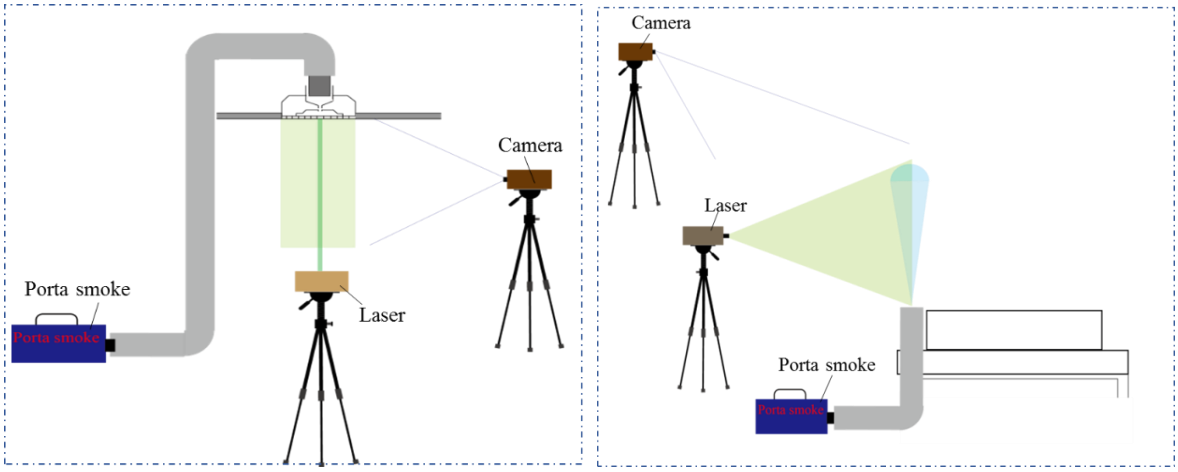

a) Smoke generated at inlet b) Smoke generated at bed

Fig. 2.61 Set-up diagram for visualization experiment

The outlet setting is under the condition of 1EC with curtain closed and open, as shown in Fig.2.62 and Fig.2.63.

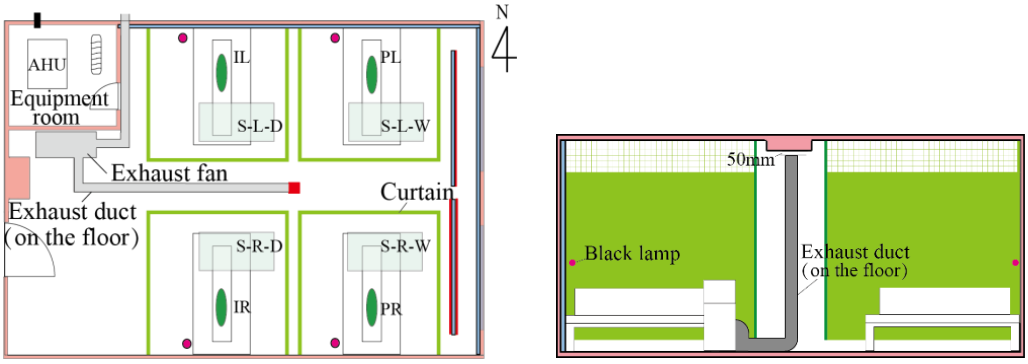

a) Plan of the outlet setting b) the outlet setting profile

Fig. 2.62 The outlet setting under the condition of 1EC with curtain closed

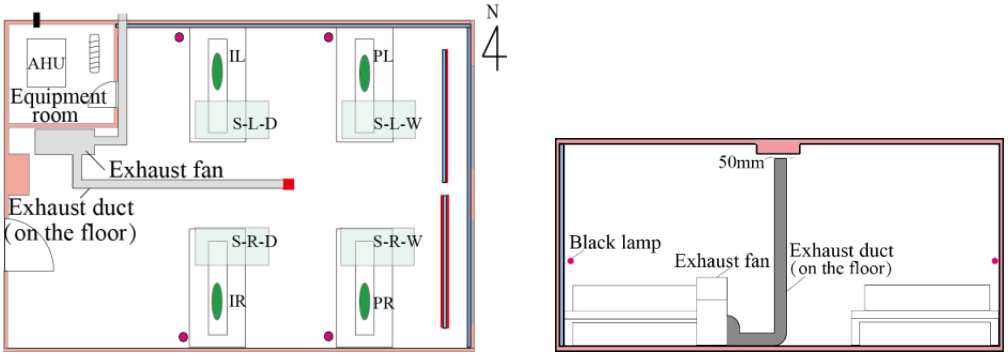

a) Plan of the outlet setting b) the outlet setting profile

Fig. 2.63 The outlet setting under the condition of 1EC with curtain removed

The location of smoke generation and object of the camera is shown in Fig. 2.64. The locations of laser and camera are shown in Fig. 2.65. While, the conditions for visualization experiment are shown in Table 2.16.

(a) Laser 1 (b) Laser 2 (c) Laser 3

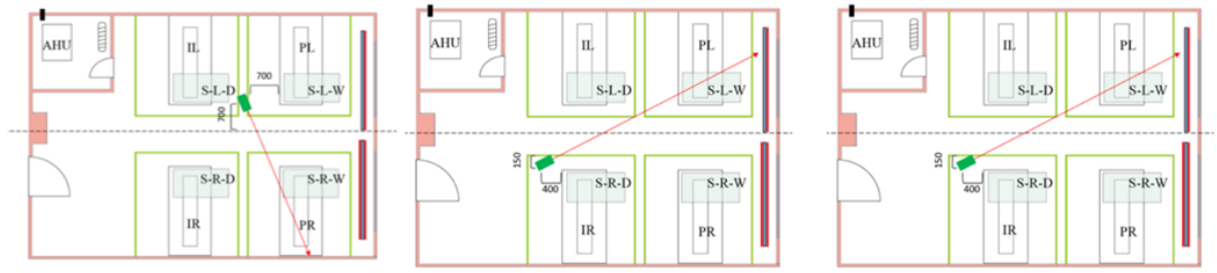

(d) Laser 4 (e) Laser 5 (f) Laser 6

Fig. 2.64 Laser location

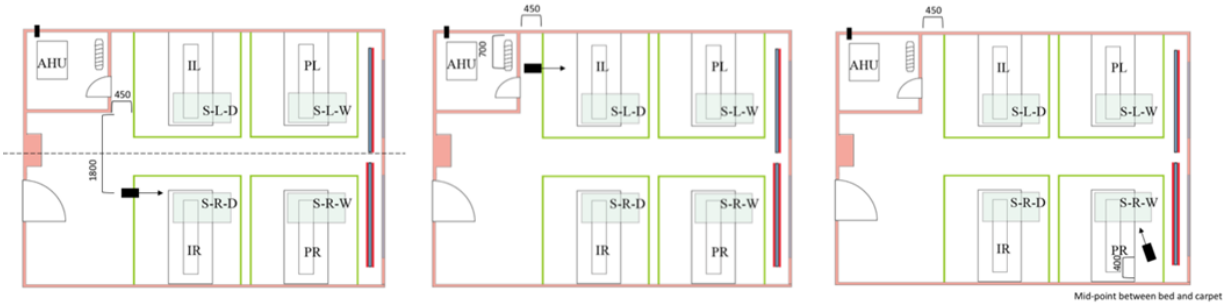

(a) Camera 1 (b) Camera 2 (c) Camera 3

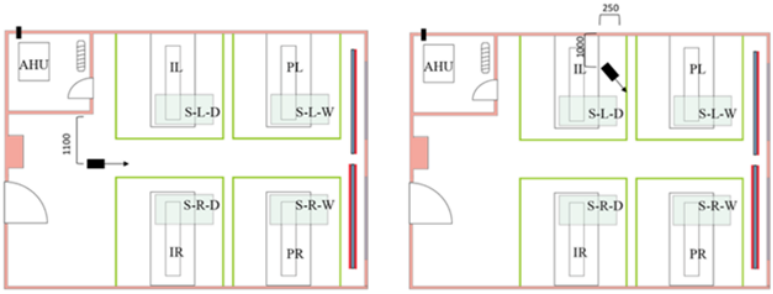

(d) Camera 4 (e) Camera 5

Fig. 2.65 Camera location

Table 2.16 Conditions for visualization experiment

	Curtain	Smoke generation	Camera object	Laser	Camera
Pattern 1	Open	Inlet	PR	1	1
Pattern 2	Open	PR	PR	2	1
Pattern 3	Open	Inlet	RL	3	3
Pattern 4	Open	RL	RL	4	2
Pattern 5	Closed	RL	RL	5	4
Pattern 6	Closed	PR	PR	6	5

2.5.2 Result and analysis

2.5.2.1 *Smoke generated at inlet (Pattern 1, Pattern 3)*

The results of Pattern 1 and Pattern 3 are under the condition that smoke is generated at inlet. The location of section is shown in Fig. 2.66 and the airflow property is shown in Fig. 2.67. The appearance of experiment is shown in Fig. 2.68~ Fig. 2.69.

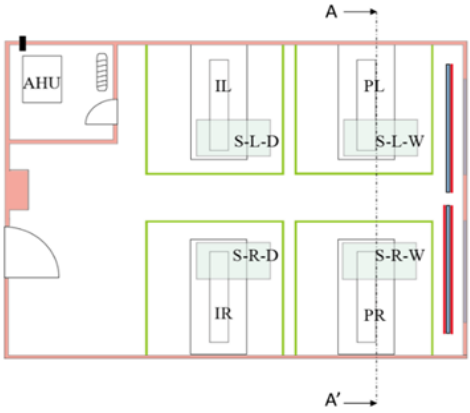

Fig. 2.66 Location of A-A' section

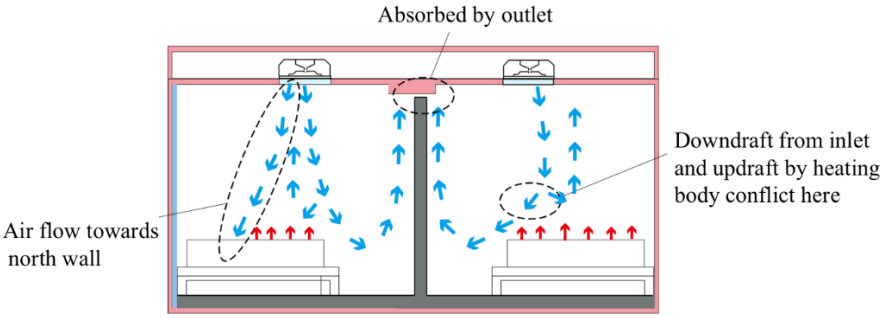

Fig. 2.67 Air flow property of A-A' section

Fig. 2.68 Airflow near RL

Fig. 2.69 Airflow near PR

In the south of the room, a large amount of airflow running out from the inlet moves to the floor. However, because of the heat generated by simulated human body, updraft and turbulence appears. Moreover, because of the induction unit, the updraft from simulated body moves to the ceiling.

While in the north side, the descending airflow divides into two streams. One of them moves to outlet and the other one flows to the north wall. From a global point of view, we consider that there is airflow moving towards the north.

2.5.2.2 *Smoke generated at bed (Pattern 2, Pattern 4)*

The experiments of Pattern 2 and Pattern 4 are conducted when smoke generation is at bed. The location of section is the same with Pattern1 and Pattern 3, and the airflow property is shown in Fig. 2.69. The appearance of experiment is shown in Fig. 2.70~ Fig. 2.72.

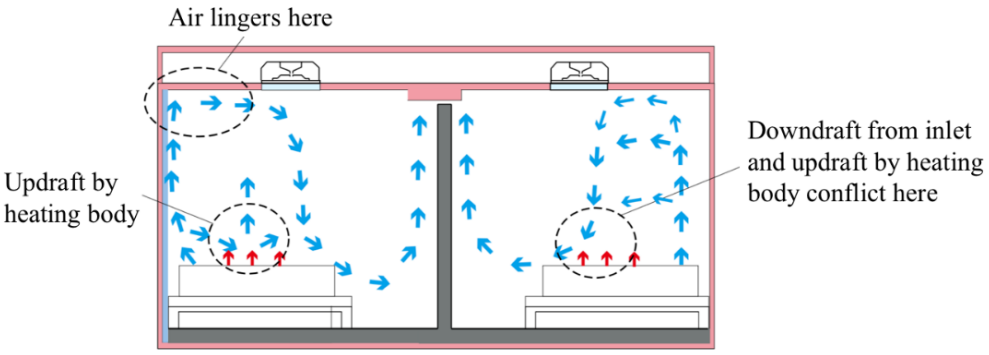

Fig. 2.70 Air flow property of A-A' section

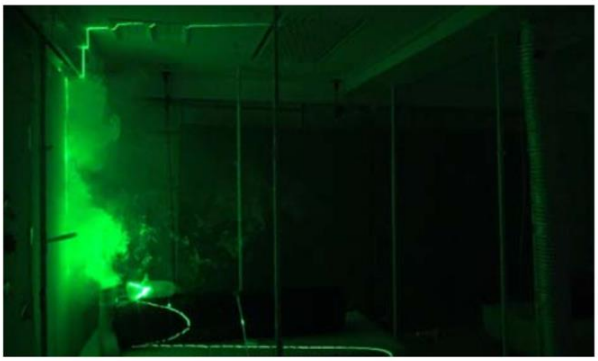

Fig. 2.71 Airflow near RL

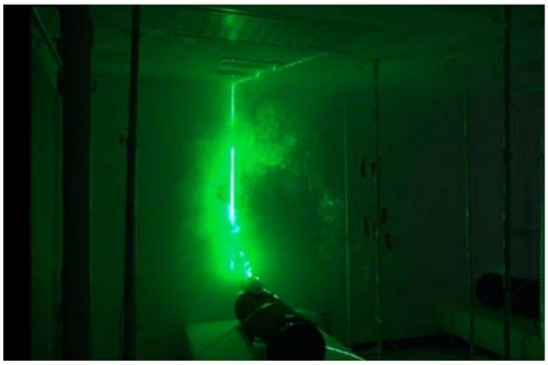

Fig. 2.72 Airflow near PR

On the north of the room, a large amount of airflow moves over bed to ceiling, and conflicts heavily with the air blown from inlet, then move down rapidly and finally inhaled by outlet. On the south of the room, the smoke accumulates at the top of room. Moreover, similar with the Pattern 1 and Pattern 3, because of the ascending flow due to the heat of simulated human body, there is turbulence near the simulated body.

On the north of the room, the air moves up along the wall and lingers around the upper corner. From a global point of view, it is considered that there is flow moving to the north.

2.5.2.3 *Airflow moving outside curtain*

Pattern 5 and pattern 6 are under the condition that the smoke is generated at bed with curtain closed. The smoke generated location if shown in Fig. 2.73 and the appearance of smoke moving over the curtain is shown in Fig. 2.74 and Fig. 2.75.

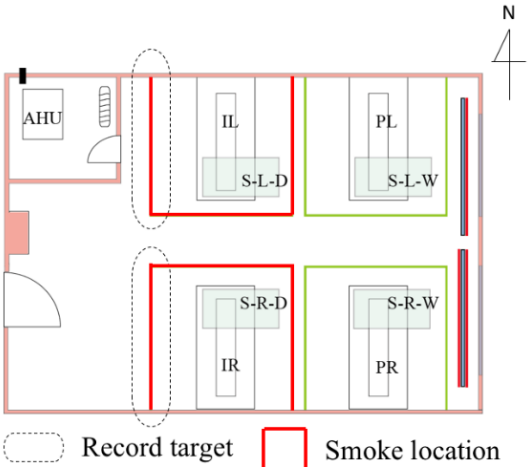

Fig. 2.73 Smoke generation location

Fig. 2.74 Airflow at the top of curtain at LR

Fig. 2.75 Airflow at the top of curtain at PR

Both BLW and BRW are generating smoke, but when flowing from the top of the curtain to the outside, it seems that it goes out from the center of the upper part of the curtain. In other words, it is conceivable that the smoke spreads out from the generation position in a planar manner and then overflows from the top of the curtain after staying.

The smoke is generated near the wall side both in RL and PR region. When flowing from the top of the curtain to the outside, airflow goes out from the center of the upper part of the curtain. Therefore, we believe that the smoke spreads out from the generation position in a planar manner and then overflows from the top of the curtain after staying.

2.6 Measurement of radiation

2.6.1 Set-ups

Fig. 2.76 Picture of long wave radiometer

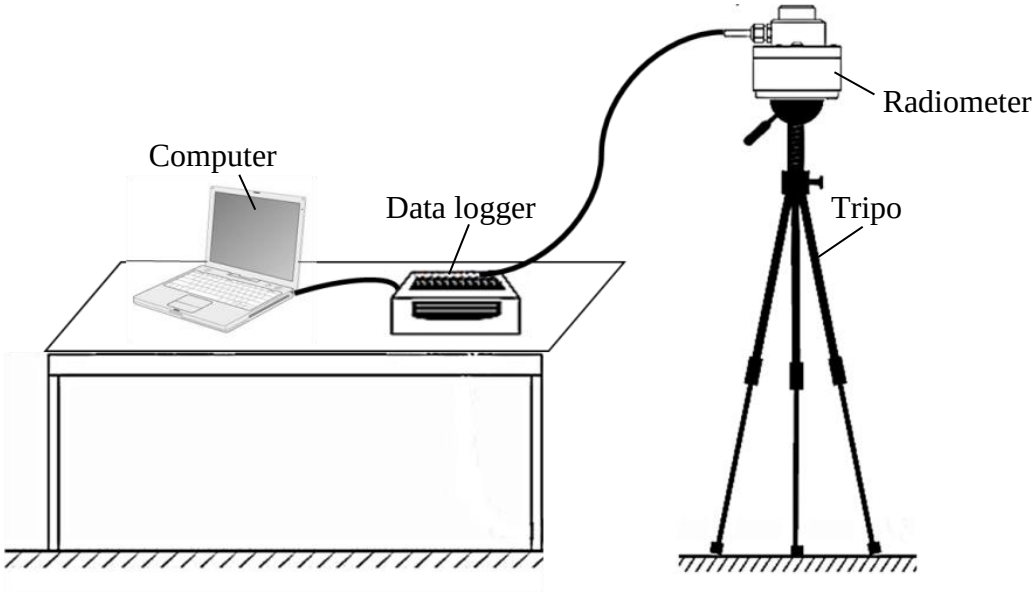

Fig. 2.77 Measurement device diagram for radiation

We conduct the radiation measurement after confirming the system reaches steady state. The measurement instrument is long wave radiometer (CFH-IR02) produced by CLIMATEX CORPORATION. The picture of long wave radiometer is shown in Fig. 2.76, and we can see Fig. 2.77 for measurement device diagram. During measurement, long wave radiometer is set at the location shown in Fig. 2.78, whose height is FL+1100mm. The experiment was conducted under two conditions: with curtain and without curtain.

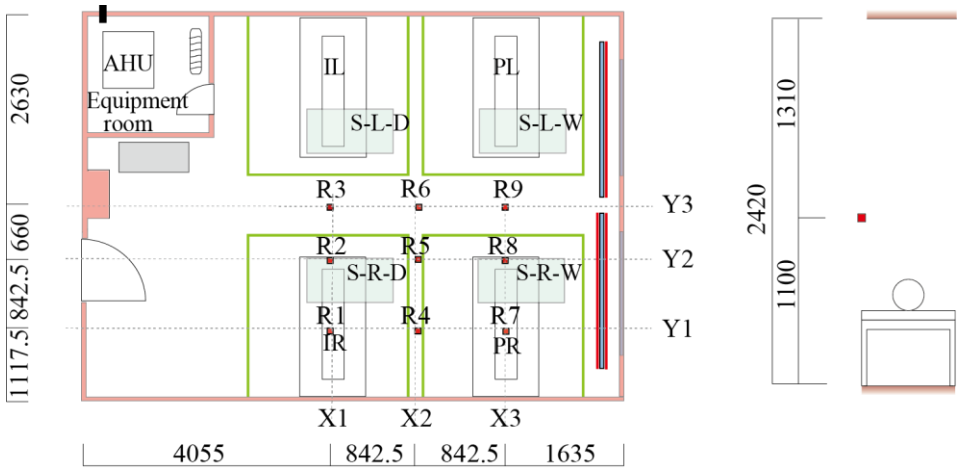

Fig. 2.78 Measurement points for radiation

2.6.2 Result and analysis

The radiation can be calculated by using the following formula:

$$E = \frac{U}{S} + s(q + 273.15)^4 \tag{2.12}$$

The temperature can be calculated as:

$$q = \sqrt[4]{\frac{E}{se}} \tag{2.13}$$

Where E is irradiance in [W/m^2], U is voltage output in [V], σ is the Stefan-Boltzmann constant in [W/(m^{2}K^4)], θ is the instrument body temperature in [$^\circ C$], S is sensitivity in [V/(W/m^2)].

The calculated radiation temperature and the indoor temperature result are shown in Fig. 2.79 and Fig.2.80.

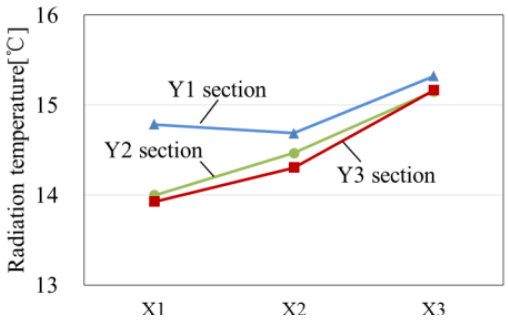

a) Radiation temperature of multiple sections (With curtain)

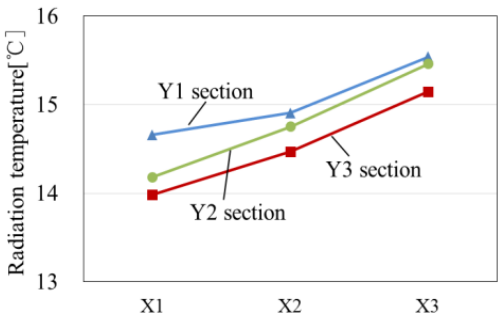

a) Radiation temperature of multiple sections (Without curtain)

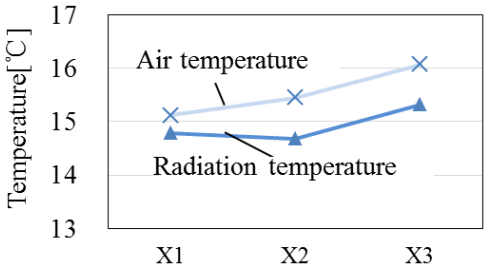

b) Section A (With curtain)

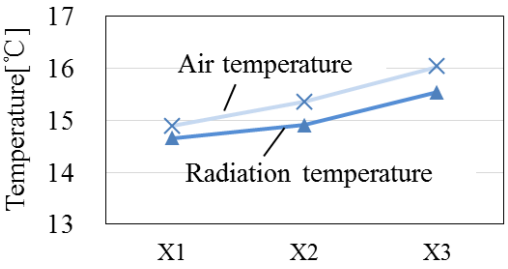

b) Section A (Without curtain)

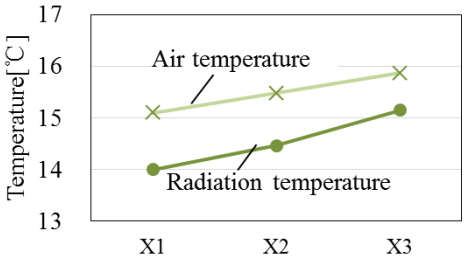

c) Section B (With curtain)

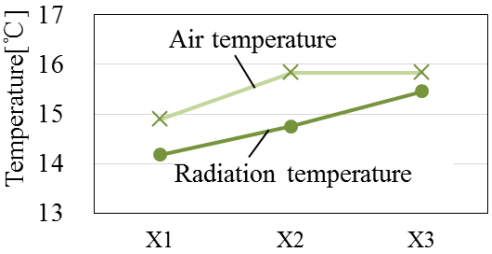

c) Section B (Without curtain)

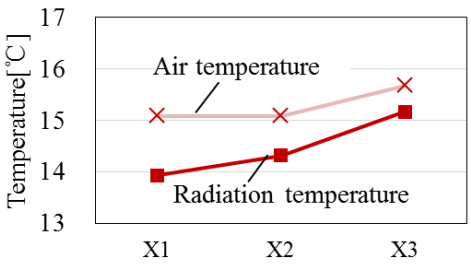

d) Section C (With curtain)

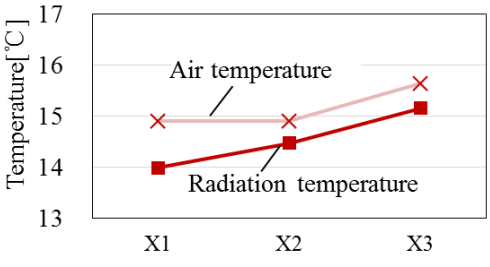

d) Section C (Without curtain)

Fig. 2.79 Radiation and indoor temperature (With curtain)

Fig. 2.80 Radiation and indoor temperature (Without curtain)

As shown in Figure, the radiation temperature is 0.3~0.5°C lower than indoor temperature. However, because of the influence of heating carpet and simulated human body, the radiation temperature is relatively higher than indoor temperature.

2.7 Measurement of air velocity

2.7.1 Set-ups

Measurement of air velocity was conducted to help understand the airflow properties in the experimental room. Three-dimensional ultrasonic anemometer (DA-700, SONIC CORPORATION) was used, so the airflow in three direction of x, y and z axis is visible and can be analysed. The picture of ultrasonic anemometer is shown in Fig. 2.81, and we can see Fig. 2.82 for measurement device diagram.

Fig. 2.81 Picture of three-dimensional ultrasonic anemometer

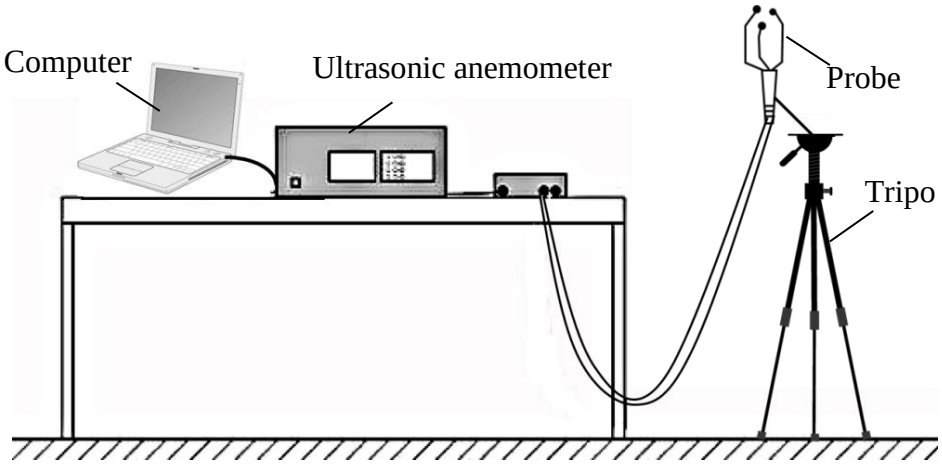

Fig. 2.82 Measurement device diagram for air velocity

Air velocity is collected at 3 points vertically (FL+600mm, FL+1100mm and FL+1700mm) at the positions of X1 - X10. Measurement points are shown in Fig. 2.83. When the indoor environment reached a steady state, measurement was started. It took 45 seconds to 1 minute 30 seconds at each measurement point by using ultrasonic anemometer.

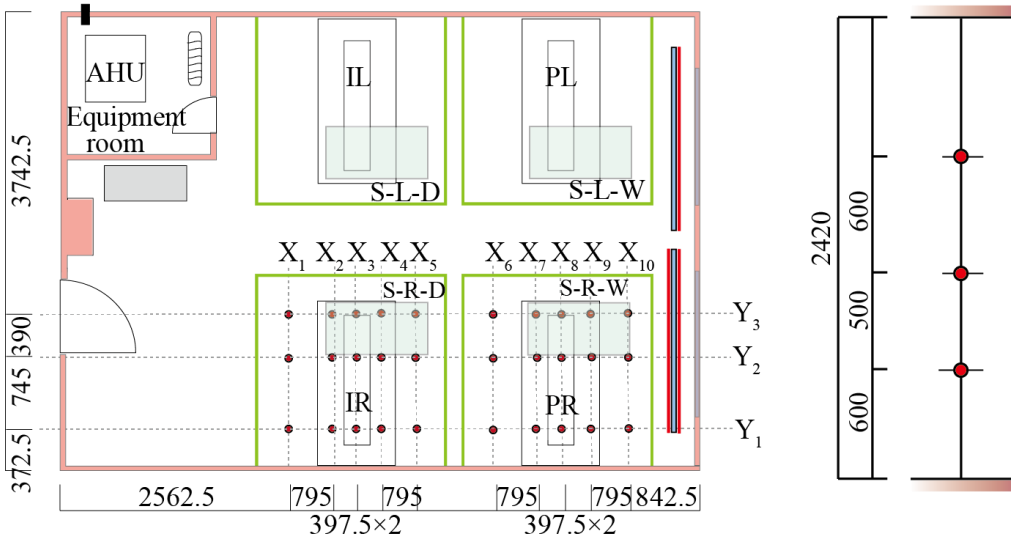

Fig. 2.83 Measurement points for air velocity

2.7.2 Result and analysis

The results of the air velocity measurement are shown in Fig. 2.84~ Fig. 2.86. The results of the vector velocity distribution in Y and X section are shown in Fig. 2.84 and Fig. 2.85, respectively. From the figure we can see, the direction of vector velocity near inlet is upward which is caused by the ascending air due to the heat of the simulated human body.

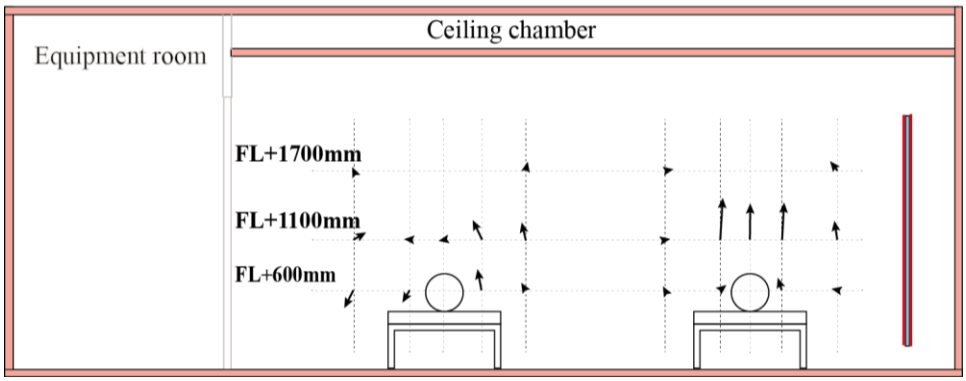

a) Section Y1

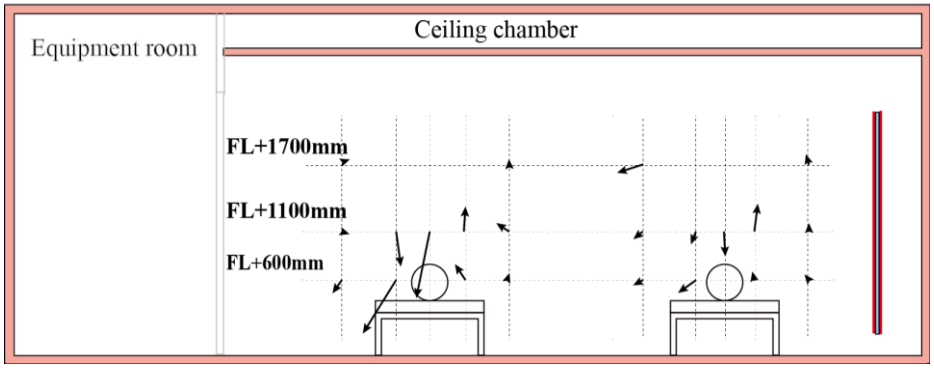

b) Section Y2

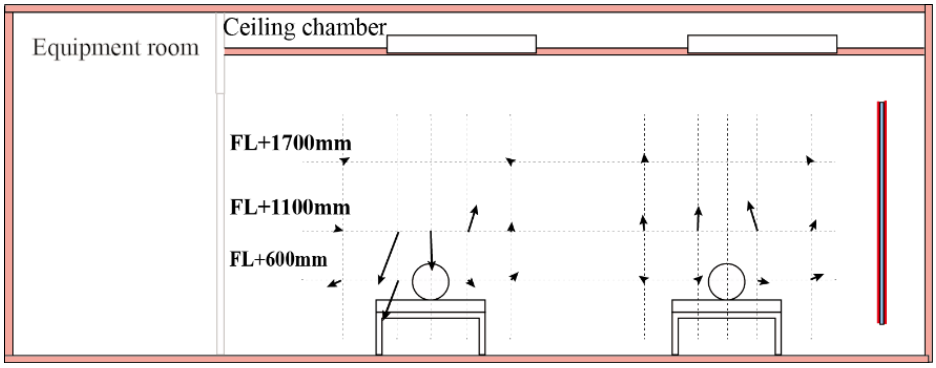

c) Section Y3

Fig. 2.84 Vector velocity distribution in Y Section

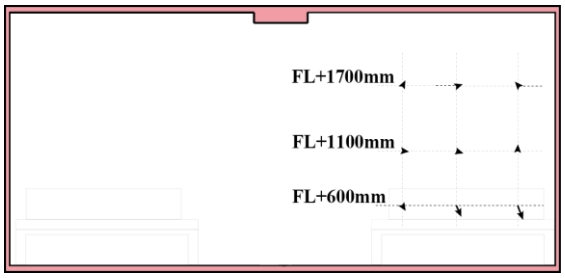

a) Section X1

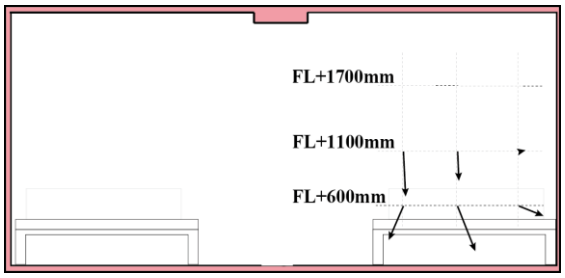

b) Section X2

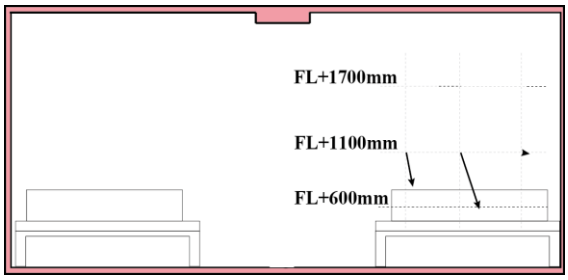

c) Section X3

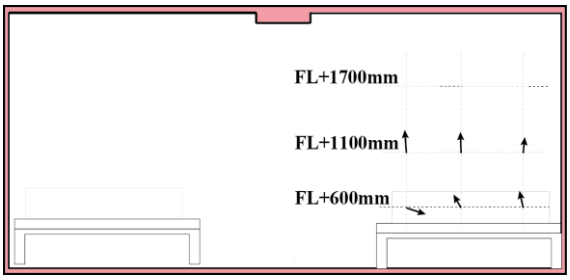

d) Section X4

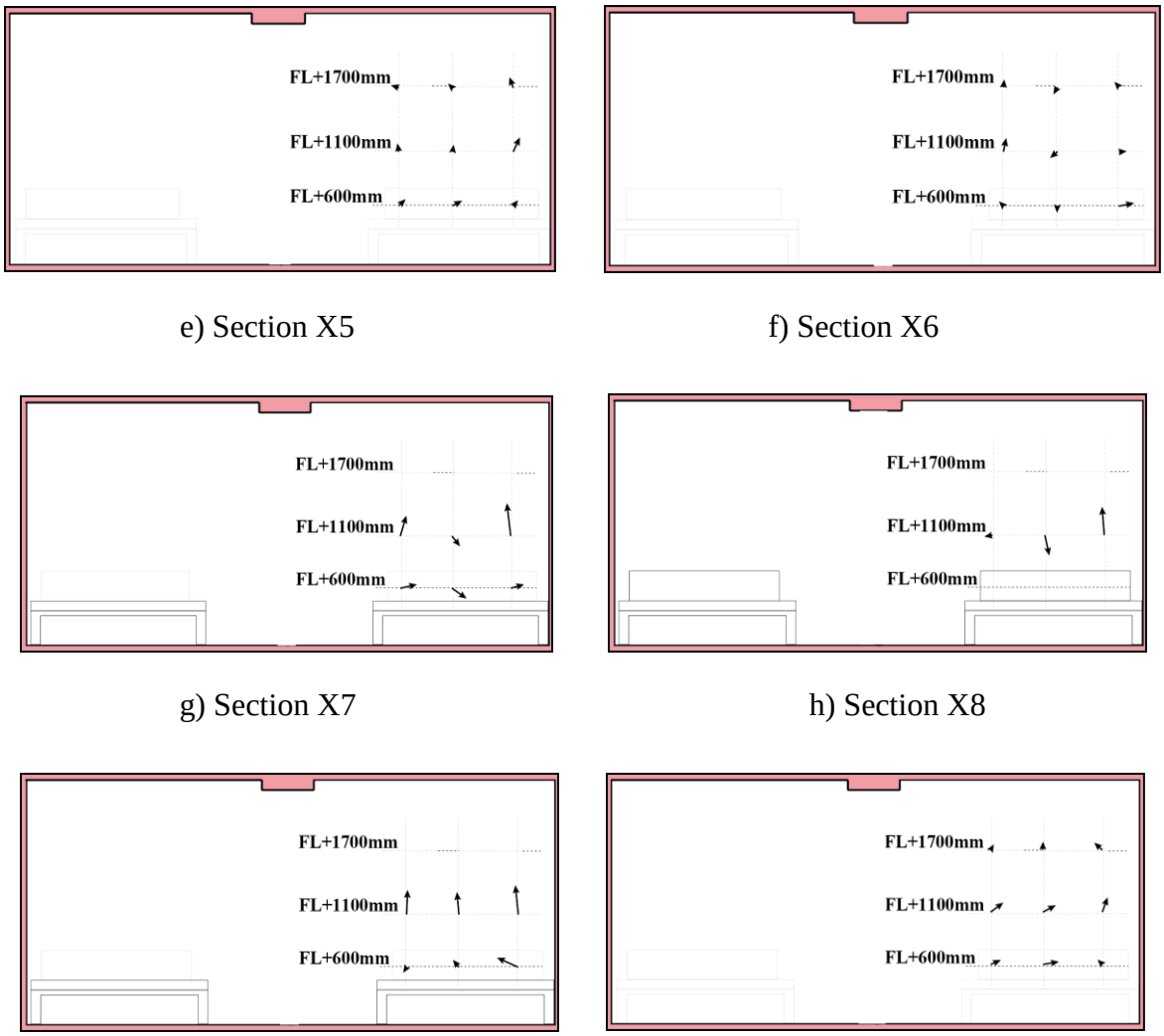

e) Section X5 f) Section X6

g) Section X7 h) Section X8

i) Section X9 j) Section X10

Fig. 2.85 Vector velocity distribution in Y Section

The scalar velocity distribution is shown in Fig. 2.86.

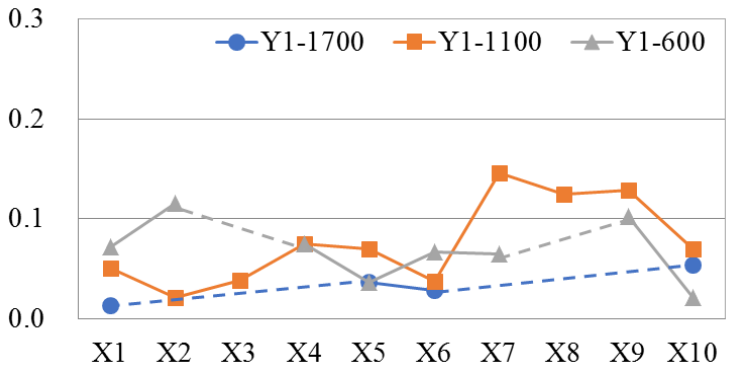

a) Section Y1

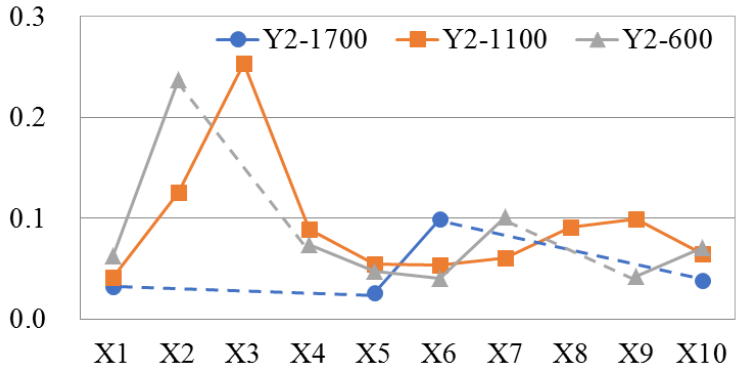

b) Section Y2

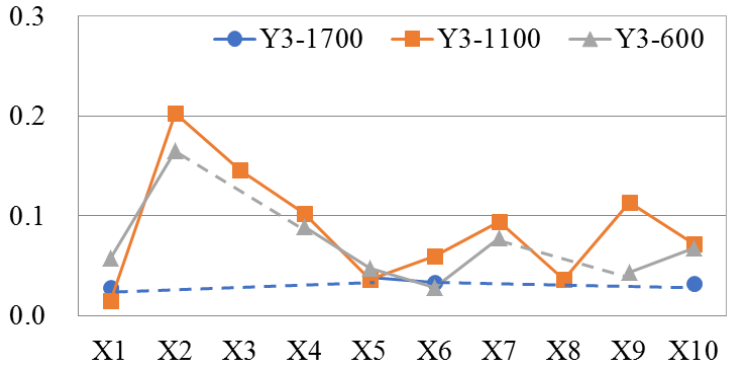

c) Section Y3

Fig. 2.86 Scalar velocity distribution

As can be seen from the figure, the air velocity at all of the measurement points is small, which is less than 0.3 m/s. In addition, at the height of FL+1700m, the air velocity is relatively smaller than the other points, and it is distributed at about 0.1 m/s or less. Moreover, at the height of FL+600mm the distributions of different sections are almost the same.

2.8 Discussion and summary

The effects on indoor air environment caused by some relevant parameters were examined. From what have been discussed above, the following conclusions were drawn:

(1) The position of the exhaust ports plays an influential role on the indoor environment. The vertical temperature difference was minor in the ward area caused by the position of the exhaust ports. However, the significant influence caused by the position of the exhaust ports was shown on the normalized concentration distributions. The appropriate position for the exhaust ports

can make the contaminant escape out of the room effectively. The optimum choice was to place the exhaust ports near the beds because this position was close to the sources of the odour gas.

(2) The height of the exhaust ports was also a major factor towards the indoor environment. Compared with the normalized concentration distributions, vertical temperature distributions showed few differences. When the height of the exhaust ports is closer to the source of gas, the contaminant will be emitted out of the room efficiently.

(3) Whether the curtains wrapped around the beds or not would bring the different effects on the indoor environment. To some extent, the curtains had an effect on the heat transmission. Basically, curtains made the indoor temperature higher than that of in without curtains. Similarly, the curtains influenced the normalized concentration distributions. The curtains around the bed would prevent the contaminant escaping out, when in patients panted.

(4) The local mean age of air influenced by the same three factors were given by these studies. The ventilation efficiency was excellent with the kind of the exhaust port condition 1EC, because the rate of the mean air exchange showed the maximum value. In terms of the horizontal distributions, the distance from the inlet to the measuring points had an effect on the air age significantly. The values of local mean age of air showed the maximums, when the measuring points were far away from the inlet. The results of the vertical distributions were close considerably, even though the heights of the exhaust ports changed. Meanwhile, the similar level of the horizontal distributions of the local mean age of air was shown when the measuring points were far away from the inlets. It can be considered that there was minor influence on the air age caused by the height of the exhaust port. Concerning the curtains, some obvious influences were presented in this study. The air movement was obstructed, when the inlets were placed inside the curtains. When the curtains wrapped around the bed, the local mean age of air within the space of curtains became small. With regard to the horizontal distributions, the contaminants spread out in the room efficiently when there was no curtain. Generally, the ventilation property of the whole room presented the same level, although the air flow was affected by the curtains to some extent.

(5) As for radiation temperature is 0.3~0.5°C lower than indoor temperature. However, because of the influence of heating element, the radiation temperature is relatively higher than indoor temperature.

(6) Regarding air velocity at all of the measurement points is small, which is less than 0.3 m/s. In addition, at the height of FL+1700m, the air velocity is relatively smaller than the other points.

(7) As for the airflow behavior, it is obvious from visualization experiment that the blowout air from the air supply port descends immediately below the air supply port although it is low initial speed (0.2 m / s to 0.8 m / s).

Chapter 3 MEASUREMENTS FOR HEATING CONDITION

3.1 Purpose of the experiments

In previous chapter, the characteristics of the air conditioning system with ceiling induction diffusers were verified under the condition of cooling. In this chapter, some experiments were conducted in winter, aimed at examining the influence of some relevant parameters on the indoor environmental quality in the same sickroom.

3.2 Experimental set-ups

All of the experiments for heating condition were conducted from January 12th to January 25th, 2017. The whole test period lasts 14 days. All of the experiments were conducted in the same showroom of KIMURA KOHKI Corporation. The experimental room is shown in Fig. 3.1 and Fig. 3.2.

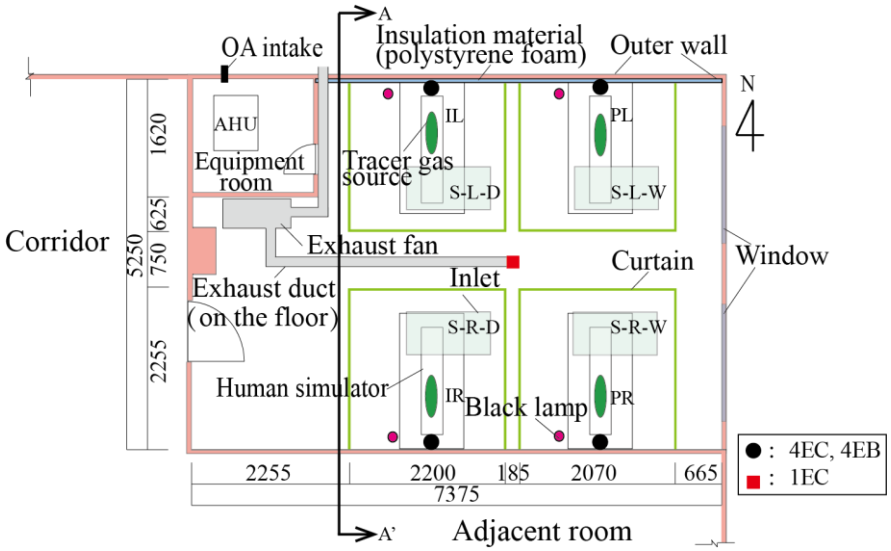

Fig. 3.1 Plan of experimental room [mm]

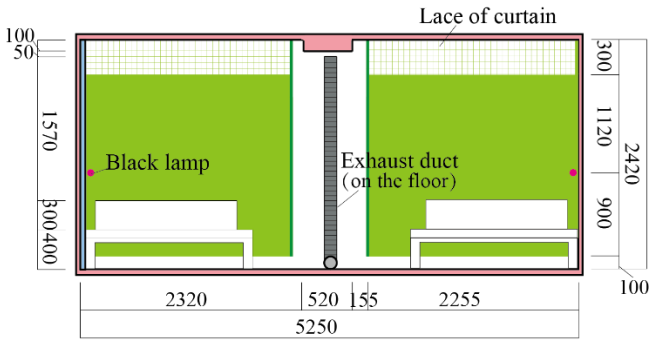

Fig. 3.2 A-A' Section of experimental room [mm]

Polystyrene foam sheets (a kind of insulation material) are pasted on the north wall. The thickness of each sheet is 15mm. There are four rectangular supply diffuser units set on the ceiling. Three conditions were designed by changing the position and the number of exhaust vents. The plane positions of the exhaust ports are displayed in Fig. 3.1, and the according heights are shown in Table 3.1.

Table 3.1 Position of exhaust ports

No.	Item	Number of exhaust ports	Position of exhaust ports
A	4EC	4	50mm below the ceiling
B	4EB	4	1200mm above the floor on the wall
C	1EC	1	50mm below the ceiling in the middle of four beds

Heat generation rate of each simulator is 40W, and four black lamps with power of each lamp 55W are placed for simulating the heat generated by household appliances. The gas mixture (density is near to the air) composed by carbon dioxide (CO_2) and helium (He) is used as tracer gas. The flow rates of CO_2 and He are regulated at 1.5L•min^{-1} and 0.9L•min^{-1} by mass flow controller, respectively and the tracer gas step-up method is conducted in this series of testing.

Two series of experiments are carried out and each series of experiments contains four cases. The main parameters are listed in Table 3.2. Moreover, the difference between the both series of experiments is the positions for tracer gas generation. Specifically, in order to investigate the temperature distribution and normalized concentration distribution in vertical profiles, the first batch of experiments simulates the contaminant from four patients (4B) and the second batch of experiments applies four diffusers to release the testing gas for analyzing the distribution of local mean age of air (4D).

Table 3.2 Experimental conditions

Item	Condition	Exhaust position	Curtains around bed
Case 1	1EC-NC	1EC	Open
Case 2	1EC-C	1EC	Closed
Case 3	4EB-C	4EB	Closed
Case 4	4EC-C	4EC	Closed
Case 5	4EC-NC	4EC	Open

3.3 Measurement points

Just like cooling condition, wall surface temperature, indoor air temperature and CO_2 concentration are measured, when the indoor environment reached steady state. The measurement points are shown in Fig. 3.3~ Fig. 3.6. The values of wall surface temperature, captured by T-thermocouple were collected from three heights in a vertical line. The measurement positions distribute in the room layout, from W1 to W9. Moreover, the other 12 measurement points (W10-W13) are set on the east wall. In terms of indoor ambient environment, the values of indoor air temperature are obtained from measurement positions P1-P12 and there are 11 measurement points along each measurement position vertically. It is worth mentioning that there are 10 measurement points at each position from P1 to P4 (there is no measurement point at the height of 2420mm) because of the existing of a beam. Measurement positions P1-P10 can monitor the concentration of CO_2, where 4 measurement points at each position vertically serve purpose of collection by CO_2 recorder.

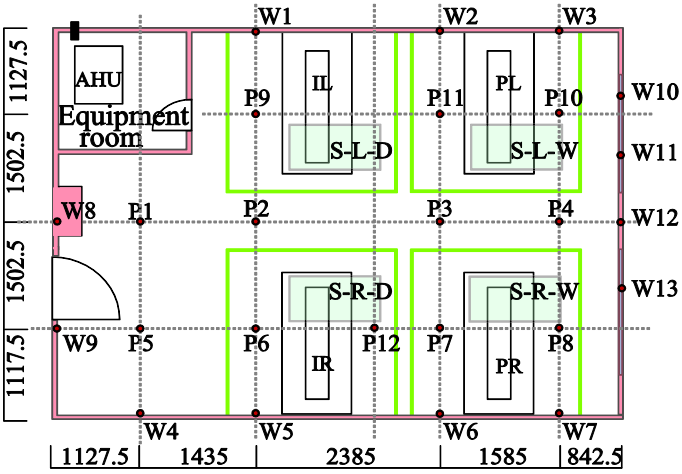

Fig. 3.3 Plane positions of measurement points [mm]

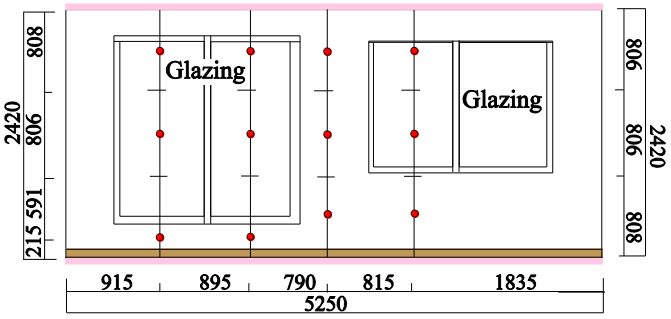

Fig. 3.4 Measurement points on the east wall

The measurement points for temperature, including indoor air temperature, wall surface temperature and supply air temperature are shown in Fig. 3.5. The values of temperature were captured by T-thermocouple.

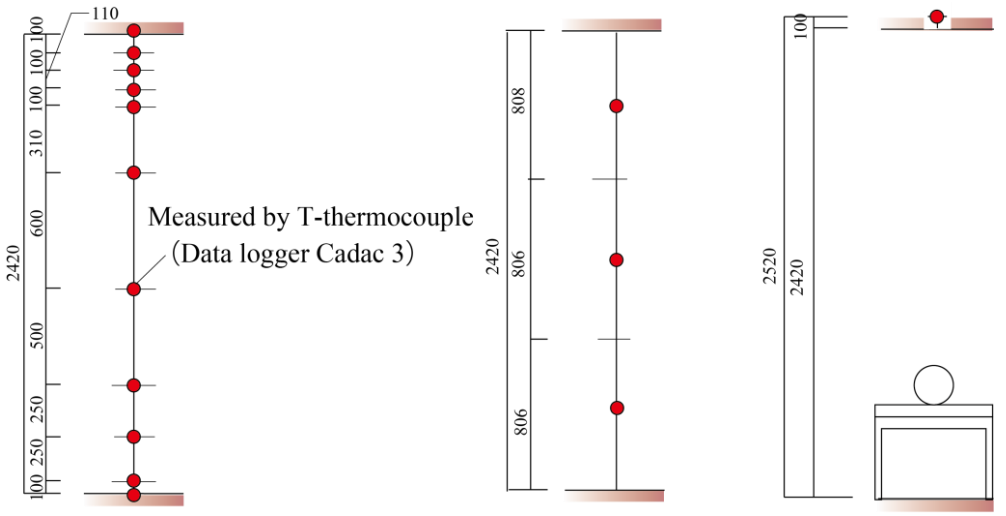

a) Air temperature b) Wall surface temperature c) Supply air temperature (SLW, SLD, SRW, SRD)

Fig. 3.5 Measurement points for temperature

The concentration measurement points are shown in Fig. 3.6, which were measured by CO_2 recorders.

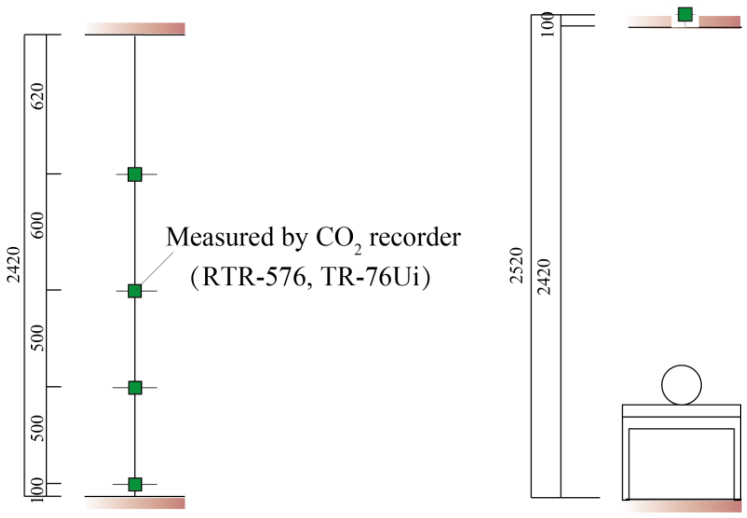

a) Air concentration b) Supply air concentration (SLW, SLD, SRW, SRD)

Fig. 3.6 Measurement points for concentration

3.4 Measurement instrument

The detail information of measurement instruments is shown in Table 3.3.

Table 3.3 List of experiment instrument

Instrument	Manufacturer	Amount
T-thermocouple		
Data logger (CADAC 3)	Etodenki Corporation	10
CO_2 recorder (RTR-576, TR-76Ui)	T&D Corporation	49
Mass flow controller (FCS-T1000L)	Fujikin	2
Read out model	Fujikin	2
Watt monitor (TAP-TST8N)	Sanwa supply	4
Slidac (V-130-3)	YAMABISHI Corporation.	2
Mini pump (MP-Σ500N2)	SIBATA	6

3.5 Result and analysis

3.5.1 Temperature

3.5.1.1 *Time variation of temperature*

The air conditioning used in the experiment is controlled so that it turns OFF when the difference between the set temperature and the temperature measured by the temperature sensor in the room becomes ±1 ℃ or more. During heating, the air conditioning operates at set temperature of 23 ℃ (Temperature change of the measurement point near the temperature sensor was shown in Fig. 3.7 (a)).

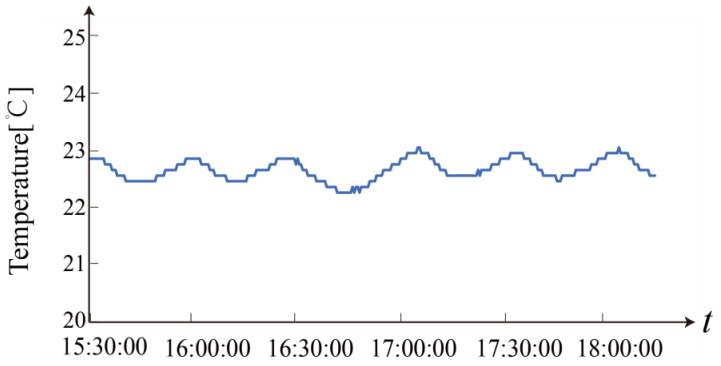

a) Temperature changes near the temperature sensor

However, when the indoor air temperature tends to rise, air conditioning turns ON/OFF repeatedly during the heating period. The reason is that the high-capacity (6.47kW) with 800m^3/h of the outdoor unit results in fluctuant temperature of supply air, when the outdoor air flow rate is small as 380m^3/h. According to the large temperature change with the elapse time, we can see that the supply air temperature fluctuates greatly (Fig. 3.7 (b)), and the indoor air temperature shows a large fluctuation (Fig. 3.7 (c)). Therefore, we focused on one cycle of temperature fluctuation and showed the vertical temperature distribution of average value, maximum value and minimum value in one cycle.

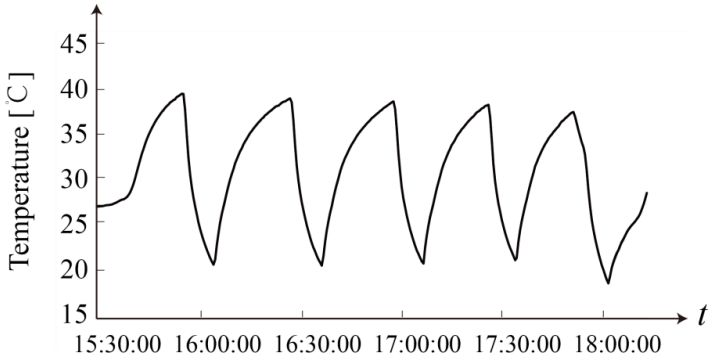

b) Changes of average temperature of supply air

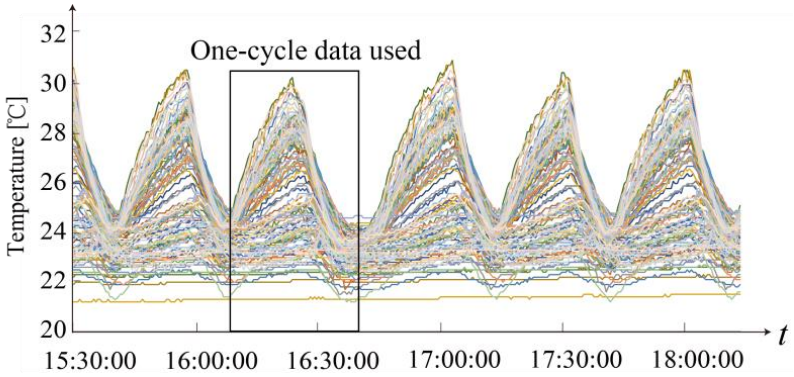

c) Temperature changes of indoor air

Fig. 3.7 Measured temperature change with time

3.5.1.2 *Vertical temperature distribution*

In order to research how the parameters influence the vertical temperature distributions, we compare the temperature of the first batch of experiments simulated the contaminants from patients.

3.5.1.2.1 Influence on vertical temperature distribution caused by the positions of exhaust ducts

By changing the positions of the exhaust ducts, some experiments are carried out. So, we fix the other two factors (curtains are wrapped and the tracer gas is breathed out from four manikins), as shown in Table 3.4 and Fig. 3.8~ Fig. 3.11.

Table 3.4 Conditions for three cases

Condition	Exhaust position	Positions of tracer gas generation	Curtains around bed
1EC-C-4B	1EC	4B	Closed
4EB-C-4B	4EB	4B	Closed
4EC-C-4B	4EC	4B	Closed

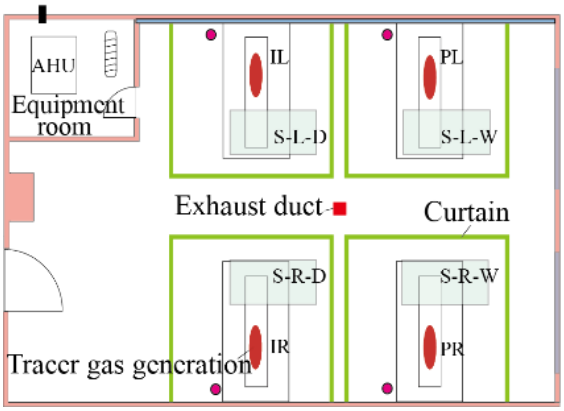

Fig. 3.8 Plan of experimental room (Exhaust duct of 1EC)

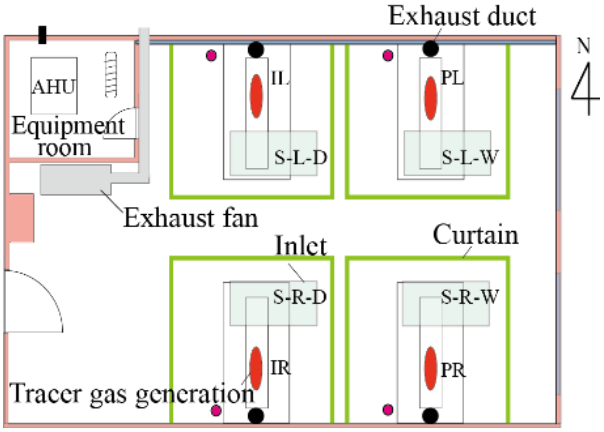

Fig. 3.9 Plan of experimental room (Exhaust duct of 4EC/4EB)

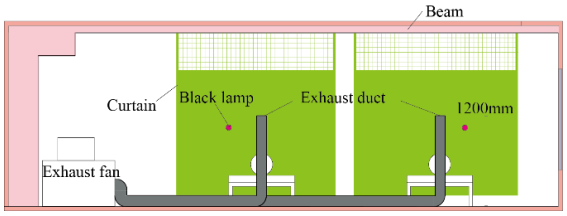

Fig. 3.10 Section of experimental room (Exhaust duct of 4EB)

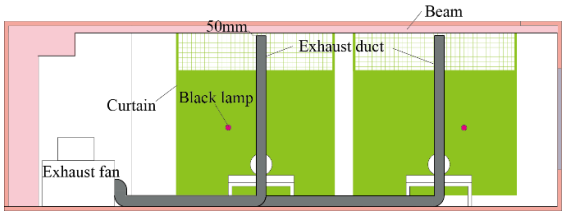

Fig. 3.11 Section of experimental room (Exhaust duct of 4EC)

Vertical temperature distributions of maximum value, minimum value and average value in one cycle were shown in Fig. 3.12~Fig. 3.14. The outdoor air temperature of condition 4EC-C-4B

conducted on 19th, Jan., 2017 is 8.2℃ and condition 4EB-C-4B on January 18th and condition 1EC-C-4B on January 16th is 9.4℃ and 6.7℃, respectively.

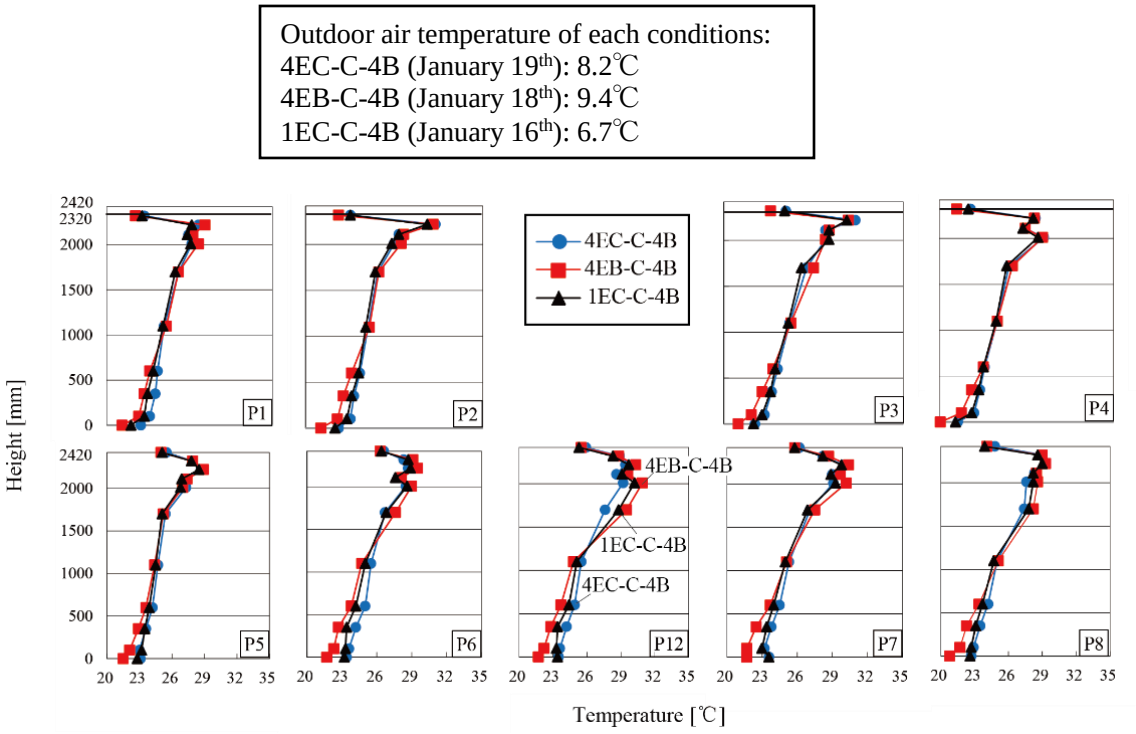

Fig. 3.12 Vertical temperature distribution of maximum value

(Contaminant source position: 4B, with curtain, position of the exhaust ducts: 4EC, 4EB and 1EC)

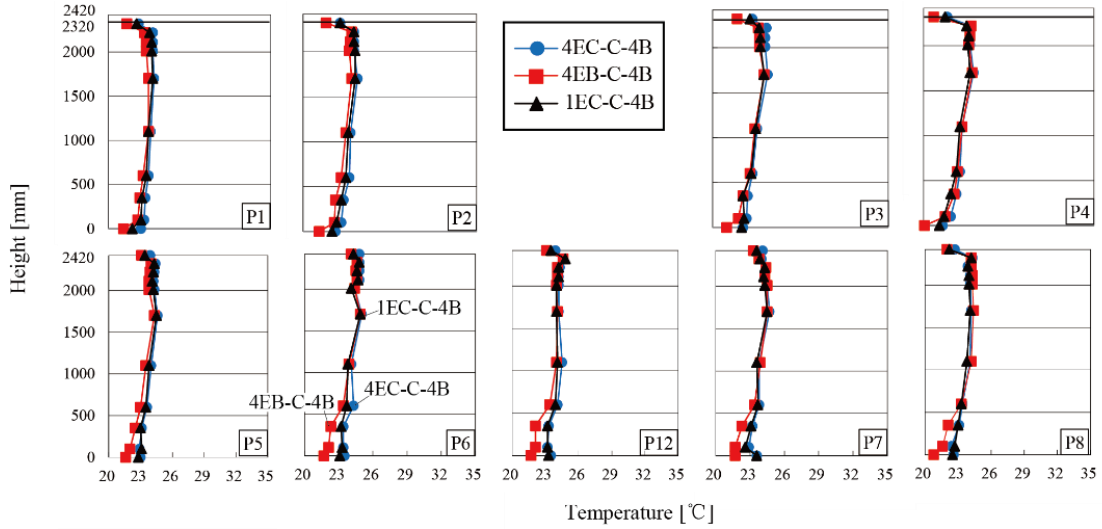

Fig. 3.13 Vertical temperature distribution of minimum value

(Contaminant source position: 4B, with curtain, position of the exhaust ducts: 4EC, 4EB and 1EC)

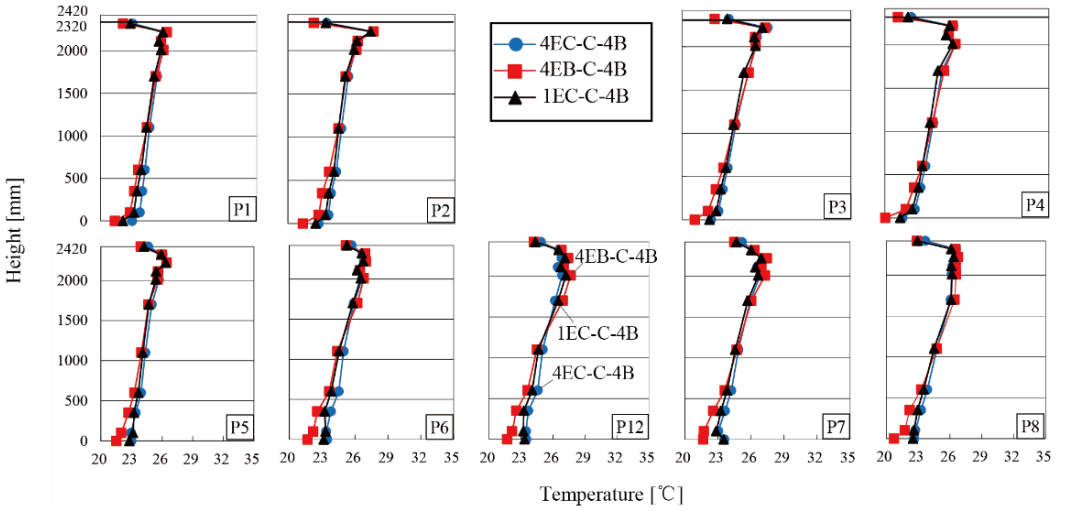

Fig. 3.14 Vertical temperature distribution of average value
(Contaminant source position: 4B, with curtain, position of the exhaust ducts: 4EC, 4EB and 1EC)

According to Fig. 3.12~ Fig. 3.14, the temperature developing tendencies change with the heights of the measurement points. Three cases collected the similar vertical temperature distribution, in which insignificant differences appeared. The values of vertical temperature show that the temperature increases gradually with the height. Especially, from the maximum values and average values, the significant temperature differences appear at the height of 2200mm, which result from the fact that the warm air has been out of the air supply diffusers stays in the upper part of the room during the heating period. It complies with the comfort evaluation standard of ISO since the temperature difference does not exceed 3℃ from FL+100mm to FL+1100mm.

3.5.1.2.2 Influence on vertical temperature distribution caused by curtains

(1) Position of the exhaust ducts: 4EC

When the exhaust ducts fixed on 4EC and tracer gas breathed out of the manikins, the experiments were carried out under the different situations of curtains. The differences between the two conditions are demonstrated in Table 3.5 and Fig. 3.13~ Fig. 3.14.

Table 3.5 Condition for mentioned cases

Condition	Exhaust position	Positions of tracer gas generation	Curtains around bed
4EC-C-4B	4EC	4B	Closed
4EC-NC-4B	4EC	4B	Open

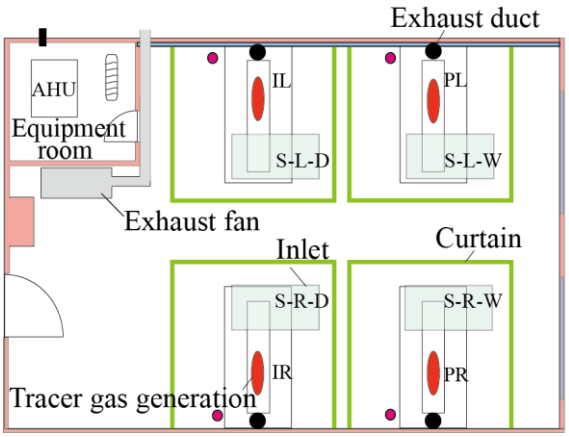

Fig. 3.13 Plan of experimental room
(Exhaust duct of 4EC, with curtain)

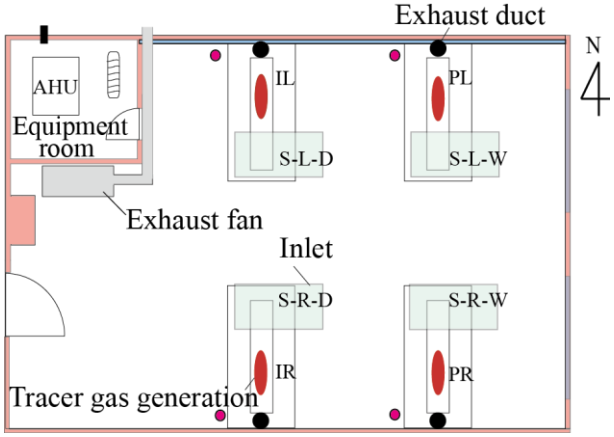

Fig. 3.14 Plan of experimental room
(Exhaust duct of 4EC, without curtain)

The vertical temperature distributions are shown in Fig. 3.15~ Fig. 3.17. The outdoor air temperature of condition 4EC- C-4B conducted on January 19th is 8.2℃ and condition 4EC-NC-4B on January 24th is 5.8℃, respectively.

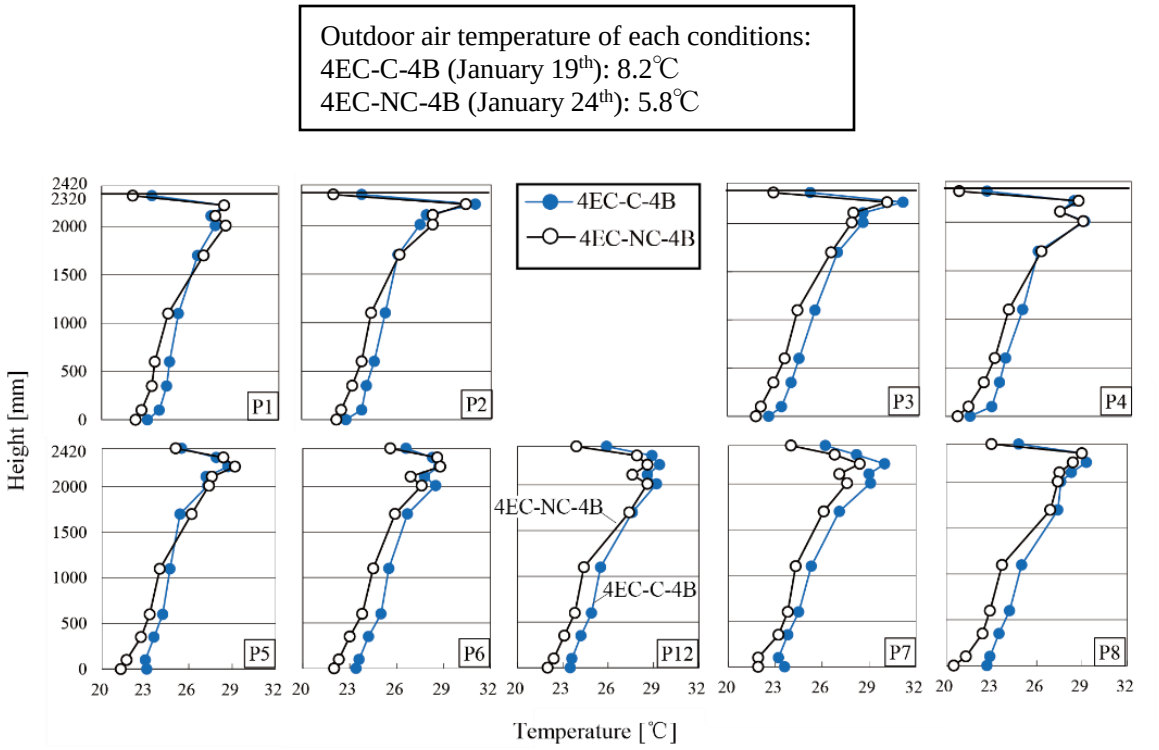

Fig. 3.15 Vertical temperature distribution of maximum value
(Contaminant source position: 4B, location of the exhaust ducts: 4EC, two different situations of the curtains)

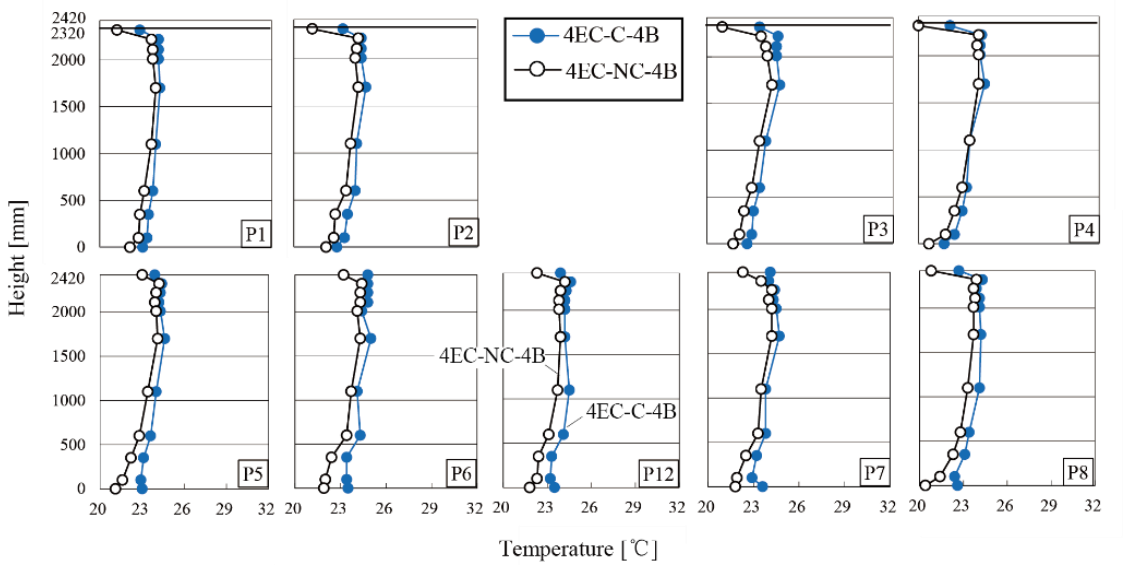

Fig. 3.16 Vertical temperature distribution of minimum value

(Contaminant source position: 4B, location of the exhaust ducts: 4EC, two different situations of the curtains)

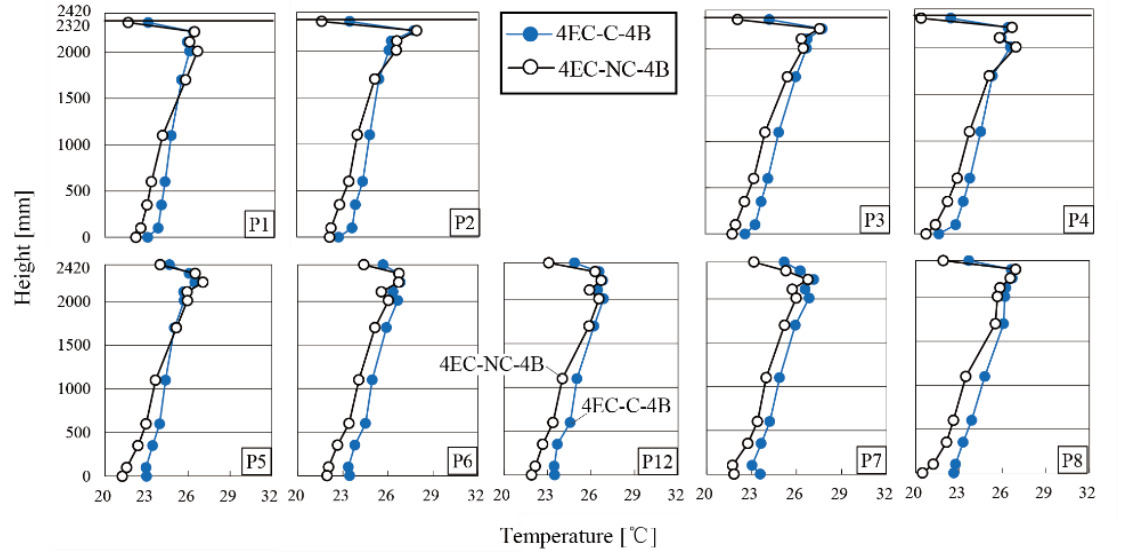

Fig. 3.17 Vertical temperature distribution of average value

(Contaminant source position: 4B, location of the exhaust ducts: 4EC, two different situations of the curtains)

It is clear that the vertical temperature between the two cases shows a few differences. It may be caused by the different temperature of outdoor air, since the two experiments were carried out on different day.

(2) Position of the exhaust ducts: 1EC

Based on the premise that the position of exhaust duct is fixed in the center of the room at the height of 50mm below the ceiling (1EC) coupled with the tracer gas breathed out of the manikins, the vertical temperature distribution in two cases are analyzed under the different situations of the curtains. The description of conditions for mentioned cases is listed in Table 3.6 and Fig. 3.18~ Fig. 3.19. Moreover, the outdoor air temperature of condition 1EC- C-4B conducted on January 16th is 6.7℃ and condition 1EC-NC-4B on January 27th is 7.4℃.

Table 3.6 Condition for mentioned cases

Condition	Exhaust position	Positions of tracer gas generation	Curtains around bed
1EC-NC-4B	1EC	4B	Open
1EC-C-4B	1EC	4B	Closed

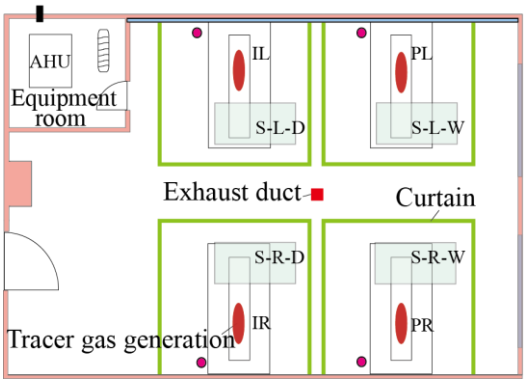

Fig. 3.18 Plan of experimental room (Exhaust duct of 1EC, with curtain)

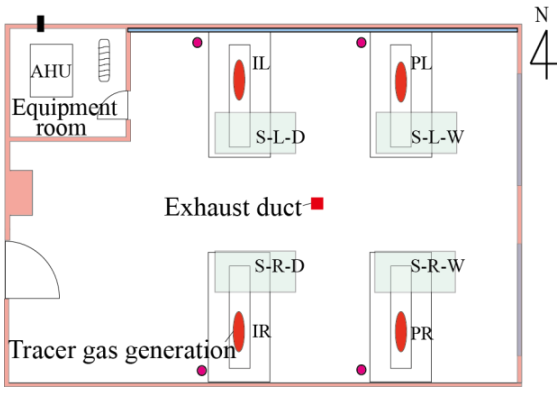

Fig. 3.19 Plan of experimental room (Exhaust duct of 1EC, without curtain)

From Fig. 3.20~ Fig. 3.2, we can see the distribution of vertical temperature between the two cases (1EC-C-4B and 1EC-NC-4B). The two cases collected the similar vertical temperature distribution, in which a few differences appeared. It may be caused by the different temperature of outdoor air. It is noteworthy that from the maximum values and average values, the significant temperature differences appear at the height of 2200mm, which result from the fact that the warm air has been out of the air supply diffusers stays in the upper part of the room during the heating period. It complies with the comfort evaluation standard of ISO since the temperature difference does not exceed 3℃ from FL+100mm to FL+1100mm.

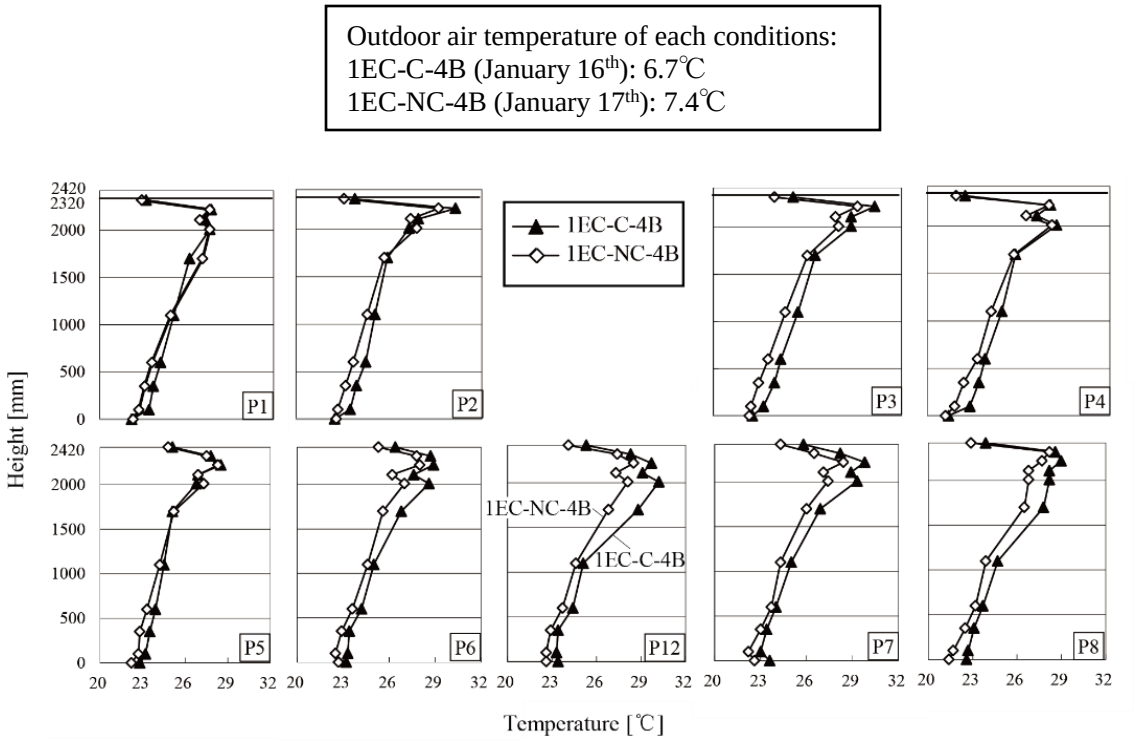

Fig. 3.20 Vertical temperature distribution of maximum value
(Contaminant source position: 4B, location of the exhaust ducts: 1EC, two different situations of the curtains)

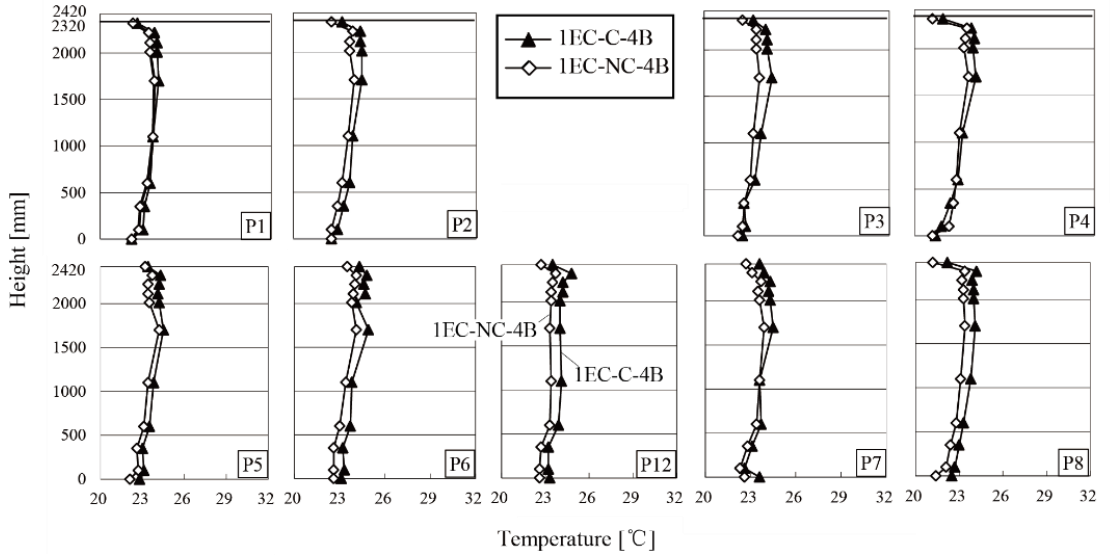

Fig. 3.21 Vertical temperature distribution of minimum value
(Contaminant source position: 4B, location of the exhaust ducts: 1EC, two different situations of the curtains)

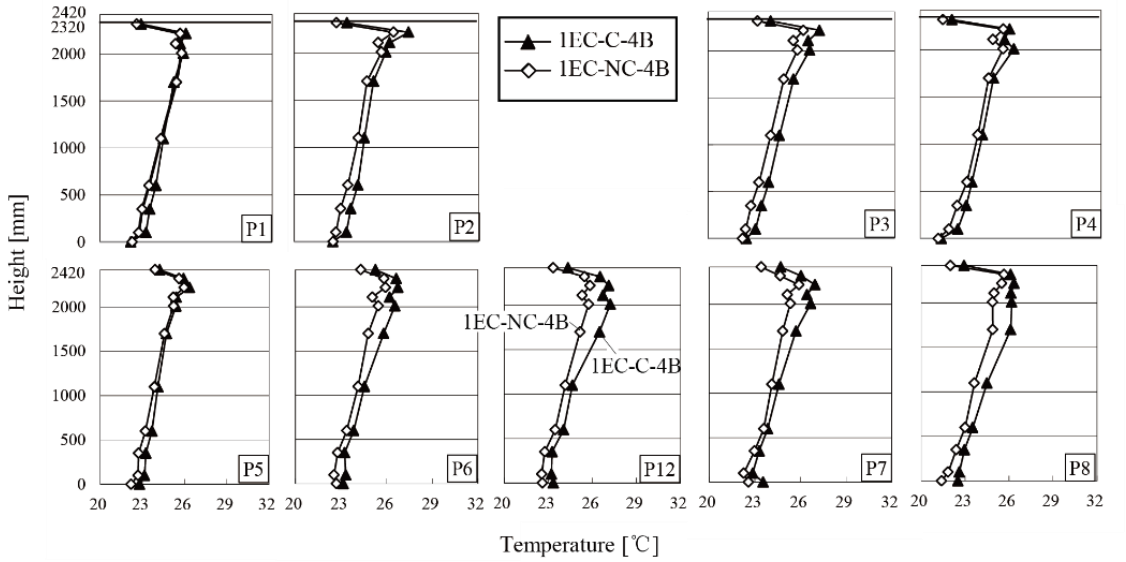

Fig. 3.22 Vertical temperature distribution of average value

(Contaminant source position: 4B, location of the exhaust ducts: 1EC, two different situations of the curtains)

3.5.2Concentration

3.5.2.1 *Time variation of concentration*

As a part of tracer gas breathed out of the manikins flowed into the equipment room through the crack between the door of the equipment room and the floor, the ratio of tracer gas remaining in the experimental room h_r of heating condition was calculated.

According to the contamination balance in equipment room, formula (3.1) can be gotten.

$$C_{OA}Q_{OA} + (1-\eta_r)M = C_{SA}Q_{SA} \tag{3.1}$$

Where, C_{OA} [ppm] is the concentration of outdoor air and C_{SA} [ppm] is the concentration of supply air, Q_{OA}, Q_{SA} [m^3/h] is the airflow rate of outdoor air and supply air, respectively, M[m^3/h] stands for emission rate of tracer gas and h_r was the ratio of tracer gas distributed in the experimental room.

Based on formula (3.1), values of h_r can be calculated as formula (3.2) and shown in Table 3.7.

$$\eta_r = 1 - \frac{C_{SA}Q_{SA} - C_O Q_O}{M} \tag{3.2}$$

Table 3.7 The ratio of tracer gas distributed in the experimental room

Item	Condition	h_r
Case 1	1EC-NC-4B	0.10~0.41
Case 2	1EC-C-4B	0.11~0.41
Case 3	4EB-C-4B	0.32~0.63
Case 4	4EC-C-4B	0.20~0.49
Case 5	4EC-NC-4B	0.24~0.54
Case 6	1EC-NC-4D	0.18~0.48
Case 7	1EC-C-4D	0.11~0.41
Case 8	4EB-C-4D	0.24~0.57
Case 9	4EC-C-4D	0.12~0.42
Case 10	4EC-NC-4D	0.26~0.56

※ It is noteworthy that the minimal values of are calculated by the outdoor air flow rate of 380m^3/h with the assumption that the airflow rate of returning air to the equipment room through the crack is 70 m^3/h, i.e. there is no exfiltration flow through the other gaps. While, the counterpart maximums are calculated by the outdoor air flow rate of 450m^3/h with the assumption that there is no returning air to the equipment room through the crack, namely, the total airflow rate of exfiltration flow through the other gaps is 70m^3/h. It may sound a kind of contradiction, because no returning airflow cannot convey any tracer gas to the equipment room. It can be suggested that some amount of mutual airflow across the door of equipment room convey the emitted tracer gas.

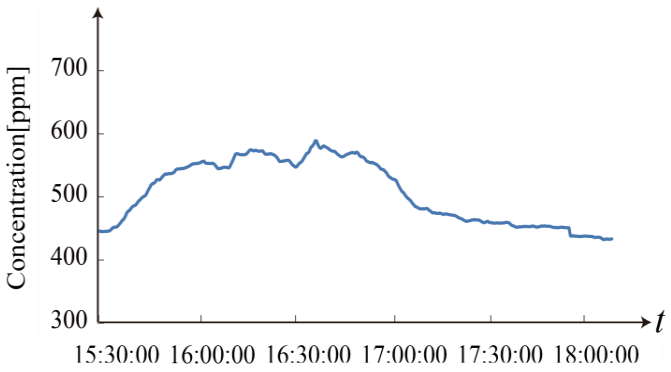

a) Concentration changes of supply air

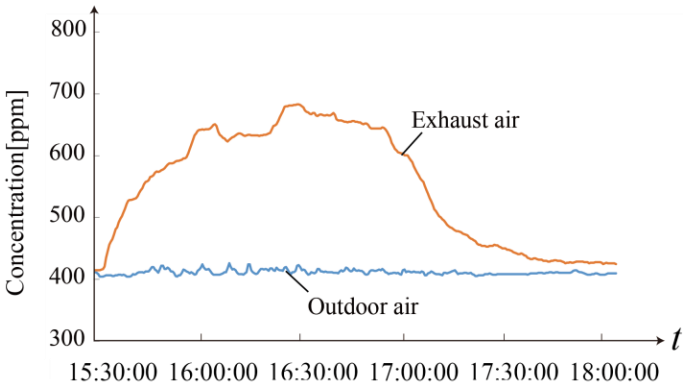

b) Concentration changes of outdoor air and exhaust air

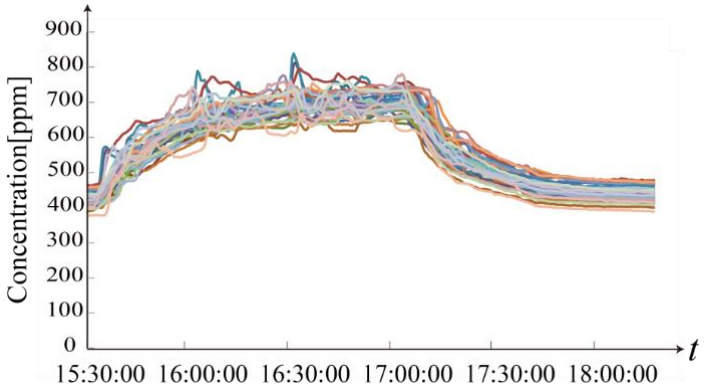

c) Concentration changes of indoor air

Fig. 3.23 Measured concentration change with time

From Fig. 3.23, the concentration of supply air increased in Fig. 3.23 (a), the concentration variation of outdoor air as well as exhaust air are illustrated in Fig. 3.23 (b) and the indoor air concentration change is shown in Fig. 3.23 (c). It can be seen that there were some slight fluctuates during the measurement period. It was found that these phenomena were related to rather the changes of outdoor air concentration than the stability of CO_2 recorders. Since CO_2 recorders were calibrated after finishing data collecting, where the data obtained was used to process experimental data.

According to the Eq. (3.3), the normalized concentration could be calculated.

$$C_n = \frac{C_P - C_{SA}}{C_{EA} - C_{SA}} \tag{3.3}$$

Here, C_n [ppm] is normalized concentration, and C_{EA} [ppm] is the concentration of exhaust air and C_P [ppm] is the concentration of point P.

3.5.2.2 *Vertical concentration distribution*

3.5.2.2.1 Influence on normalized concentration distribution caused by the positions of exhaust ducts

In order to research how the positions of the exhaust ducts influence normalized concentration distributions, the other two factors are fixed (curtains are wrapped and the tracer gas is breathed out from four manikins). By changing the positions of the exhaust ducts, experiments are carried out. The differences among each condition is illustrated in Table 3.8 and Fig. 3.24~ Fig. 3.27.

Table 3.8 Conditions for three cases

Condition	Exhaust position	Positions of tracer gas generation	Curtains around bed
1EC-C-4B	1EC	4B	Closed
4EB-C-4B	4EB	4B	Closed
4EC-C-4B	4EC	4B	Closed

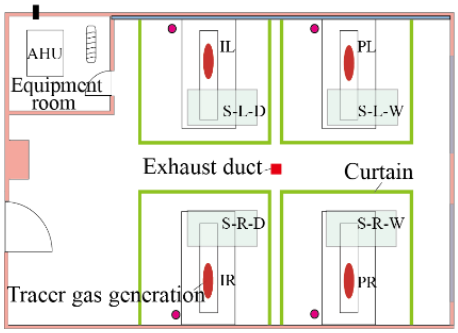

Fig. 3.24 Plan of experimental room (Exhaust duct of 1EC)

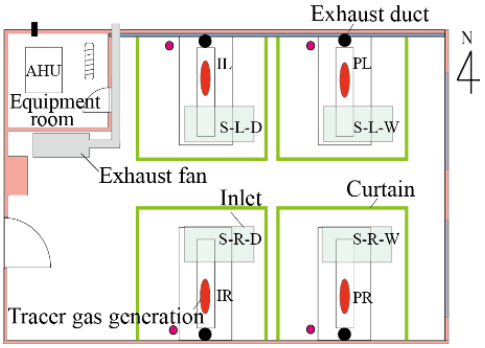

Fig. 3.25 Plan of experimental room (Exhaust duct of 4EC/4EB)

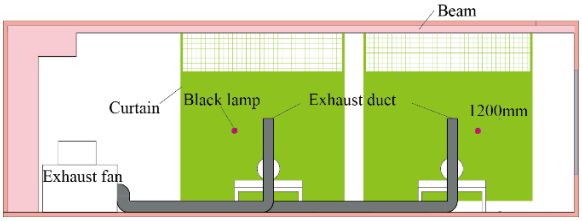

Fig. 3.26 Section of experimental room (Exhaust duct of 4EB)

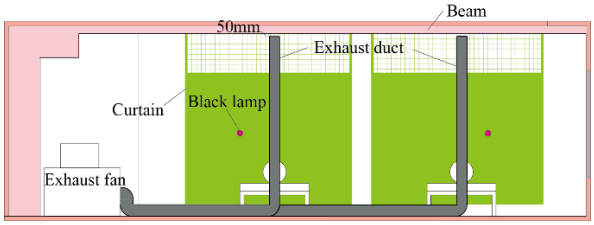

Fig. 3.27 Section of experimental room (Exhaust duct of 4EC)

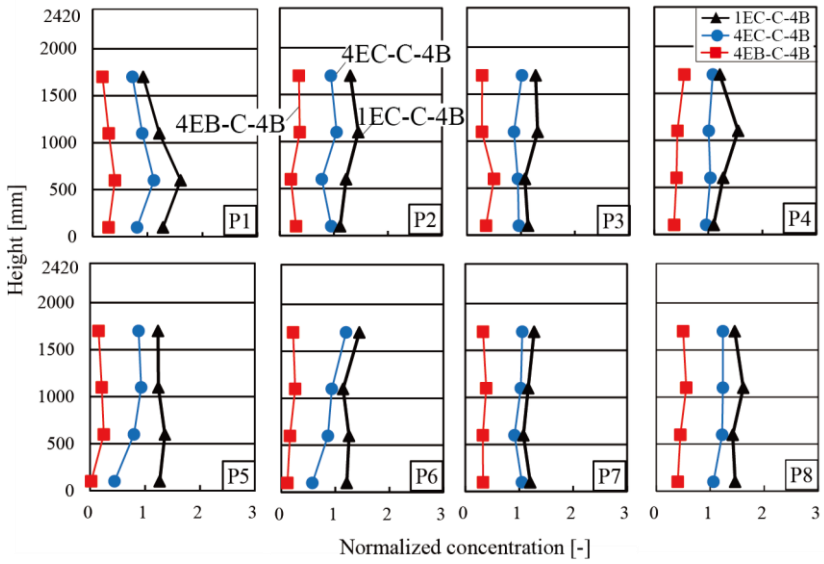

Fig. 3.28 Normalized concentration distribution

(Contaminant source position: 4B, with curtain, position of the exhaust ducts: 4EC, 4EB and 1EC)

Supply air concentration and the exhaust concentration were defined as 0 and 1, respectively. Fig. 3.28 provides some noteworthy data with respect to the vertical concentration distributions. It was clear from the subgraphs that CO_2 spread to the entire room uniformly. It can be seen that the ventilation efficiencies were high due to four exhaust ducts, and the values of normalized concentration in the case 4EB-C-4B was smaller than those of in the other two cases. This demonstrates that the condition 4EB presents the excellent ventilation efficiency, in which the exhaust duct is close to the resource of contaminant.

3.5.2.2.1 Influence on normalized concentration distribution caused by curtains

(1) Position of the exhaust ducts: 4EC

On the premise of the position of the exhaust ducts fixed on 4EC and tracer gas breathed out of the manikins, the experiments were carried out under the different situations of curtains. The differences between the two conditions are demonstrated in Table 3.9 and Fig. 3.29~ Fig. 3.30.

Table 3.9 Condition for mentioned cases

Condition	Exhaust position	Positions of tracer gas generation	Curtains around bed
4EC-C-4B	4EC	4B	Closed
4EC-NC-4B	4EC	4B	Open

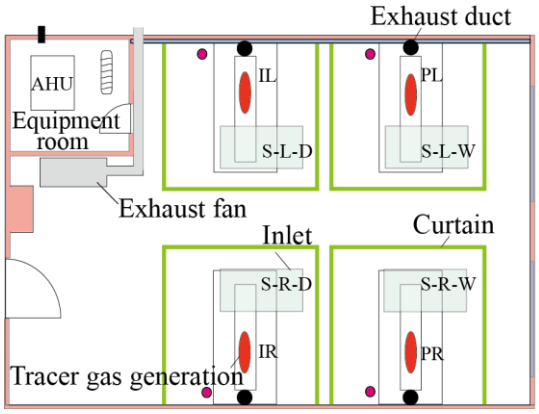

Fig. 3.29 Plan of experimental room
(Exhaust duct of 4EC, with curtain)

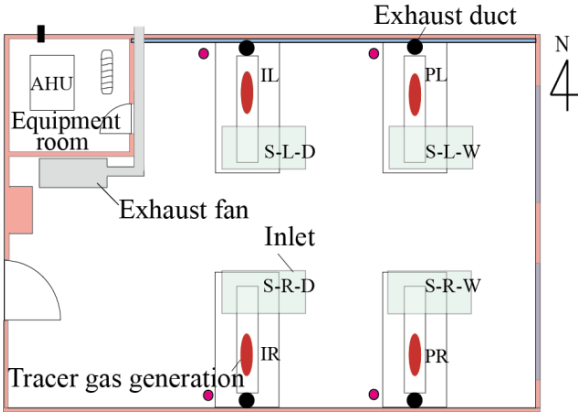

Fig. 3.30 Plan of experimental room
(Exhaust duct of 4EC, without curtain)

The normalized concentrations in vertical profiles are shown in Fig. 3.31.

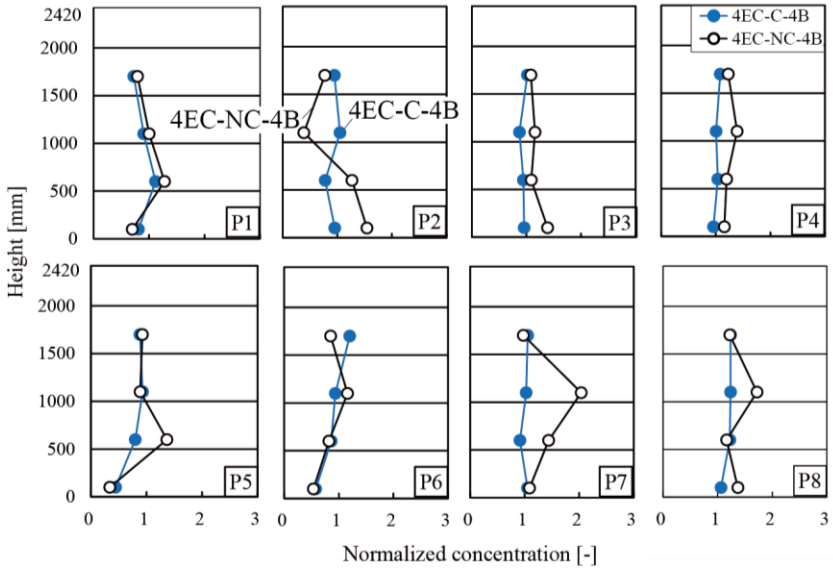

Fig. 3.31 Normalized concentration distribution
(Contaminant source position: 4B, location of the exhaust ducts: 4EC, two different situations of the curtains)

It is clear that the normalized concentration shows a few differences among these cases. Generally speaking, the normalized concentration is higher at the case under the situation of curtain being open. However, some obvious differences are observed at some measurement points inside the curtain, because of the barrier function of curtains to the contaminants. As a whole, the influence of the curtains on the contaminant removal efficiency is reckoned to be minor.

(2) Position of the exhaust ducts: 1EC

When the position of exhaust duct is fixed in the center of the room at the height of 50mm below the ceiling (1EC) coupled with the tracer gas breathed out of the manikins, the normalized concentrations in two cases are analyzed under the different situations of the curtains. The description of conditions for mentioned cases is listed in Table 3.10 and Fig. 3.32~ Fig. 3.33.

Table 3.10 Condition for mentioned cases

Condition	Exhaust position	Positions of tracer gas generation	Curtains around bed
1EC-NC-4B	1EC	4B	Open
1EC-C-4B	1EC	4B	Closed

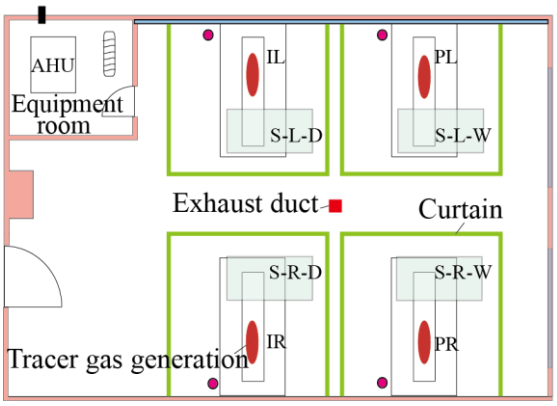

Fig. 3.32 Plan of experimental room (Exhaust duct of 1EC, with curtain)

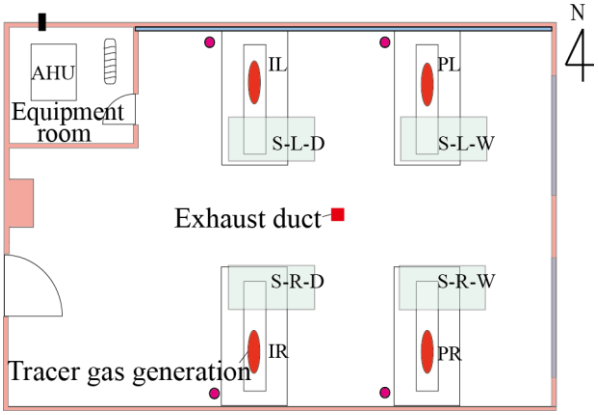

Fig. 3.33 Plan of experimental room (Exhaust duct of 1EC, without curtain)

Fig. 3.34 illustrated the distribution of normalized concentration between the two cases (1EC-C-4B and 1EC-NC-4B). The value of normalized concentration is higher as the curtain is wrapped around the bed. Contaminant generated from the patients is prone to flow to the exhaust duct when the curtains are removed, because the position of the exhaust duct is outside the curtain. The contaminant removal efficiency is better than that in situation of beds being wrapped when exhaust duct is fixed at 1EC.

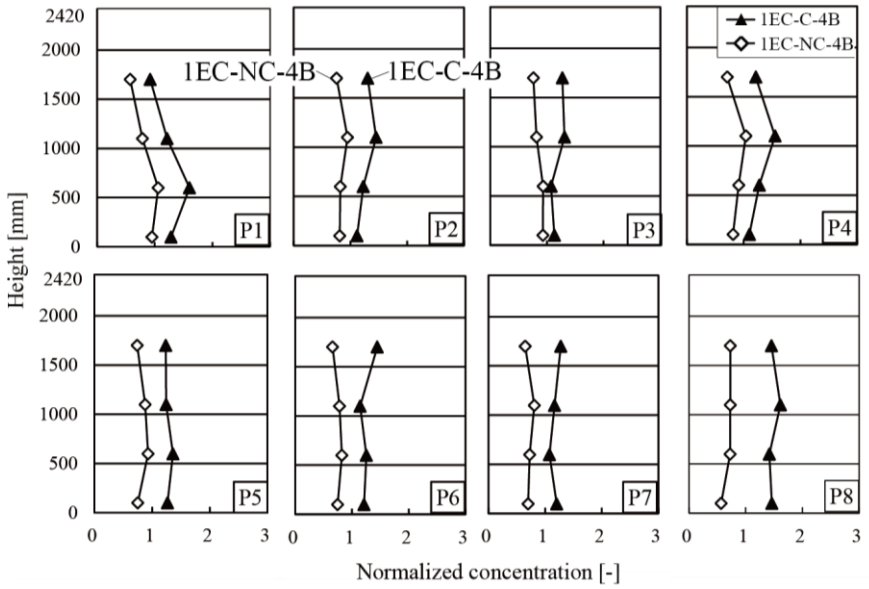

Fig. 3.34 Normalized concentration distributions

(Contaminant source position: 4B, location of the exhaust ducts: 1EC, two different situations of the curtains)

3.5.3Local mean age

3.5.3.1 *The average age of air <τ>*

Local mean age of air is calculated by the same improved step-up method as used in cooling condition. Changes of concentration and response function of heating condition are illustrated in Fig. 3.35.

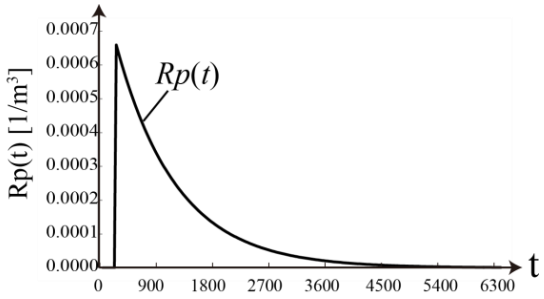

a) Impulse response function at supply diffuser

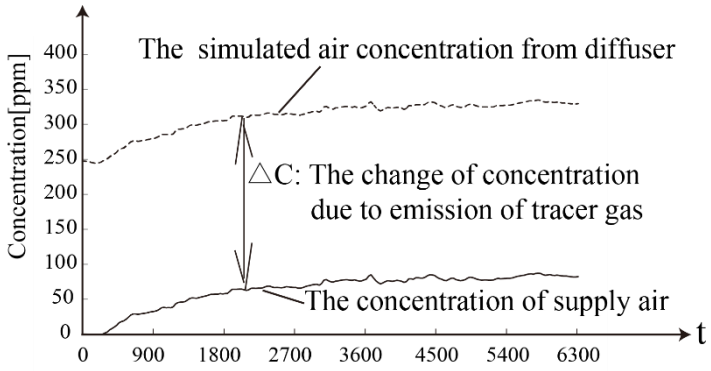

b) Change of supply air concentration at inlet

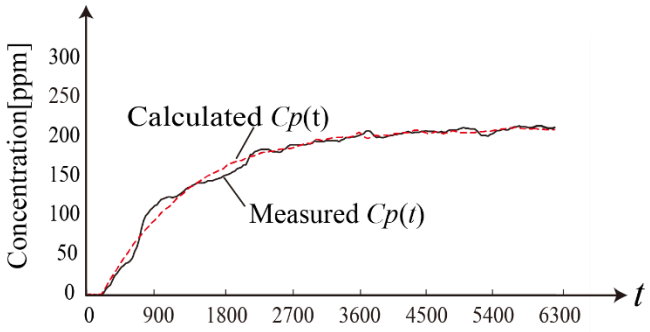

c) An example for the concentration curve at a certain point

Fig. 3.35 Changes of concentration and response function of heating condition

In addition, the results of both the average age of air <τ> and the air exchange efficiency η of heating condition were listed in Table 3.11.

Table 3.11 Room average age of air and the air exchange efficiency

τ_n=11.16

Condition	Room average age of air τ [min]	Air exchange efficiency η [-]
1EC-NC-4D	17.0	0.66
1EC-C-4D	16.1	0.69
4EB-C-4D	14.1	0.79
4EC-C-4D	15.0	0.74
4EC-NC-4D	14.7	0.76

3.5.3.2 *Vertical distributions of local mean age of air*

The influence of relevant parameters on local mean age of air and the results of the vertical distributions is shown below.

Firstly, the effect of the positions of exhaust ducts on the local mean age of air is analyzed, under the situation of the bed being wrapped by the curtains. Table 3.12 and Fig. 3.36~ Fig. 39 show the condition of the three cases, in which the difference is the position of the exhaust ducts.

Table 3.12 Conditions for three cases

Condition	Exhaust position	Positions of tracer gas generation	Curtains around bed
1EC-C-4D	1EC	4D	Closed
4EB-C-4D	4EB	4D	Closed
4EC-C-4D	4EC	4D	Closed

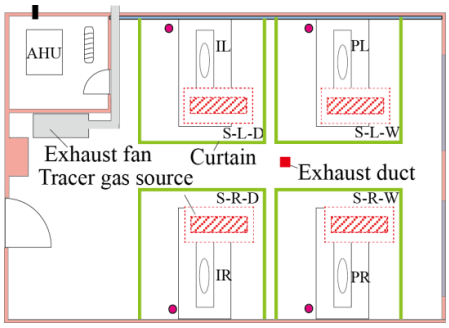

Fig. 3.36 Plan of experimental room (Exhaust duct of 1EC)

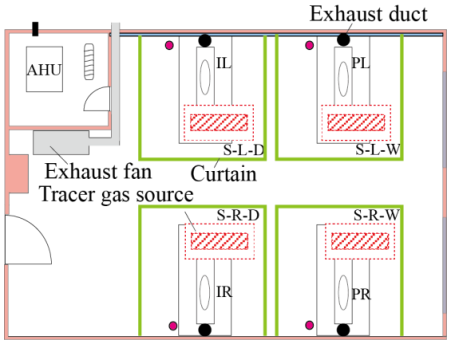

Fig. 3.37 Plan of experimental room (Exhaust duct of 4EC/4EB)

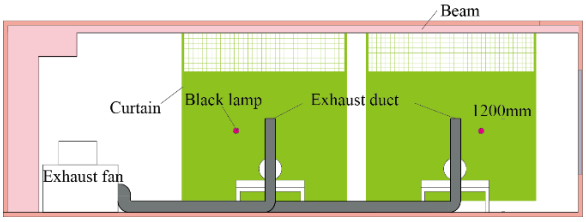

Fig. 3.38 Section of experimental room (Exhaust duct of 4EB)

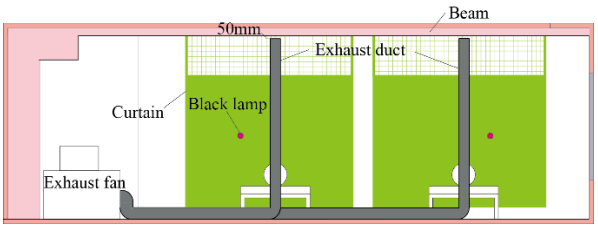

Fig. 3.39 Section of experimental room (Exhaust duct of 4EC)

Fig. 3.40 shows the results of the air age when the positions of the exhaust ducts are changed. It can be seen that the local mean ages of air under the condition of 4EB are smaller than those of at the other two conditions, where the positions of four exhaust ducts are laid at approximately 1200mm above the floor on the wall. It can be inferred that the air from the air supply diffusers goes down quickly and the air flows to the lower space within the curtains earlier.

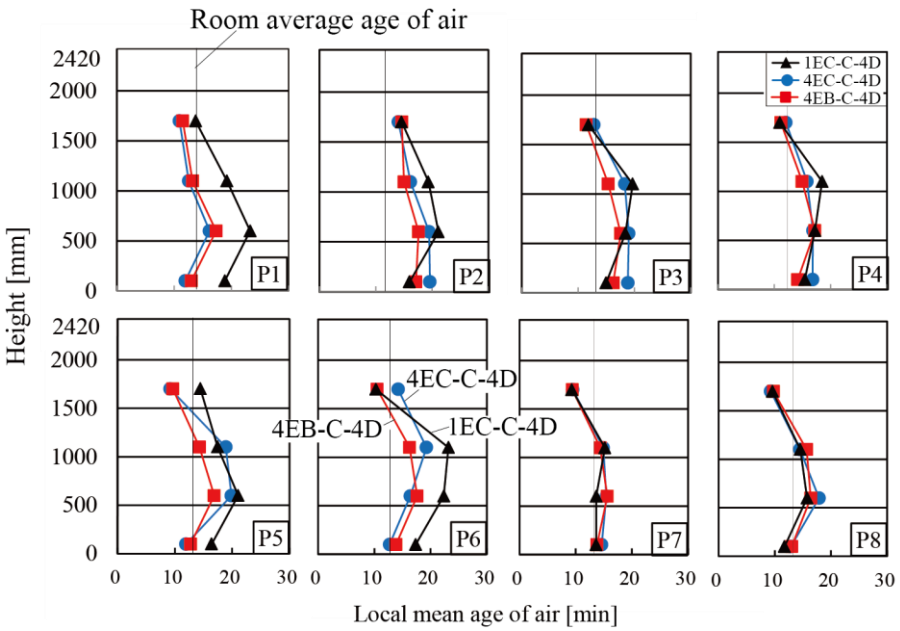

Fig. 3.40 Local mean age of air
(Contaminant source position: 4D, with curtain, position of the exhaust ducts: 4EC, 4EB and 1EC)

Then, in Table 3.11, comparing the conditions of 4EC and 1EC, the room average age of air under the condition of 4EB is the lowest and the air exchange efficiency under the condition of 4EB show the maximum values. It can be considered that the ventilation efficiency of 4EB is excellent.

Subsequently, the influence of curtains is studied. The difference is the situations of the curtains under the same condition of 4EC, as shown in Table 3.13 and Fig.41~ Fig.3.42.

Table 3.13 Condition for mentioned cases

Condition	Exhaust position	Positions of tracer gas generation	Curtains around bed
4EC-C-4D	4EC	4D	Closed
4EC-NC-4D	4EC	4D	Open

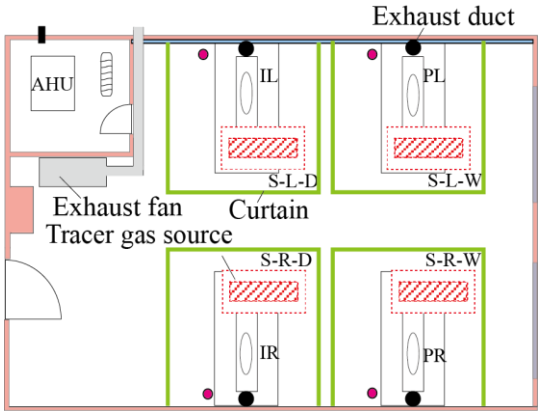

Fig. 3.41 Plan of experimental room
(Exhaust duct of 4EC, with curtain)

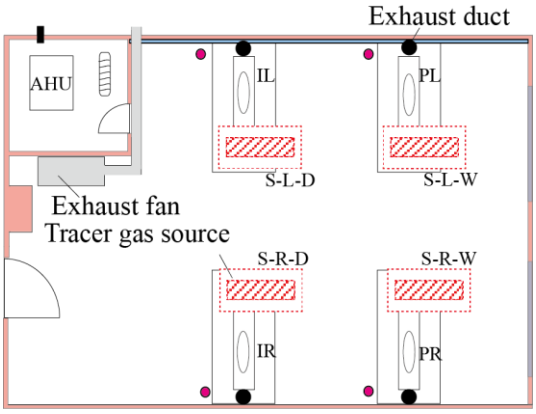

Fig. 3.42 Plan of experimental room
(Exhaust duct of 4EC, without curtain)

From the Fig. 3.43, it can be seen that the results of the vertical distributions are similar in the both conditions. Specifically, the air exchange efficiency is 0.74 (in Table 3.11) under the situation of the bed being wrapped by the curtains and it is 0.76 under the situation of curtains removed. The exhaust duct is included in the inner space of the curtain under the condition of 4EC, which results in that curtains show a minor influence on the mean age of air. To some extent, curtains prevent the contaminants escaping from the closed space around the bed.

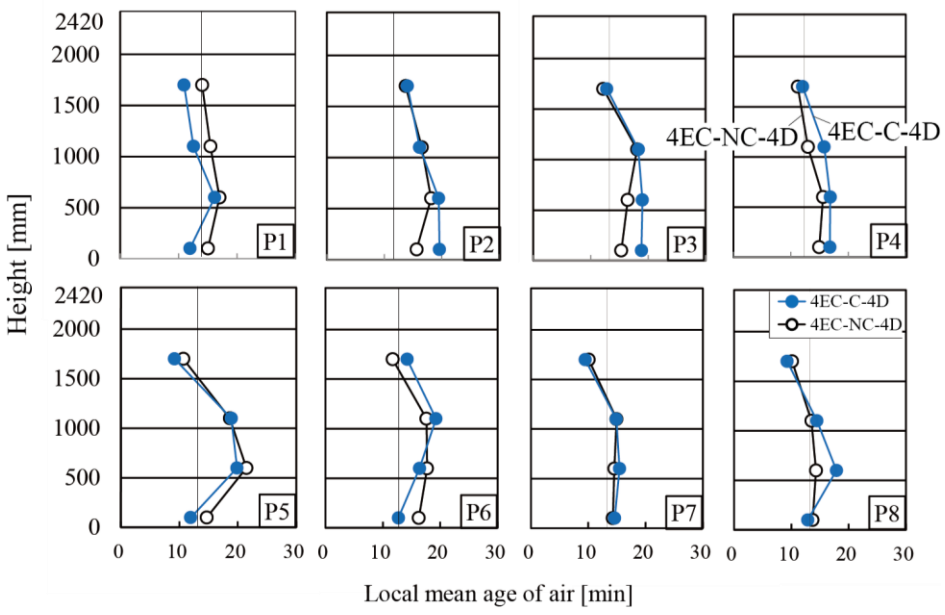

Fig. 3.43 Local mean age of air
(Contaminant source position: 4D, location of the exhaust ducts: 4EC, two different situations of the curtain)

Eventually, the local mean ages of air in two cases are analyzed under the different situation of the curtains, where the exhaust ducts are laid in the center of the room at the height of 50mm below the ceiling (1EC). (see Table 3.14 and Fig. 3.44~Fig. 3.45)

Table 3.14 Condition for mentioned cases

Condition	Exhaust position	Positions of tracer gas generation	Curtains around bed
1EC-NC-4D	1EC	4D	Open
1EC-C-4D	1EC	4D	Closed

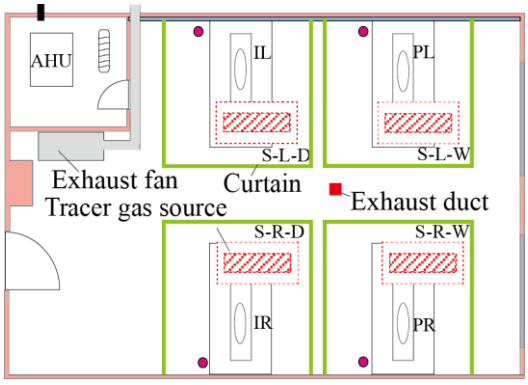

Fig. 3.44 Plan of experimental room
(Exhaust duct of 1EC, with curtain)

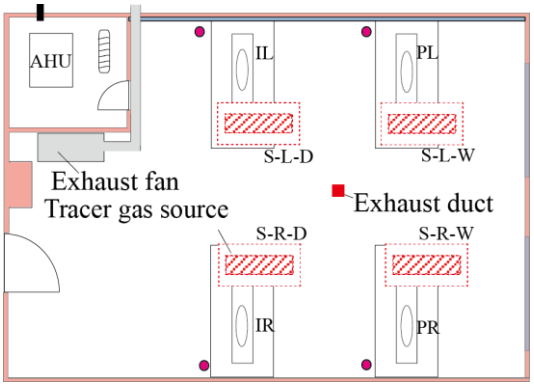

Fig. 3.45 Plan of experimental room
(Exhaust duct of 1EC, without curtain)

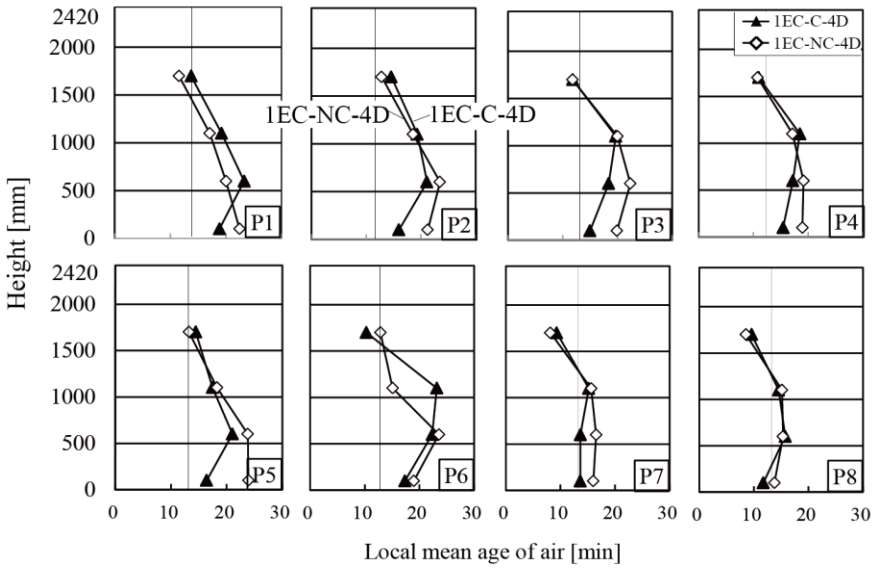

Fig. 3.46 Local mean age of air
(Contaminant source position: 4D, location of the exhaust ducts: 1EC, two different situations of the curtain)

According to the Fig. 3.46, the measured points at the lower position outside the curtains (P1-P5) have the lower local mean ages of air, which results from air movement in the lower position inside the space of curtains. Air exchange efficiency for two different situations of curtain are 0.66 and 0.69, respectively. The better performance can be found under the condition of 1EC and the curtains being removed.

3.6 Discussion and summary

1) The indoor temperature fluctuates obviously with the change of supply air temperature due to the fact that air conditioning turns ON/OFF repeatedly during the heating period, which results from the large capacity of the outdoor unit ($800m^3/h$) and the low outdoor air flow rate ($380m^3/h$).

2) Insignificant differences of vertical temperature distribution exist in different cases which have the different conditions. The values of the wall temperature and air temperature almost show the constants at some measured points, which are placed at the high positions. The related fact is that the warm air has been out of the air supply diffusers stays in the upper part of the room during the heating period.

3) The positions of the exhaust ducts play an influential role on the normalized concentration distributions. Basically, the contaminant removal efficiency improves obviously when the exhaust ducts are closer to the source of contaminants.

4) In terms of the influence of the curtains on the indoor environment, to some extent, the barrier function of curtains to the contaminants is verified.

5) The positions of the exhaust ducts have strong influence on the mean age of air. The lower local mean age of air and the better efficiency of average air exchange can be obtained when the exhaust ducts close to the source of contaminants. There is a minor influence of curtains on the local mean age of air, though it can change the directions of the air flow.

6) Compared with cooling, the lower air exchange efficiency ($\eta < 1.0$) is obtained under heating condition because of the vertical temperature stratification (only 2.8 ℃). However, it measures up the comfort evaluation criteria of ISO since the temperature difference does not exceed 3 ℃ from FL+100mm to FL+1100mm in residential area. In addition, according to the values of η,

although the system does not reach complete mixing ventilation thoroughly, normalized concentration distributions show the minor difference, i.e., there are fewer contaminants to be stuck.

Chapter 4 CONCLUSION

4.1 Overview and objectives

In this study, we used the air conditioning with Ceiling Induction Diffusers (CID) in sickroom with 4-bed ward. In order to examine the practicability and validity of CID system, several experiments are conducted in a simulation sickroom whose size and appearance are set as the real sickroom. In order to cater to the real environment of the ward, manikins who can exhale the gas with contaminant are arranged and black lamps are also set for simulating the heat generated by household appliances such as TV, refrigerator etc. Moreover, the gauge points in the monitoring process were widely arranged, including the horizontal and vertical distributions. The layout of device and decoration in the ward probably has influence on the indoor environment, therefore, these factors were also considered in this study.

Some indicators related to the indoor environment quality of ward are collected and analyzed, such as indoor air temperature, the concentration of contaminant and local mean age of air, air velocity and radiation etc., under both cooling condition and heating condition.

4.2 Result of cooling condition

4.2.1 All condition

Vertical temperature distribution

Regarding the vertical temperature distribution, the vertical temperature difference in the residential area under all conditions is within 3°C, which means that a good thermal environment is formed. In addition, temperature fluctuation in the residential area is smaller than the temperature fluctuation of the whole measurement point with time.

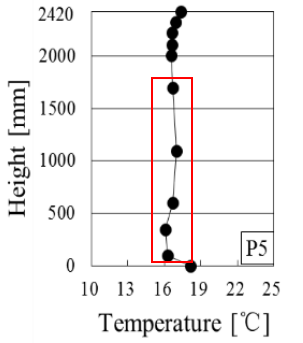

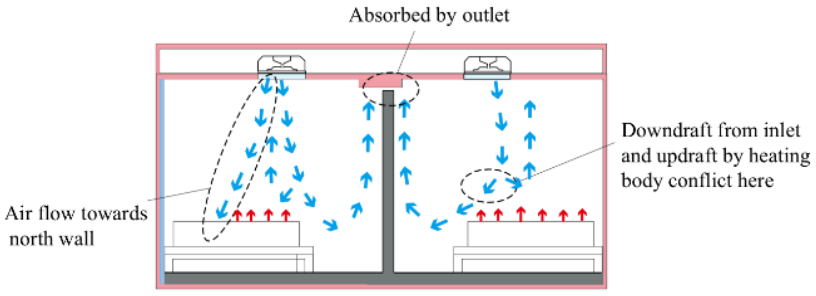

Fig. 4.1 Temperature vertical distribution **Fig. 4.2** Air flow in one section

Vertical normalized concentration distribution

Regarding the normalized concentration distribution of contaminant, in most cases, the value is about 1, indicating that the contaminants diffuse throughout the entire room.

Local mean age of air

In general, the air exchange efficiency is 1 in the case of perfect mixing and 2 in the case of piston flow, whereas if it is smaller than 1 it is presumed that a retention zone due to a short circuit flow is generated. The step-up method gives a larger value, but in either case it is around 1, indicating that the ventilation performance is mixing exchange.

Airflow behavior

It is obvious from visualization experiment that the blowout air from the air supply port descends immediately below the air supply port although it is low initial speed (0.2 m/s to 0.8 m/s).

Also, regarding the flow from the room to the machine room, the ratio of gas remaining in the room has an increasing order as 4EB> 4EC> 2EC> 1EC, and the flow to the machine room is decreasing. Comparing the presence or absence of a curtain, the curtain presence condition has a larger remaining ratio. It is conceivable that the flow of air to the machine room is blocked by the curtain.

Air velocity

Air velocity at all of the measurement points is small, which is less than 0.3m/s. In addition, at the height of FL+1700mm, the air velocity is relatively smaller than the other points.

Radiation

Radiation temperature is 0.3~0.5°C lower than indoor temperature. However, because of the influence of heating element, the radiation temperature is relatively higher than indoor temperature.

4.2.2 Different conditions

Influence of curtain

There was no big difference in temperature.

Regarding the contaminant concentration and age of air, when the contaminant source and air supply port are inside the curtain, if the curtain is closed, the contaminants can be exhausted without flowing to the outside of the curtain. On the other hand, if there is no curtain, it is conceivable that contaminants and air supply are spreading throughout the entire room. Therefore, although the effect of preventing the contamination diffusion of the curtain is different depending on the positions of the exhaust port and the air supply port, it is considered that there is a diffusion prevention effect in both cases.

Also, it can be concluded from the vertical distribution of the age of air in each case under the condition with curtains that the age of air at the low position was small outside the curtain, furthermore, we can conclude that the air is flowing out from the lower part of the curtain to the outside.

Effects of exhaust port position

In the cooling experiment, comparison experiment was made at the four exhaust port positions.

First of all, there was no big difference in temperature.

Moreover, as the contaminant concentration takes the lowest value at the exhaust port condition 4EB located near the pollutant source, it can be seen that the contaminant removal efficiency is improved by providing the exhaust port near the contaminant.

In addition, when comparing the values between the conditions for the room-average air exchange efficiency, in the case of the exhaust port condition 1EC, the value is large. But in a one-time experiment, it is difficult to conclude that the ventilation performance is good and more experiments are required

Comparing the exhaust port conditions 4EC and 2EC, the vertical distributions of air ages roughly match, despite the large difference in the horizontal position. What’s more, the air age became smaller as the air supply port became closer to the air inlet, it can be concluded that the position of the air supply port more affects the air supply distribution performance than the position of the air outlet.

4.3 Result of heating condition

4.3.1 All condition

Vertical temperature distribution

Regarding the vertical temperature distribution, the temperature variation is large at high measurement points' locations, and it can be seen that it fluctuates greatly with time. On the other hand, the temperature is almost a constant value at low measurement points. This is because that the warm air blown out from the inlet is staying in the upper part of the room.

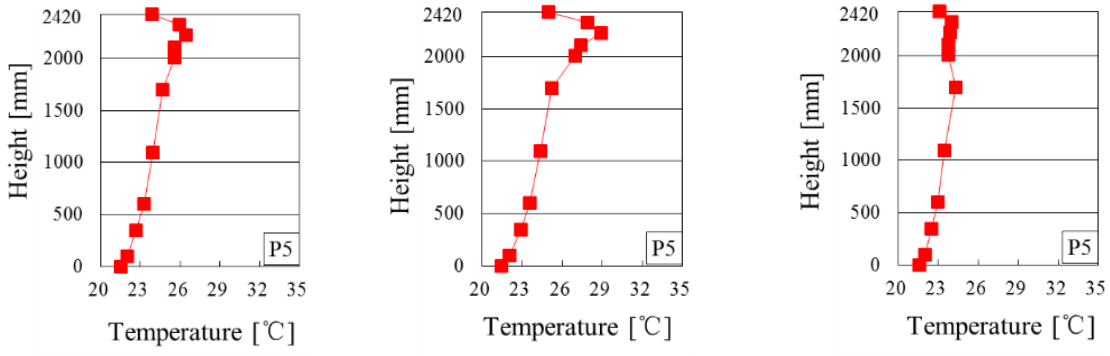

(a) Average temperature (b) Maximum temperature (c) Minimum temperature

Fig. 4.3 Vertical temperature distribution

Concentration distribution

In the case of 4 human body emission, the concentration repeatedly increases and decreases, and never reach a steady state even after a long time. This is because the indoor air temperature fluctuated greatly together with the supply air temperature fluctuation.

In the case of a diffuser emission, the steady state could be reached after the concentration rising. This is because air at the top flows downward by gravity without staying.

Local mean age of air

As for age of air, air exchange efficiency is 1 under cooling condition, but less than 1 under heating condition. This can be considered to be the reason to the formation of temperature stratification in the vertical direction.

Finally, the remaining air ratio has the increasing order as 4EB > 4EC>1EC, which means the air flowing to the machine room is decreasing. It is also observed that, when curtain is closed, remaining air is larger which is due to the obstruction of curtain.

4.3.2 Different conditions

Influence of the existence of curtain

Regarding the temperature distribution, it can be seen that hot air easily reaches a lower position with curtain closed.

Regarding the normalized concentration, when the exhaust port is inside the curtain, the influence by the existence of curtain is small. However, when the exhaust port is outside the curtain, the flow to the exhaust port is obstructed when there is a curtain, and the contaminant removal efficiency deteriorates.

Regarding the age of air, when the exhaust port is inside the curtain, the influence by the existence of the curtain is small. When the exhaust port is outside the, the ventilation efficiency is slightly improved.

Influence of exhaust port position

First, the influence on the temperature distribution was small, and with regard to the normalized concentration, the exhaust port provided near the pollutant generation position became smaller, and the contaminant removal efficiency was slightly improved. Regarding the age of air, the deviation of horizontal age distribution became large if there is only one exhaust port. The ventilation efficiency of the entire room is better at the exhaust port position of 4EC.

Next, the influence of the exhaust port height is considered by comparing the exhaust port position 4EC (50 mm down from the ceiling) and 4 EB (FL + 1150 mm). At the exhaust port position 4 EB, the hot air did not reach the position lower than the exhaust port, and the vertical temperature difference became larger. Moreover, for the normalized concentration, the exhaust port position 4 EB near the gas generation position became smaller, and the contaminant removal efficiency is remarkably improved. The age of the air is almost identical inside of the curtain and the ventilation efficiency of the entire room is slightly higher at the exhaust port position 4EB.

Correlation of temperature fluctuation and concentration fluctuation

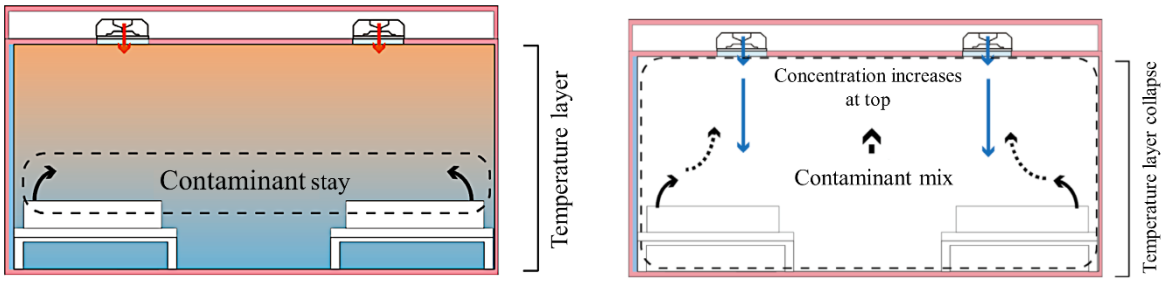

(a) Temperature layers exist (b) Temperature layers collapse

Fig. 4.4 The change of gas when supply air temperature changes

The concentration becomes smaller when the indoor air temperature at FL+1700mm is high, and the concentration becomes larger when the temperature is low. This is because when the temperature at the high position at FL+1700 mm is high, the gas leaving from the bed stays below, temperature stratification therefore appears, and when the temperature at FL+1700 mm is low, the temperature stratification collapses and the gas rises to a high position as well.

By observing the correlation between temperature stratification (vertical temperature difference) and concentration fluctuation, the following conclusion can be obtained.

In the absence of curtains, when there is temperature stratification, contaminants flow in the horizontal direction from the source. When the thermal stratification collapses, it flows in the vertical direction and diffuses greatly in the horizontal direction.

When there is a curtain, it flows in the vertical direction inside the curtain and flows out from the top of the curtain.

When the exhaust port is set in the vicinity of the pollutant source, the contamination removal efficiency is remarkably improved. Although contaminants can be removed efficiently when temperature stratification is formed, contaminants are diffused when temperature stratification is broken, as a result the concentration rises.

4.3.3 Future prospect

Through the findings from the experiments conducted in the simulation sickroom under cooling condition and heating condition, some proposals are made for four-bed ward design. The

ventilation efficiency is not only related to the position of the exhaust port, but also closely related to the position of the supply diffuser. It is considered that the position of supply diffuser has an effect on the local mean age of air significantly. Therefore, both of these two positions are essential factors to be considered whilst a four-bed ward is designed. The experiments were conducted under an optimum condition (each of the four bed was set a supply diffuser overhead). In terms of reducing cost of installation, only one or two inlets are arranged in the real ward. The effect of the number of supply diffuser and setting position will be studied and discussed in the further research.

In order to make the contaminants escape out of the ward efficiently, exhaust ports in appropriate position are necessary. Specifically, the optimum choice is that each of four exhausts ports are placed near the one bed. Taking the cost of installation and ventilation efficiency into account, setting a central exhaust port in the ceiling of ward is feasible.

However, the above suggestions for design are based on the experimental results, CFD simulation will be used to verify the results in further analysis of research and the suggestions will be improved.

REFERENCES

1-1) Kosonen R., Tan F. (2005): "A feasibility study of a ventilated beam system in the hot andhumid climate: a case-study approach", Building and Environment, 40 (9): pp.1164–1173.

1-2) Virta M., Butler D., Gräslund J., Hogeling J., Lund K. E., Reinikanen M., Svensson G. (2004): "Chilled beam application guidebook", Brussels : Rehva. 3.

1-3) Trox USA, Inc.: "Chilled beam design guide".

1-4) Tang J.W., Li Y., Eames I., Chan P., Ridgway G.L. (2006): "Factors Involved in the Aerosol Transmission of Infection and Control of Ventilation in Healthcare Premises", *Journal of Hospital Infection*, 64(2):pp.100–14.

1-5) Li Y., Huang X., Yu I., Wong T., Qian H. (2004): "Role of Air Distribution in SARS Transmission During the Largest Nosocomial Outbreak in Hong Kong", *Indoor Air*, 15(2):pp. 83–95.

1-6) Azizpour F., Moghimi S., Lim C., Mat S., Zaharim A., Sopian K. (2011): "Thermal Comfort Assessment in Large Scale Hospital: Case Study in Malaysia", in: 4th WSEAS International Conference on Recent Researches in Geography Geology, Energy, Environment and Biomedicine, Corfu Island, Greece, pp. 171–174.

1-7) Parsons K.C. (2003): "Human Thermal Environments: The Effects of Hot, Moderate, and Cold Environments on Human Health, Comfort and Performance" *Taylor and Francis*, London, pp. 196–228.

1-8) ASHRAE (2003): "Chapter seven: Healthcare Facilities", *HVAC Applications Handbook*.

1-9) Kameel R., Khalil E. (2003): "Thermal Comfort VS Air Quality in Air-conditioned Healthcare Applications", *the 36th AIAA thermophysics conference*, Orlando, the U.S.

1-10) Sattayakorn S., Ichinose M. and Sasaki R. (2017): "Clarifying Thermal Comfort of Healthcare Occupants in Tropical Region: A Case of Indoor Environment in Thai Hospitals". *Energy and Buildings*, 149: pp. 45–57.

1-11) Hashiguchi N., Hirakawa M. and Tochihara Y., Kaji Y., Karaki C. (2008): "Effects of Setting up of Humidifiers on Thermal Conditions and Subjective Responses of Patients and Staff in a Hospital during Winter", *Applied Ergonomics*, 39: pp. 158–165.

1-12) Balaras C., Dascalaki E, Gaglia A. (2007): "HVAC and Indoor Thermal Conditions in Hospital Operating Rooms", *Energy and Buildings*, 39: pp. 454–470.

1-13) Wang X., Bi X., Chen D., Sheng G., Fu J. (2006): "Hospital Indoor Respirable Particles and Carbonaceous Composition", *Building and Environment*, 41: pp. 992–1000.

1-14) Mendes A., Bonassi S., Aguiar L., Pereira C., Neves P., Silva S., Mendes D., Guimarães L., Moroni R., Teixeira J. (2015): "Indoor Air Quality and Thermal Comfort in Elderly Care Centers", *Urban Climate*, 14: pp. 486–501.